MODELING THE SPECTROSCOPY OF A LIGHT COLLECTING MOLECULE COUPLED TO A NANOCRYSTALLINE SEMICONDUCTOR

By

GREGARY C. ZWEIGLE

A thesis submitted in partial fulfillment of
the requirements for the degree of

MASTER OF SCIENCE IN CHEMISTRY

WASHINGTON STATE UNIVERSITY
Department of Chemistry

MAY 2009

To the Faculty of Washington State University

The members of the Committee appointed to examine the thesis of GREGARY C. ZWEIGLE find it satisfactory and recommend that it be accepted.

_____

Dr. Jeanne McHale, Ph.D., Chair

_____

Dr. Kirk Peterson, Ph.D.

_____

Dr. Aurora Clark, Ph.D.

ACKNOWLEGEMENT

Don Wiseman, my good friend, diagnosed with cancer in 2000, provided my initial motivation to renew chemistry and physics studies. I wanted to understand, at a fundamental, scientific level, why cancer is not always cured and why our remedies are primitive. Also, our country, the United States of America, is unnecessarily dependent on external energy resources. I wanted to understand why we have not significantly developed sources of energy other than fossil fuels. Energy propels life forward to advance, conquer, discover. Are we satisfied taking hours to travel across the world? Going faster requires new energy technology. How about clothing that keeps us at a constant temperature regardless of the environment, or nanomachines that continuously move around inside our bodies to clean up toxins, diseases, cancerous cells, and fix cell deterioration? Building infrastructure and cities on other planets, enabling the developing world to more fully enjoy the benefits of modern technology such as continuously available and reliable electricity, helping our planet support an exponentially growing human population; it all requires new ways to convert energy from one form to another and in the process, work. As an engineer, and now a scientist, I am curious to understand key challenges for solving problems such as these. And why it takes so long to get them accomplished. Nothing, it sometimes seems, moves slower than the pace of technology.

When I considered returning to school in 2004 Dr. Kirk Peterson was very encouraging. Probably I am in the Chemistry department, instead of the Physics department, because of him. I enjoyed the instructors at WSU: Dr. Ron Poshusta (Quantum Physics), Dr. Ursula Mazur (Thermodynamics), Dr. Jeanne McHale (Statistical

Mechanics and Spectroscopy), Dr. Scot Wherland, Dr. Ken Nash, Dr. Jim Hurst (Inorganic Chemistry), Dr. K.W. Hipps (Group Theory), Dr. Sue Clark, Dr. Jim Bruce (Analytical Chemistry), and Dr. Jim Schenk (Electrochemistry).

Schweitzer Engineering Laboratories, Inc. paid for my entire graduate study. I am grateful to Dr. Schweitzer for his vision of education's importance and our responsibility of contributing to society. I have the privilege of helping solve energy problems every day working as an Engineer at SEL.

Dr. Jeanne McHale suggested the research topic, provided excellent guidance, and was kind enough to answer my many weekend phone calls and e-mails. "Theory guides, experiment decides"!

My family Tina, Taylor, and Kelsey are always awesome in their support of my continuing interest in learning new engineering and scientific fields. Our cat, Midnight, provides the example in my introduction.

MODELING THE SPECTROSCOPY OF A LIGHT COLLECTING MOLECULE COUPLED TO A NANOCRYSTALLINE SEMICONDUCTOR

Abstract

By Gregary C. Zweigle, M.S.
Washington State University
May 2009

Chair: Jeanne McHale

The solar cell based on sensitizing a mesoporous array of nanocrystaline semiconductors with a small, light collecting molecule, depends on coupling between the semiconductor and molecule for proper operation. This coupling provides a pathway for solar energy generated electron injection from the molecule into the semiconductor. Modeling this coupling is important to obtain fundamental insight into the physics of solar cell operation and design future innovative solar energy transforming systems. Starting from first principles of quantum physics a model of the coupling effect on the molecule spectroscopy is created. The model estimates how molecule energy levels are affected by the semiconductor. A key advantage of this model is its simplicity. This enables easy comparison against experimental data and aids insight into parameters influencing the coupling.

Effects of both semiconductor bulk and surface states are included. The model utilizes experimentally available spectroscopic parameters. Spectroscopy provides a convenient method to probe the nature of this coupling. The model qualitatively predicts an absorption spectrum red-shift, an intensity change, and reproduces coupling induced broadening of the molecule vibronic absorption spectrum. A strength parameter is

identified and numerical values are calculated. The model is amenable to including arbitrary number of normal mode vibrations.

The spectral broadening characterization utilizes basic spectroscopy parameters of the molecule and the semiconductor. But the model requires only a single adjustable parameter for reproducing the full vibronic absorption spectrum experimental data. Comparison of the model absorption spectrum broadening prediction against experimental absorption data for 8'-apo-β-caroten-8'-oic-acid attached to colloidal nanoparticle TiO_2 provides a validation test of the theory.

TABLE OF CONTENTS

Page

LIST OF TABLES

Page

LIST OF FIGURES

Page

1.0 Introduction

Imagine an isolated physical system and a set of rules for calculating a single number based on the motion and position of objects in the system. The rules also include properties of the objects such as their mass and charge. An infinite variety of such rules are possible. Now allow the system to change. Recalculate the single number using the same rules. A new number results.

What is interesting about creating rules and calculating numbers? It is this. A certain set of rules have been discovered with a surprising result. The calculated number never changes. The rules always result in the same number, for a given system. Let the system evolve in any way imaginable. The objects can consist of planets, cars, exploding fireworks, sunlight reflecting from the ocean, cats, shuffling electrons inside a microprocessor, even the interactions of living creatures. Calculate the number after every change and as many times as desired. The same number always is found. This number is called energy. Energy is constant, it is conserved.

Two broad classes of rules for calculating energy are known. One is called kinetic energy. These rules are based on the motion of the objects in the system. The second is called potential energy. These rules are based on the position of the objects in the system. Because energy is conserved, kinetic energy can trade for potential energy, and potential for kinetic energy. In this sense, energy measures the ability of a system to create motion.

Finer classifications of energy are also possible. A moving cat has kinetic energy proportional to the mass of the cat multiplied by the velocity of the cat squared. The

water behind Grand Coulee dam has potential energy proportional to its mass multiplied by height above the ground. A photon has kinetic energy proportional to the color observed when it strikes a human eye. The surrounding space of an electron has potential energy proportional to the electric and magnetic fields associated with the electron.

Notice the language of energy. Objects are said to have energy. Yet they only have energy in the sense that total energy is conserved and therefore individual energy values are tradable. Transform the energy of an electron for the energy of a photon. The electron decreases energy by exactly the gain in energy, from zero, of a new photon. Or, attach the cat to a string, using a harness to avoid harm, and make a pendulum. Nudge the cat from equilibrium. Watch kinetic energy trade with potential energy. These relationships enable predictions. Given the position and velocity of the cat, conservation of energy enables finding other possible positions and velocities because they must have the same energy. These are allowed states of the system, assuming no other interaction with the surroundings.

Conservation of energy is necessary for predictions, but not sufficient to actually formulate predictions. A system may have many states with the same energy but the conservation property does not predict which state is preferred. Why does the firecracker explode when sparked? A resting firecracker has the same energy, mostly potential, as flying bits of paper, mostly kinetic. Fortunately, a second property of these sets of rules has been discovered. Energy prefers to spread out. Select a system. Calculate all configurations with the same energy. Find the configuration in which the energy is maximally distributed, to available states. This is the preferred configuration. Given sufficient time, the system always finds this final configuration. Therefore, the future is

known. Predictions are available. Energy is a property that enables creating systems, machines, acting predictably and doing useful things. Engineering is possible.

Although the diffusing property of energy may appear abstract at first, it is very understandable. The physical world contains a large number of objects. A cat is constructed of, perhaps, 10^{27} individual particles. And an even larger number of particle configurations are possible, all with the same energy. Imagine an isolated room filled with oxygen molecules. One possible arrangement is the molecules localize in one corner of the room. Another possible arrangement is the molecules evenly distributed throughout the room. Many more arrangements for uniform distribution are available, in comparison to tight distribution. Therefore, a system with the molecules localized in one corner eventually changes into a system with all molecules evenly distributed.

The measure of energy distribution is called entropy. Entropy always increases during a spontaneous change of an isolated system. Spontaneous means no external influences. At maximum entropy the system reaches equilibrium. No further changes are possible. The system is dead.

Energy and entropy are fundamental to life. Sunlight is the origin of most energy on Earth, and therefore is the energy of life. The photosynthesis process involves transforming kinetic energy of a photon into potential energy of separated carbon and oxygen. The initial photosynthetic step is photon capture. Molecules with an energy spectrum tuned to the wavelength of visible light collect the photon, turning the original energy into a potential and kinetic energy change of electrons. These electrons return to their initial energy, not by releasing heat, but by transferring this energy to a water molecule. The water fragments into pieces: an oxygen molecule, a pair of electrons, and

a pair of protons. The oxygen is dumped into the atmosphere. Plants have little regard for the environmental impact of releasing such a dangerous chemical as oxygen (O_2) into the atmosphere. The electrons and protons, meanwhile, are sufficiently energetic to drive the creation of plant-parts, along with atmospheric carbon dioxide.

Low entropy systems, far from equilibrium, are useful. The system consisting of separated oxygen and plant-parts is not at equilibrium. Humans and animals consume the plant-parts and biologically burn them with inhaled oxygen. Vehicles, designed by humans, burn the plant-parts as well, in the form of gasoline and jet fuel, with exciting and violent reactions. Burning plant-parts returns them to the original water and carbon dioxide system. Meanwhile, solar kinetic energy is conserved into kinetic energy of cats and airplanes.

Solar kinetic energy coupled to chemical potential energy has provided significant benefit to life. However, the conversion process is inefficient and slow. Inefficiency means much of the original energy is wasted as heat, and is radiated away. Slow means low power. Power is the rate of change of energy per unit time. Energy may drive life, but power lets it win. Slow energy conversion creatures, such as the Triceratops, are greatly disadvantaged to the fast energy converting Tyrannosaurus rex. Slow armies, soldiers on foot, are greatly disadvantaged to fast armies, soldiers riding in machines. In the limit, slow always loses to fast.

Also, life in its present form depends on the present concentration of atmospheric oxygen. Returning the original water and carbon dioxide back into the atmosphere changes this concentration. Better methods of utilizing solar energy are needed.

Several types of machines are possible which convert solar energy into useful energy. An artificial photosynthetic process converts solar kinetic energy into separated oxygen and other useful chemicals such as molecular hydrogen or an alkane [1], [2]. Another possibility is to directly use excited electrons in a cyclic process as electricity. While the latter approach is investigated in this research, the work is fundamental and applicable to both systems.

A solar cell operates by capturing photons in the energy bands of highest intensity radiated from the sun. The excited electrons can return to their original energy state, radiating heat as required meeting energy conservation. Alternatively, a machine can direct the path of the electrons by the use of an asymmetry. The most common type of solar cell, based on crystalline bulk silicon semiconductors, utilizes a junction between two dissimilar materials as the asymmetry. At the interface, mobile electric charge redistributes between the two materials, in a similar process to the example of oxygen molecules diffusing into the large volume of a room. Complete diffusion is prevented by the charged nature of the electrons and equilibrium is reached when the diffusion process is exactly canceled by the electric field of the charged particles.

When an electron is excited into higher energy by a received photon it migrates aimlessly through the semiconductor material. If the electron happens to interact with the electric field then it is swept across the junction. The electric field prevents return. The field is, effectively, a one-way valve. Therefore the system is forced away from equilibrium and the only return path is for the electron to travel through an external circuit, back to its original side of the junctions. These devices are popular because they are simple, easy to understand, and with well known manufacturing methods. Although

an active area of research is improving the solar to electron energy conversion efficiency. Also, silicon is relatively expensive, the manufacturing process is complicated, the cells are heavy, inflexible, and fragile.

Recently a new type of solar cell, the dye sensitized solar cell (DSSC), was proposed and tested [3]. In this case the asymmetry is based on time-domain dynamics of transfer rates, in addition to static junction barriers. This makes the system more difficult to understand and analyze.

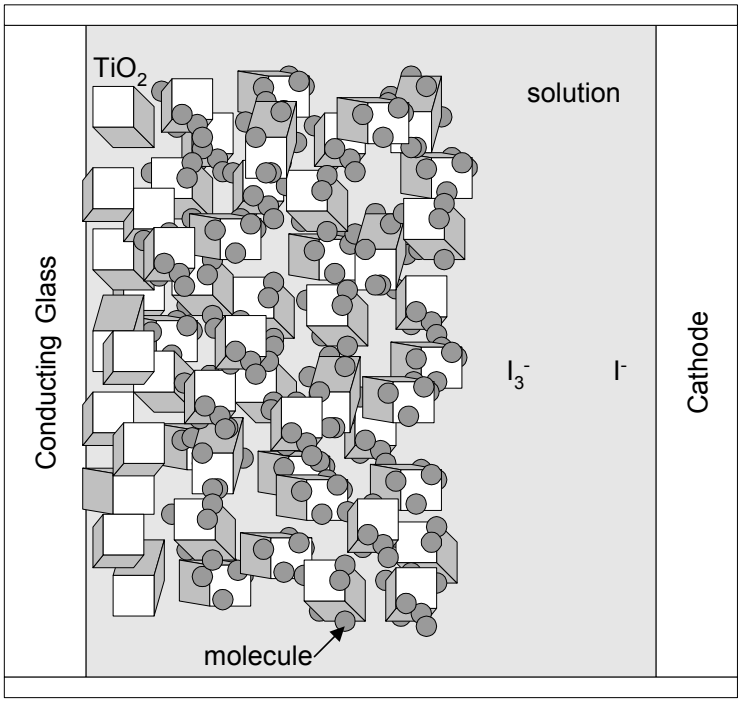

Figure 1.1. Basic structure of dye sensitized solar cell.

The DSSC, schematically shown in Figure 1.1, operates by placing a light collecting molecule, a chromophore, sometimes also called a dye, in contact with a semiconductor [4] [5], [6], [7], [8], [9]. The chromophore is tuned to collect specific bands of incident electromagnetic radiation. Efficiency is improved with nanosize

semiconducting crystalline particles because a higher surface area leads to a high concentration of light collecting molecules available to absorb solar energy. The chromophore, with few available states, couples to the semiconductor, with a tremendous number of available states. The excited electron injects into the semiconductor because of the associated entropy increase [6]. Energy is conserved and so the original solar kinetic energy is transferred into the electron potential and kinetic energy. The electron is prevented from returning to the original molecule because of the relatively large volume of states available in the semiconductor and the coupling strength. The system is bathed in an electrolyte solution which enables the electron to return to the chromophore after transport through an external circuit. Many research systems use iodide / iodine as the electrolyte. Iodide (I^-) is created by a reduction of iodine/tri-iodide (I_3^-) when it receives the returning electron at the counter cathode electrode. The iodide then diffuses to the semiconductor / molecule system. The molecule's missing electron is returned by an oxidation step of converting iodide to iodine/tri-iodide.

Figure 1.2 shows the DSSC electron path. The initial light energy, represented by $h\nu$, excites a molecule and then results in injection of an electron from a molecule into the semiconductor array. The electron injection process depends on the coupling relationship between semiconductor and molecule. The electron eventually migrates to the external circuit, represented by a resistor. After returning to the DSSC the electrical energy reduces I_3^- which diffuses back to a chromophore molecule, thereby completely the electrical loop. Unwanted paths, reducing the solar cell performance, include the electron returning immediately to the molecule, without following the external circuit

route and the electron reducing I_3^- at the TiO_2 interface, again without following the external circuit route.

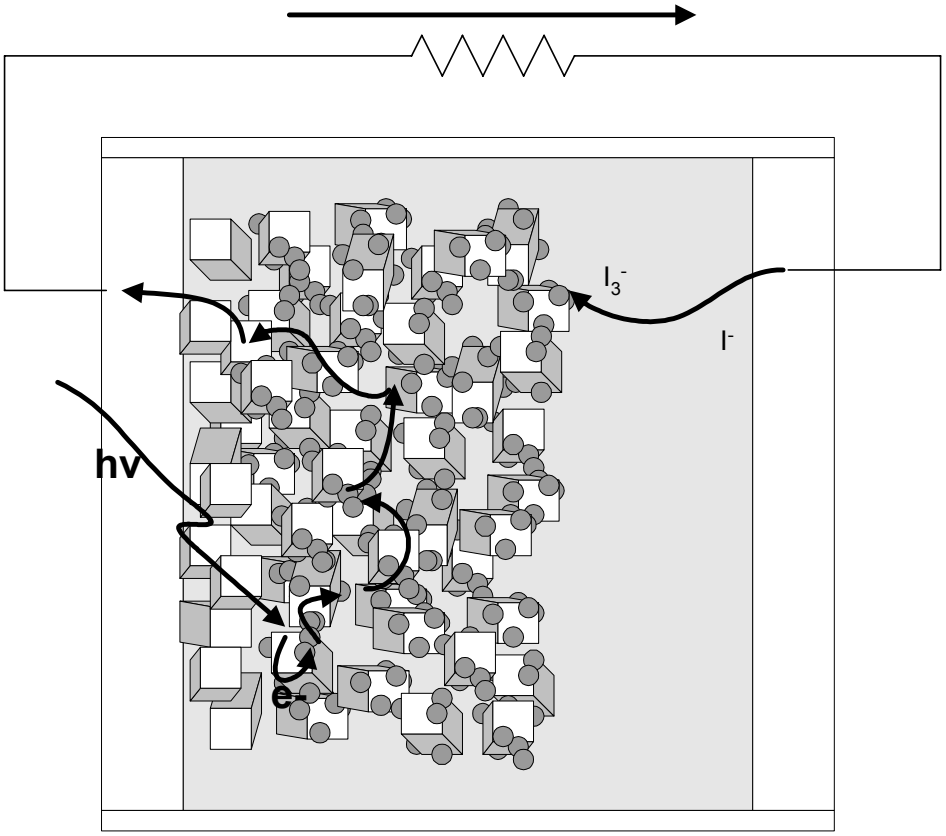

Figure 1.2. Electron path through DSSC.

The DSSC has the advantage of low cost, a simple manufacturing process, the possibility of creating flexible solar cells, and the possibility of tuning the absorption characteristics of the light absorbing molecule to the exact incident spectrum [10]. The disadvantages include low efficiency and poor reliability. Improving efficiency requires understanding the details of physical operation and this is a challenge because of the fairly complex interactions.

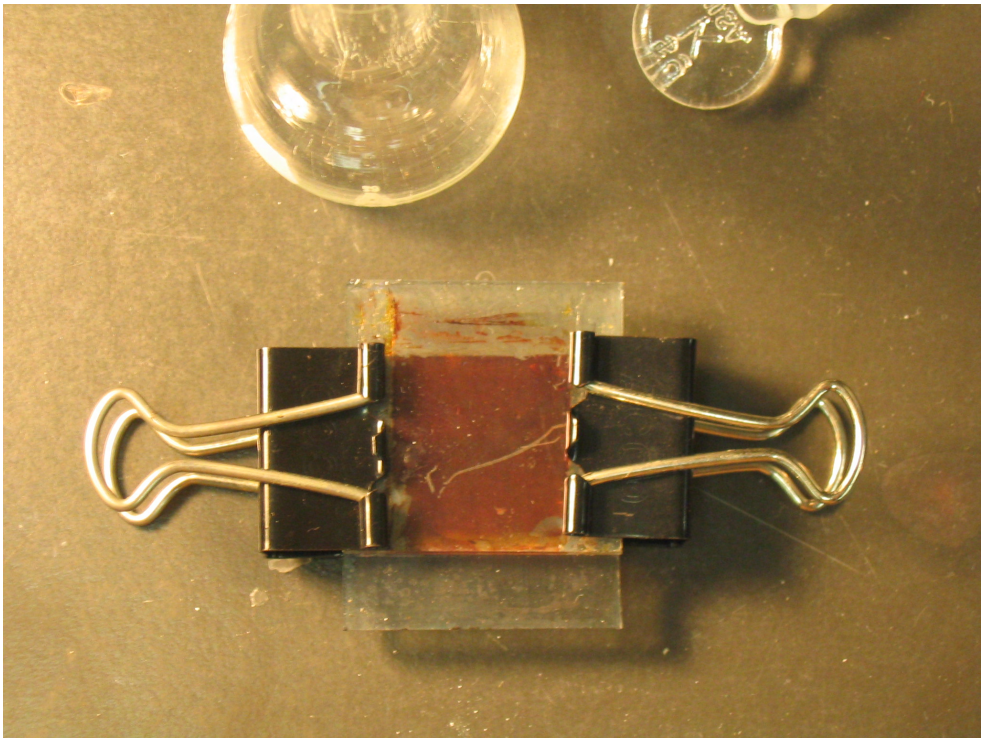

Figure 1.3. Photograph of a DSSC suitable for experimental use.

One important physical step of operation requiring better understanding is the coupling process of a light collecting molecule to the semiconductor. This coupling is important to the mechanism of electron injection, the ideal conditions for injection, and minimizing the reverse reaction. Strong coupling increases the rate of electron injection. However, if the coupling is too strong then the reverse reaction rate is increased. The reverse reaction is a pathway for converting solar energy without flowing through the external circuit. Think of this as a parallel low-resistance path and it decreases the efficiency of the cell.

A very simple solar cell model, Figure 1.4, is a current source, representing excitation due to the incident photon, a series resistance representing propagation of the

electron to the external contacts, and a parallel resistance representing recombination of the electron internal to the cell before arriving at the external contact. The diode represents a critical voltage beyond which excited electrons return immediately to their initial state. For the DSSC this is the junction potential of the TiO_2 / electrolyte interface. The simplicity of this model results in its applicability to nearly all classes of solar cells. Based on this model, a few important tradeoffs of solar cell design are observable.

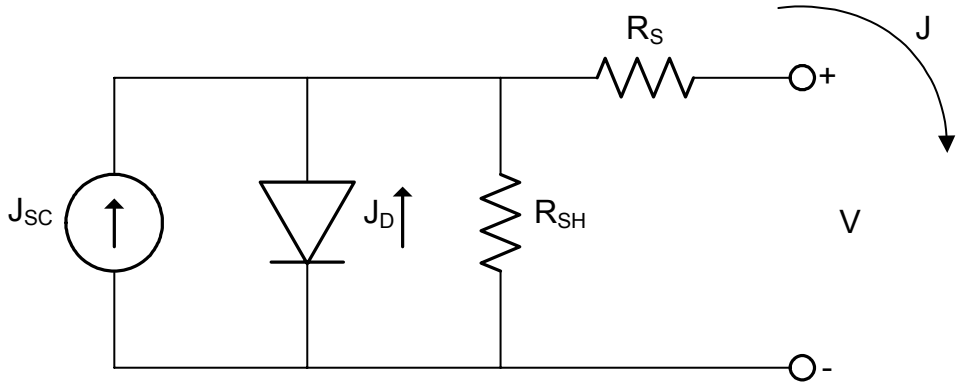

Figure 1.4. A simple solar cell model.

Figure 1.5 shows the performance of the Figure 1.4 circuit for a typical silicon based solar cell and the solar spectrum observed on planet Earth. The vertical axis is current density, J, flowing through the external circuit. The horizontal axis is the external voltage V.

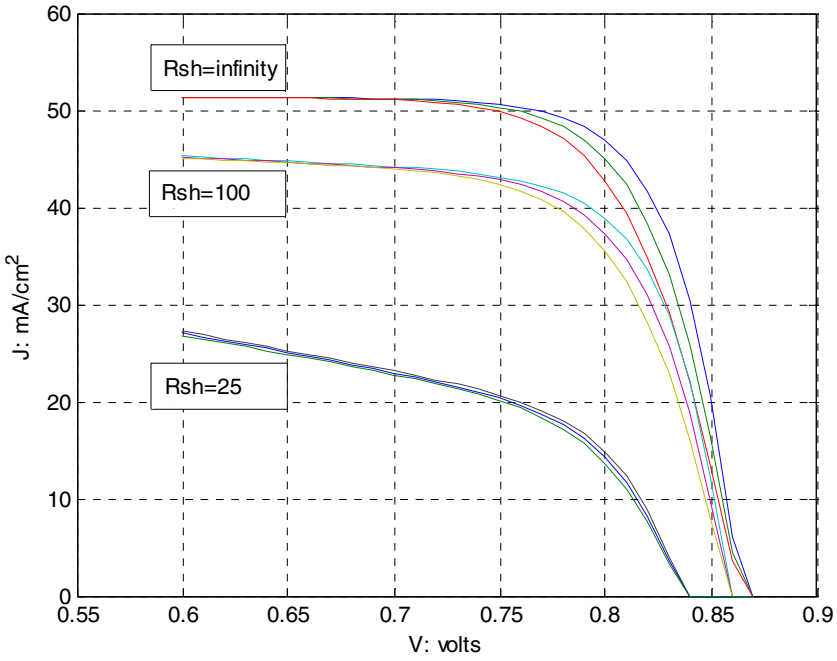

Figure 1.5. Current vs. voltage relationship of the Figure 1.4 solar cell model.

Three sets of three curves are shown in Figure 1.5. Each set of curves represent a different R_{SH}. The top set is for $R_{SH} = \infty$. The middle set is for $R_{SH} = 100\Omega cm^2$. The lower set is for $R_{SH} = 25\Omega cm^2$. Within each set of curves are three finer resolution curves. These are for $R_S = \{0, 0.2, 0.4\}\Omega cm^2$ respectively. The parallel shunt resistance R_{SH} models unwanted paths which short-circuit electron ability to flow through the external circuit. The series resistance R_S models the migration path of the electron through the TiO_2 matrix and also diffusion properties back through the electrolyte. The open circuit (peak) current is limited by the ability of the molecule to receive solar energy and depends, in part, on the match of the molecule absorption spectrum to the incident solar spectrum.

The power output of the solar cell is $V \cdot J$. Peak power output, the desired operating point, is at the point of $V \cdot J$ maximum. This is approximately between 0.75 and 0.8 volts for the conditions shown in Figure 1.5. Any change to the solar cell which increases the current (larger vertical value of the curves) or pushes out the point where the current begins to roll off from its initial value, results in an improvement in the power output of the cell. Divide the power output by the power input. This is the solar cell efficiency. Figure 1.6 shows efficiency for the conditions of Figure 1.5.

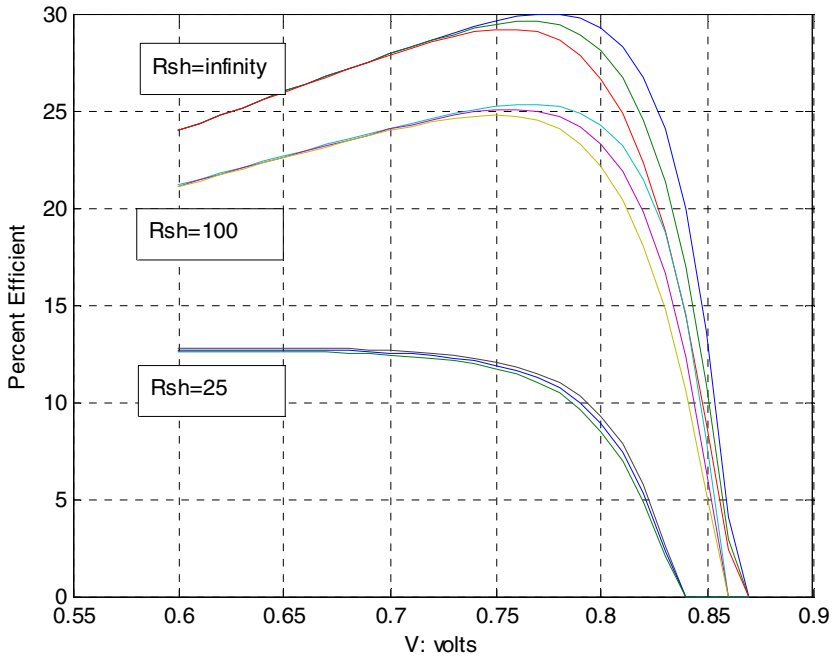

Figure 1.6 Efficiency of the Figure 1.4 solar cell model.

The maximum current value is set by J_{sc}. Increasing molecule coupling to the semiconductor is one method to increase J_{sc}. Increasing the molecule coupling also decreases R_{SH}. Notice that as R_{SH} decreases, so does the total amount of current, the slope of the current as a function of voltage increases, and the efficiency decreases.

Understanding coupling helps design molecules and their interface to the semiconductor with the goal of simultaneously increasing J_{sc} and R_{SH}.

One helpful method of studying the coupling is with spectroscopic measurements. Spectroscopy is a method of applying an electromagnetic signal to a system and observing the electromagnetic effect. An absorption experiment measures the change in intensity of the original signal, as a function of frequency, after passing through the system. A scattering experiment measures the change in intensity and frequency of the incident light after scattering by the system. The frequency of a photon is directly proportional to its energy. Therefore, spectroscopy measures the system energy. This provides important information for designing solar cells. For example, the energy levels of the chromophore in a DSSC must be properly matched to the energy levels of the nanocrystalline semiconductor for proper coupling. The excited electron needs sufficient energy to transfer to the conduction band of the semiconductor. Too much energy and the excess is wasted as heat in the transfer process, while too little energy prevents the electron from transferring, or the rate of electron transfer is slow which lowers the maximum short circuit current available. Also, the energy of the excited chromophore compared to the electrolyte is important. A relatively large concentration of I_3^- hovers near the chromophore, having recently reduced adjacent light harvesting molecules. For proper operation, the iodine/tri-iodide must diffuse back to the counter electrode. The diffusion process is driven by this concentration gradient. However, this large concentration of an oxidizing agent is a tempting target from the perspective of the excited chromophore electron. An electron transferring directly from an excited chromophore to the iodine/tri-iodide is a parasitic process, effectively reducing R_{SH}.

Proper separation of chromophore and electrolyte energy levels are important to minimize this undesired transfer path.

Studies of coupling using spectroscopy of various molecules attached to nanocrystalline semiconductors show the coupled spectrum has a shifted frequency and scaled intensity when attached to the semiconductor, compared to the molecule in isolation. The fact that the semiconductor influences the energy levels of the chromophore complicates the design of solar cells. The interaction is influenced by many factors such as surface states, the electrolyte, and the size of nanoparticles.

A simple model to help understand these effects is needed. The model can help improve understanding of the interface between the molecule and the semiconductor. In this research a model is proposed, limitations and approximations are identified, and experimental results are predicted. The predictions are based on a simple model of the semiconductor absorption spectrum. The model aspires to include experimental data as much as possible and avoid computationally intensive quantum calculations. Sometimes models are very accurate but are so complicated that they provide little physical intuition. Ideally, the model developed by this research is simple and contributes to new understanding of the solar cell underlying physical coupling mechanisms.

In creating this model, first, in Chapter 2, the present state of understanding DSSC coupling is referenced. Then the applicable basics of quantum mechanics, both static and time-dependent are derived in Chapter 3 and Chapter 4, respectively. This introductory work is well known and is included to define the basic equations and notation required for the theory. Next the original work begins. Physical models of the molecule and semiconductor system, the coupling, and the effect of the semiconductor on the molecule

are proposed in Chapter 5 and Chapter 6. The development is based on variational theory. Chapter 7 defines and derives the expansion states used in the variation summation. Next a mathematical prediction of the molecule energy level change due to the semiconductor is developed in Chapter 8 and a prediction of the intensity change is developed in Chapter 9. Two variants for each are included in the development, one for use with electronic levels only and one that includes vibrational levels. Comparison against experiment requires the semiconductor spectroscopic properties. A useful approximation is developed in Chapter 10. The energy level shift, intensity change, and vibronic spectra are quantified.

Finally, the model predictions are compared with experiment in Chapter 11. Two classes of chromophores are organic-based and metal-based. Metal-based molecules have resulted in the highest efficiency solar cells. However, the complexity of the electronic and vibrational levels make them unsuitable for the present study. Comparison is made against several reported experimental results in the literature using organic chromophores such as the carotenoid family. It is shown that the model makes reasonable predictions, therefore justifying the underlying theory. This means intuition gained by studying the model is helpful in understanding parameters which affect the molecule semiconductor coupling. Hopefully this understanding will lead to the design of better energy conversion systems.

2.0 State of the Art

Many physical systems include small molecules interacting with metals and semiconductors [11]. Surface enhanced Raman scattering (SERS) utilizes a metal amplifying the intensity and scattered light associated with vibronic transitions in an adsorbed molecule [12]. Highly sensitive detection of target molecules is a useful application. Innovative hydrogen generation systems utilize solar energy based charge injection systems [13] [14]. In the system under study a small molecule injects electrons into a semiconductor after excitation by electromagnetic radiation. Improving the understanding of these interactions is essential for future energy conversion devices.

Charge transfer is a related field. An excited molecule can inject an electron into metals or semiconductors under certain circumstances. Studies utilize reaction rate constants to determine features of the electron transfer process. Research includes calculating electron transfer rate constants for semiconductor electrode / liquid interfaces [15] [16]. Several studies of charge injection as ultra fast interfacial heterogeneous electron transfer from a small molecule to semiconductor are available and absorption spectra are predicted based on transfer rates [17] [18]. Charge injection rates across the metal-molecule interface based on Marcus theory are calculated [19]. The electron transfer is influenced by density of states in the semiconductor [20].

In contrast to charge injection, which describes rates in terms of electron injection across the interface, this thesis investigates photon-induced electron excitation within the molecule. The effect of the semiconductor on the molecule states is researched using

electronic absorption spectroscopy. Work in this area includes understanding the SERS phenomena [21] [22]. Metal states are the intermediate excitation state. The referenced study is of vibronic scattering enhancement in terms of frequency and time-domain Raman.

Time-domain dynamics of perylene coupled to TiO_2 has been extensively studied [23] [24] [25] [26] [27] [28][29] [30]. A model using the time-domain Schrödinger equation includes the electronic states and a set of vibrational coordinates for the modes which participate in the electron transfer process. The perylene ground state, first excited state, and the quasi continuum states of the semiconductor are included [23]. The reorganizational energy and its effect on the decay times of this system have been studied [24]. When the system is excited by a short laser pulse, the product state decay shows a staircase time dependence. This demonstrates the vibrational wave packet of the chromophore crossing between the reactant and product potential energy curves [25].

Further work on the perylene TiO_2 coupling system includes a detailed study of the time-dependent energy distribution and trends in absorption line broadening and heterogeneous electron transfer rates with different bridge-anchor groups [26]. Although perylene vibronic spectra consist of multiple Franck-Condon active vibrational modes, the model is based on a single perylene C-C stretching vibration at 1370 cm^{-1}. Experimental evidence shows this approximation is valid at room temperature. However, a model that is amenable to including more vibrational modes could be useful. The model developed in this thesis is not limited to a set number of vibrational modes. The perylene TiO_2 systems are dissolved as colloids in toluene and four different bridge-anchor groups are studied. The model calculates the absorption coefficient based on the

Fourier Transform theory of spectroscopy. It is interesting that although the data shows red-shifting in the spectrum (obscured due to the interaction of vibronic progression with the broadening), the author does not indicate in the tabulated data any change of the perylene electronic energy level when coupled to TiO_2. Investigation to understand the effect of coupling on energy levels is addressed in the present thesis.

Perylene spectra are broadened and different transitions have changes in the intensity. The vibronic transition 0-1 becomes stronger than the vibronic transition 0-0. The change in intensity is claimed due to a change in the reorganization energy which shifts the curves with respect to the normal coordinate. It is interesting that the transition 0-1 is a higher energy transition, closer to the conduction band TiO_2 energy. An investigation into the effect of vibronic level energetic proximity to the semiconductor conduction band is needed and this is addressed in the present thesis.

The perylene TiO_2 system has also been studied by varying different parameters such as the coupling strength of the excited chromophore state to the TiO_2 continuum states, dependence on reorganizational energies of the intramolecular vibrations coupled to the electronic transitions, and the effect of different semiconductor density of state models [27]. The chromophore injection level is slightly below the band edge. Previous studies include absorption spectra, both calculated and experimental, for perylene in solution and perylene absorbed to the TiO_2 surface [27]. It is interesting that the perylene absorption spectrum is broadened when attached to TiO_2. The spectrum does not appear to shift in frequency. This is because the combination of broadening and red shift of the individual vibronic transition frequencies causes the total spectrum to appear unchanged in the frequency location of its peak [27]. Also, it is shown that using different models of

the semiconductor density of states can move the predicted absorption spectrum peak by several hundredths of eV.

For further theoretical verification of the accuracy of the time-domain model, a quantum calculation has been performed [28]. The model consists of a $(TiO_2)_{60}$ cluster and the perylene model with several different anchor groups. The 6-31G(d,p) basis set was applied to a density functional theory (DFT) calculation. The results are primarily focused on dynamic effects. One interesting result is that the lowest unoccupied molecular orbital (LUMO) level is approximately 0.5 eV above the lower edge of the conduction band energy level.

A recent paper studying the perylene TiO_2 system addresses a potential Fano [29] effect that is possible when direct excitation from the ground perylene state to the semiconductor continuum states interferes with an intramolecular charge transfer from the perylene excited state to the semiconductor continuum states. [30]. Again, a single intramolecular vibrational coordinate, 1370 cm^{-1} (0.17 eV), a C-C stretching vibration, is included with the model, along with the full semiconductor conduction band states. The model enables calculation of the linear absorption spectra when the direction CT transition occurs in parallel with an intramolecular excitation. It is expected that the intramolecular excitation results in charge injection as a second stage of the process. Photoexcitation followed by charge transfer is a two step process.

To summarize the studies on perylene coupled to TiO_2, the result is a model showing excellent agreement with experiment. However, the model is based on a time-domain expansion and does not directly calculate molecule energy level changes due to semiconductor effects. What is needed is a static model, simpler in scope, addressing the

movement of the energy levels themselves, and unlimited in ability to include vibrational modes. The model should include as few adjustable parameters as possible.

The original motivation for the present research was experimental results showing a red-shift of Ru(4,4'-dicarboxylic acid-2,2'-bipyridine)$_2$(NCS)$_2$ on TiO_2 when dissolved in acetonitrile solvent but not with ethanol [31]. This chromophore, consisting of a ruthenium metal pyridine complex and often referred to as N3, has numerous excited states and this makes theoretical analysis difficult. It is desired to select simpler systems and derive a theoretical framework to help understand these phenomena. The perylene chromophore also may have shown red-shift behavior but the results were inconclusive due to the spectral broadening on attachment of perylene to TiO_2 [27].

An investigation of experimental results of coupling induced absorption spectral shifts show a variety of results. The ruthenium metal systems are typically blue-shifted upon attachment [32]. Thiophene-functionalized coumarin is also blue-shifted [33]. This shift is due to a deprotonation of the carboxylic acid group in the course of the chemical reaction of chromophore interacting with semiconductor. More complicated perylene chromophores also show a blue-shift [34]. This is due to a ring opening upon attachment to form two carboxylates. Systems which show absorption spectral shifts attributed to chemical reactions changing the basic structure of the chromophore are not useful for the present investigation. This is because a model of the chemical reaction is unduly complicated and masks the essential nature of the phenomena of interest. When the structure of the molecule is chemically changed then the model of this thesis does not apply and so these systems are not considered further.

Some systems show no shift of the absorption spectrum. The spectrum of carbocyanine shows no changes when mixed with acetonitrile and either TiO_2 or silver core TiO_2 nanoparticles [35]. This is because the interaction is primarily electrostatic [35]. Meanwhile, some other systems are red-shifted due to a chemical reaction of the system [36] [37]. Red-shift is also seen due to a direct excitation from the ground chromophore state into the conduction band of the semiconductor. This effect results in a large red-shift [38] [39]. All of these systems are primarily influenced by physical effects which are not covered by the model developed in this thesis and are not considered further.

Although many parameters affect the vibronic spectral shift of the chromophore when attached to a semiconductor, it is interesting to investigate the effect when the coupling is weak. A set of experimental results with systems that seem to fit the approximations of the present thesis model includes the progression of absoprtion spectra found for a sequence of retinoic acid and carotenoic acid chromophores [40] [41] [42]. The molecules bind to TiO_2 through the carboxyl group, then coupling to the light absorbing portion of the molecule through a relatively long bridge conjugated bridge sequence of conjugated double bonds. Alizarin, while not quite as simple, also has some characteristics making it useful for comparison against theory in the present work [43] [44].

The variety of results motivated this research to investigate the conditions under which spectral broadening, shifting, and intensity increasing occur. Certain simplifying assumptions are critical to make the problem tractable. One constraint is weak coupling. The work is studying weak physical relationships, not effects of chemical bonding. Also,

the role of solvent is neglected. This is added later using phenomenological information, a typical simplifying assumption necessary due to the significant complexity of solvent effects. The present study is related to intensity borrowing. This is different from the formation of a charge transfer complex (as found with catechol or vitamin C). Charge transfer cannot be treated by the present theory.

The basic purpose of the research is to help understand basic physics behind the solar cell operation. Coupling is important because a strong coupling is desired so that charge injection is fast. However, if the coupling is too strong then reverse charge transfer is also fast and that limits the efficiency of the cell. Some researchers have proposed designing molecular chromophores to be tuned for certain wavelenghts [10]. The effect of the semiconductor is important to include in this design work.

3.0 Quantum Physics

The mechanics of macroscopic systems are modeled using Newtonian laws of motion. These equations describe systems with force, mass, position, and time. At human level scale Newtonian mechanics work well. At the extremes of velocity, gravity, and mass they fail. The classical equations of mechanics do not predict, for example, electrical conduction characteristics of semiconductors, periodicity of atomic elements, and the energy of light.

Macroscopic systems behave as independent objects and trajectories of objects. Microscopic systems have an inherent wave-like behavior. For example, experiments show two electrons interfere with properties similar to the interference characteristics of two macroscopic waves on the surface of water. This interference manifests itself as a probability of identifying each electron location, unlike a macroscopic system where the location of an object is known without significant affect by the measurement process.

In 1926 Erwin Schrödinger proposed an equation describing the wave behavior of physical systems. This equation results in an energy relationship fundamental to what is called quantum physics. And, while the Schrödinger equation has successfully predicted the experimental behavior of microscopic systems, it also predicts the behavior of macroscopic systems. In the limit of these larger sized systems, the world at a human level, the Schrödinger predicted behavior is exactly the Newtonian predicted behavior [45].

3.1 Postulates of Quantum Physics

The Schrödinger equation is not derived from experimental measurements. It is a postulated physical model. The resulting mathematical equation is only useful because experiments have demonstrated its accuracy. The full theory of quantum mechanics consists of six postulates [45].

Postulate #1 – State Function

There exists a state function containing all knowable information about a physical system. Although the origins of quantum mechanics found wave-like behavior of particles as the basis for a proposed new physics, the extension to many-particle systems results in predicted behavior difficult to visualize with wave properties. Therefore, the quantum mechanical description of a system is sometimes called a state function. The state function is single valued and continuous.

A typical symbol for the state function is Ψ. It is a function of all coordinates of all objects in the system, along with the mass of each object, and time. For certain systems a time-independent version of the state function is also available.

Postulate #2 – Linear Hermitian Operator

There exists a linear Hermitian operator for every physically observable property of a system. Operator operations are written using Dirac's bra-ket notation.

$$\iint \cdots \int g_n^* \hat{A} g_m d\sigma \equiv \langle g_n | \hat{A} | g_m \rangle \tag{3.1}$$

Each g_n is a well-behaved function. In some cases it is the quantum mechanical state function. The integration runs over all coordinates. The linear operator is $\hat{A}$. Write the complex conjugate transpose property of a Hermitian operator using Dirac notation.

$$\langle g_n | \hat{A} | g_m \rangle^* = \langle g_m | \hat{A} | g_n \rangle \tag{3.2}$$

Additional properties of Hermitian operators include real valued eigenvalues and eigenfunctions either orthogonal, or, in the case of degenerate eigenfunctions, optionally converted to orthogonal. In this research degenerate eigenfunctions are always orthonormal. Given f_n, an eigenfunction of a Hermitian operator. Orthonormality means the inner product of two eigenfunctions is either zero or unity.

$$\langle f_n | f_m \rangle = \delta(n-m) \tag{3.3}$$

The appropriate Hermitian operator for any system starts with the classical expression in Cartesian coordinates. Replace each coordinate x with the operator $\hat{x}\cdot$. Replace each momentum component p_x with the operator $-j\hbar\partial/\partial x$.

Note the use of j to represent $\sqrt{-1}$. The state function is complex-valued. Physically observable systems are not complex. The implication is that a state function in isolation does not describe any physical property of a system. No measurement of a system can produce a state function.

Postulate #3 – Only eigenvalues are measurable.

If a physically observable system is in a state which is an eigenfunction of an operator $\hat{B}$, then the result of measuring that physical property must be one of the eigenvalues of $\hat{B}$.

$$\hat{B}f_k = \beta_k f_k \tag{3.4}$$

In Equation 3.4, $\hat{B}$ is the Hermitian operator, f_k is one of the eigenfunctions of $\hat{B}$, and β_k is an observed physical property. One possible operator is the energy operator, denoted as $\hat{H}$. Equation 3.4, with the energy operator, is exactly the time-independent version of the Schrödinger equation. In this case the eigenvalue β_k is the total energy of the system, written as E_k, and f_k is the state function.

Postulate #4 – Completeness of eigenfunctions.

The eigenfunctions of a Hermitian operator form a complete set. This means an arbitrary function, as long as it obeys identical boundary conditions, can be expanded in terms of the eigenfunctions.

$$g = \sum_k \alpha_k f_k \tag{3.5}$$

This is an important property because it enables approximating state functions of more complicated systems using state functions of known systems. Determine the coefficients α_k by operating on both sides of Equation 3.5 with the corresponding operator, integrating over all space, and using orthonormal properties of the eigenfunctions.

$$\alpha_k = \langle f_k | g \rangle \tag{3.6}$$

Postulate #5 – Average value of a physical observable value

The function $\langle \Psi | \hat{B} | \Psi \rangle$ is the manner in which a state function contains all knowable information about a physical system. Take many identical and independent systems, each in the same state Ψ, and measure the physical property corresponding to $\hat{B}$ for each system. The average value of these measurements is the most-likely experimental outcome.

$$\langle B \rangle \equiv \langle \Psi | \hat{B} | \Psi \rangle \tag{3.7}$$

The operator $\hat{B}$ corresponds to the measured physical quantity. However, only an eigenvalue of $\hat{B}$ can be measured. Therefore, expand the state function as a linear combination of the eigenvalues of $\hat{B}$.

$$\Psi = \sum_k \alpha_k f_k \tag{3.8}$$

Substitute Equation 3.8 into Equation 3.7 and solve, along the way using the orthogonality of the eigenfunctions of $\hat{B}$.

$$\langle B \rangle = \sum_k |\alpha_k|^2 \beta_k \tag{3.9}$$

Equation 3.9 indicates that the probability of finding measurement β_k in an experiment that measures property B is equal to the magnitude squared of the coefficient in an expansion of the state function over the eigenfunctions of the operator $\hat{B}$. According to Equation 3.9, a measurement does not provide any knowledge of the system prior to the measurement. And, in the absence of any measurement, the best available prediction is probabilistic at best. Note that the expansion coefficients normalize to unity.

$$\sum_n |\alpha_n|^2 = 1 \tag{3.10}$$

<u>Postulate #6 – Schrödinger Equation</u>

There exists an equation expressing the state function Ψ.

$$\hat{H}\Psi = i\hbar \frac{\partial}{\partial t} \Psi \tag{3.11}$$

This is the Schrödinger equation. As time progresses, the state function Ψ evolves according to Equation 3.11. The Hermitian operator $\hat{H}$ is the system Hamiltonian.

For a time-independent Hamiltonian Equation 3.11 reduces to an eigenfunction form.

$$\hat{H}\psi = E\psi \tag{3.12}$$

$$\Psi(x,t) = e^{-jEt/\hbar}\psi(x) \tag{3.13}$$

The Hamiltonian operator of the system and consists of both kinetic and potential energy components. Equation 3.14 shows this operator for a one-dimension single particle system. The first term is the quantum mechanical operator corresponding to the kinetic energy of the system. The second term, for potential energy, is only a function of the position and charge of the particle.

$$\hat{H} = \frac{-\hbar^2}{2m}\frac{\partial^2}{\partial x^2} + V(x,t) \tag{3.14}$$

The state function is always normalized.

$$\langle \Psi | \Psi \rangle = 1 \tag{3.15}$$

$$\int_{-\infty}^{\infty} |\Psi|^2 \, dx = 1 \tag{3.16}$$

An interesting property of state functions is that when the kinetic and potential energy terms in the Hamiltonian in Equation 3.16 are constrained in a certain way then the Schrödinger solution results in a discrete set of solutions [46]. The constraint is that

the energy relationship for a classical system limits the particle to a definite region of space. The solutions are energy values. This property is the reason for the quantization in quantum physics, hence the name. A typical system has a set of state functions, each state function associated with a discrete energy. When the Hamiltonian has symmetric aspects then multiple state functions can be associated with a single energy value. These are degenerate systems. The state associated with the smallest energy value is called the ground state.

3.2 State Function Approximation

Equation 3.11, which provides the means to determine the state function for a given system, is deceptively simple in appearance. In fact, it is unsolvable for all systems except a select few. Systems with exact solutions include a single particle-in-a-box, a harmonic oscillator, and two charged particles interacting according to their mutual electronic potential energy. The system of this research consists of a molecule interacting with a semiconductor and a stream of photons. It contains tens of thousands of individual particles. This system cannot be solved using Equation 3.11.

Several methods are available for approximating the state function, or, set of state functions, for a given Hamiltonian. The approximation method chosen for this research is based on variation theorem. This theorem states that for a time-independent Hamiltonian, with state function described by Equation 3.12, the quantum mechanical average of any function produces a result larger than that produced by the state function.

$$\frac{\langle \Phi | \hat{H} | \Phi \rangle}{\langle \Phi | \Phi \rangle} \geq E_1 \tag{3.17}$$

Equation 3.17 writes the result in terms of the ground state energy E_1. Find an approximate state function by trying every possible mathematical function Φ with the same boundary conditions as the state function Ψ. Select as an approximation to Ψ the function Φ that produces the smallest result for Equation 3.17.

Unfortunately, such an algorithm is impossibly difficult because of the vast number of possible trial functions Φ. In some cases an ad-hoc trial and error approach is useful because the general form of Ψ is known.

A systematic approach to finding the best Φ writes the trial function as a linear combination of expansion trial functions. The trial functions are chosen as a complete set. For example, the eigenfunctions of a Hermitian operator form a complete set and therefore can provide the expansion functions.

$$\Phi = \sum_{k=1}^{K} \alpha_k f_k \tag{3.18}$$

Now define a function according to Equation 3.17.

$$W \equiv \frac{\langle \Phi | \hat{H} | \Phi \rangle}{\langle \Phi | \Phi \rangle} \tag{3.19}$$

Compute the derivative of W with respect to each of the coefficients α_k in Equation 3.18. Set the result to zero. Solve for the coefficients. The result is a set of coefficients casting the minimum of the total surface of Equation 3.19 in terms of the coefficients.

$$\frac{\partial W}{\partial \alpha_k} = 0 \tag{3.20}$$

In the course of solving Equation 3.20, a matrix equation results which provides a means for determining specific values of W. For a complete derivation, see [45].

$$\left(\overline{H} - \overline{S}W\right)\overline{\alpha} = \overline{0} \tag{3.21}$$

An overbar indicates a matrix. The matrix $\overline{H}$ is a collection of all matrix elements of the Hamiltonian operator.

$$\overline{H} \equiv \begin{bmatrix} \langle f_1|\hat{H}|f_1\rangle & \langle f_1|\hat{H}|f_2\rangle & \cdots & \langle f_1|\hat{H}|f_K\rangle \\ \langle f_2|\hat{H}|f_1\rangle & \langle f_2|\hat{H}|f_2\rangle & & \\ \vdots & & \ddots & \\ \langle f_K|\hat{H}|f_1\rangle & \langle f_K|\hat{H}|f_2\rangle & & \langle f_K|\hat{H}|f_K\rangle \end{bmatrix} \tag{3.22}$$

The matrix $\overline{S}$ is the inner product of all basis functions. In this thesis these functions are chosen orthonormal and therefore $\overline{S}$ is the identity matrix. The full version of $\overline{S}$ is shown next.

$$\overline{S} \equiv \begin{bmatrix} \langle f_1|f_1\rangle & \langle f_1|f_2\rangle & \cdots & \langle f_1|f_K\rangle \\ \langle f_2|f_1\rangle & \langle f_2|f_2\rangle & & \\ \vdots & & \ddots & \\ \langle f_K|f_1\rangle & \langle f_N|f_2\rangle & & \langle f_K|f_K\rangle \end{bmatrix} \tag{3.23}$$

Equation 3.21 has a solution if the determinant of $\overline{H} - \overline{S}W$ is zero.

$$\left|\overline{H} - \overline{S}W\right| = 0 \tag{3.24}$$

Equation 3.24 provides an estimate of the total system energy, with the limitation of how good the basis functions are at representing the state function. Typically it is more interesting to find the energy than the actual state function. This is because, although the state function enables knowing all properties of a system, it is the energy that is the most interesting property for the work of this thesis. Equation 3.24 is a key equation in the derivation of the semiconductor impact on the molecule energy for the model derived in this thesis.

4.0 Time-Dependent Quantum Physics

Studying the interaction of a molecule with sunlight, when in contact with a semiconductor, requires a model of the light. Variation theory provides means to approximate the time-independent Schrödinger equation. Electromagnetic radiation, meanwhile, is time-dependent. And while the time-independent Schrödinger equation is nearly impossible to solve, the time-dependent equation is even more challenging. When attempting to model the interaction of light with matter, an approximation is required that simplifies the time-dependent Equation 3.11 into the time-independent Equation 3.12. Subsequently, solve with a time-independent approximation, such as variation theory.

The result of this section is an equation which relates the absorption cross section to the individual light collecting molecule energy levels and transition dipole moments. In subsequent sections the energy levels and transition dipole moments are approximated. Then, they are substituted back into the equation derived in this section to complete the absorption spectrum model.

4.1 Time-Dependent Approximation

Treat the Hamiltonian as a portion independent of time and a perturbation that depends on time.

$$\left(\hat{H}_o + \hat{H}'(t)\right)\Psi = i\hbar\frac{\partial}{\partial t}\Psi \tag{4.1}$$

In Equation 4.1 the Hamiltonian $\hat{H}_o$ is exactly the time-independent Schrödinger equation Hamiltonian.

$$\hat{H}_o\psi_n = E_n\psi_n \tag{4.2}$$

Use the eigenfunctions of Equation 4.2 as a complete basis set to expand the time-dependent solution.

$$\Psi = \sum_n \left(a_n(t) e^{-jE_n t/\hbar} \right)\psi_n \tag{4.3}$$

Equation 4.3 is exactly the time-dependent state function when the coefficients $a_n(t)$ are known. To find them, substitute Equation 4.3 into Equation 4.1, multiply both sides by the complex conjugate of a basis function, and integrate over all space.

$$\sum_n a_n(t) e^{-jE_n t/\hbar}\left\{\langle\psi_m|\hat{H}_o|\psi_n\rangle + \langle\psi_m|\hat{H}'|\psi_n\rangle\right\} = i\hbar\sum_n \frac{\partial}{\partial t}\left\{a_n(t)e^{-jE_n t/\hbar}\right\}\langle\psi_m|\psi_n\rangle \tag{4.4}$$

The eigenvalues of $\hat{H}_o$ are derived later. The orthonormal property of the eigenfunctions results in $\langle\psi_m|\psi_n\rangle = 0$ for $m \neq n$. Then rearrange so the derivative of the expansion coefficient is on the left side of the equation.

$$\frac{\partial a_m}{\partial t} = -\frac{j}{\hbar}\sum_n a_n \langle \psi_m | \hat{H}' | \psi_n \rangle e^{-jt\frac{(E_n - E_m)}{\hbar}} \tag{4.5}$$

Simplify the notation by defining $H'_{nm}(t) \equiv \langle \psi_m | \hat{H}' | \psi_n \rangle$ and $\omega_{nm} \equiv \frac{(E_n - E_m)}{\hbar}$.

$$\frac{\partial a_m(t)}{\partial t} = -\frac{j}{\hbar}\sum_n a_n(t) H'_{nm}(t) e^{-jt\omega_{nm}} \tag{4.6}$$

Equation 4.6 provides a mathematical approach for finding the coefficients $a_n(t)$ of Equation 4.3. However, it cannot be solved because each coefficient depends on the full integral of all other coefficients. A simplifying approximation assumes that the time-dependent perturbation is sufficiently weak to minimally change the system from its initial state. For electromagnetic radiation with the intensity of normal sunlight, this is a reasonable approximation. In this case set all $a_n(t)$ coefficients on the right side of Equation 4.6 to zero except a single coefficient. Call this nonzero coefficient the initial state, $a_i(t)$, and set its value equal to unity.

$$\frac{\partial a_m(t)}{\partial t} = -\frac{j}{\hbar} H'_{im}(t) e^{-jt\omega_{im}} \tag{4.7}$$

Integrate Equation 4.7 to find a solution for $a_m(t)$.

$$a_m(t) = -\frac{j}{\hbar}\int_0^t H'_{im}(t') e^{-jt'\omega_{im}} dt' \tag{4.8}$$

Equation 4.8 describes the time evolution of the coefficients of Equation 4.3. In an experiment measuring the energy of the system, the probability of finding the system in

one of the time-independent states ψ_m, with energy E_m, is $|a_m(t)|^2$. Examples of an experiment to measure this probability are absorption spectroscopy or Raman scattering.

Next the appropriate time-dependent perturbation $\hat{H}'(t)$ for the application under consideration is required. For electromagnetic radiation the Hamiltonian consists of the electric field vector potential, along with a time and space dependent periodic component [47]. The position vector $\vec{r}$ is a quantum mechanical operator. The arrow indicates a vector operator.

$$\hat{H}'(t) = \frac{-e}{2m}\left\{e^{j(\vec{k}\cdot\vec{r}-\omega t)} + e^{-j(\vec{k}\cdot\vec{r}-\omega t)}\right\}\vec{A}_o \cdot \vec{p} \tag{4.9}$$

Expand the complex exponentials of Equation 4.9 into a Taylor series.

$$e^{j\vec{k}\cdot\vec{r}} = 1 + j\vec{k}\cdot\vec{r} + \frac{1}{2}\left(j\vec{k}\cdot\vec{r}\right)^2 + \cdots \tag{4.10}$$

Simplify by keeping only the first term of Equation 4.10. This simplification is justified because the wavelength of visible light is long compared to the size of a molecule. For example, the highest frequency visible light, in the deep purple range, has a wavelength of, say, 413 nm. An atom has dimensions of less than one nanometer. Therefore, to a molecule, the radiation appears as if it is a constant in space. Substitute the first term of Equation 4.10 into Equation 4.9. Also, write Equation 4.9 in the form of $H'_{im}(t')$ by treating as an operator on the state function ψ_m.

$$H'_{im}(t') = \frac{-e}{2m}\left\{e^{j\omega t} + e^{-j\omega t}\right\}\left\langle \psi_m \left| \vec{A}_o \cdot \vec{p} \right| \psi_i \right\rangle \tag{4.11}$$

Write the dipole operator as the product of the electromagnetic frequency with a dipole operator [47].

$$\langle \psi_m | \vec{p} | \psi_i \rangle = \frac{-jm\omega_{mi}}{e} \langle \psi_m | \vec{\mu} | \psi_i \rangle \tag{4.12}$$

Also, apply a well-known relationship between the vector potential and electric field.

$$\vec{A}_o = \frac{-\vec{E}_o}{\omega} \tag{4.13}$$

Substitute Equation 4.12 and Equation 4.13 into Equation 4.11.

$$H'_{im}(t') = \frac{-j\omega_{mi}}{2\omega} \left\{ e^{j\omega t} + e^{-j\omega t} \right\} \langle \psi_m | \vec{E}_o \cdot \vec{\mu} | \psi_i \rangle \tag{4.14}$$

Now place the resulting time-dependent perturbation Hamiltonian, Equation 4.14, into the equation for the time-dependent coefficients, Equation 4.8.

$$a_m(t) = -\frac{\omega_{mi}}{2\omega\hbar} \langle \psi_m | \vec{E}_o \cdot \vec{\mu} | \psi_i \rangle \int_0^t \left\{ e^{j(\omega_{mi}-\omega)t'} + e^{j(\omega_{mi}+\omega)t'} \right\} dt' \tag{4.15}$$

The integral of Equation 4.15 is easy to compute.

$$a_m(t) = \frac{j\omega_{mi}}{2\omega\hbar} \langle \psi_m | \vec{E}_o \cdot \vec{\mu} | \psi_i \rangle \left[\frac{e^{j(\omega+\omega_{mi})t} - 1}{\omega + \omega_{mi}} - \frac{e^{-j(\omega-\omega_{mi})t} - 1}{\omega - \omega_{mi}} \right] \tag{4.16}$$

Because of the possible singularity in the denominator of Equation 4.16, one of the two terms dominates the probability $|a_m(t)|^2$. This is the resonant electromagnetic energy. The $\omega = \omega_{mi}$ case corresponds to excitation from state ψ_i to ψ_m. The $\omega = -\omega_{mi}$

case corresponds to excitation from state ψ_m to ψ_i. Select the $\omega = \omega_{mi}$ case and compute the magnitude squared of $a_m(t)$. This provides the probability of find the system in a state with energy E_m, given an initial state with energy E_i.

$$|a_m(t)|^2 = \frac{\omega_{mi}^2}{4\omega^2\hbar^2}\left|\langle\psi_m|\vec{E}_o\cdot\vec{\mu}|\psi_i\rangle\right|^2 \frac{\sin^2\left(\frac{(\omega-\omega_{mi})t}{2}\right)}{\left(\frac{\omega-\omega_{mi}}{2}\right)^2} \tag{4.17}$$

In a typical absorption experiment the length of time the system is exposed to radiation is long in comparison to the time scale of atomic transitions. In the limit as time goes to infinity, the sine term approaches a delta discontinuity. The transition rate r_{im} is equal to $|a_m(t)|^2$ divided by time. Also, separate the electric field out of the matrix element because it is a constant.

$$r_{im} = \frac{\left|\vec{E}_o\cdot\langle\psi_m|\vec{\mu}|\psi_i\rangle\right|^2}{4\hbar^2}\delta(\omega-\omega_{mi}) \tag{4.18}$$

Equation 4.18 is convenient to use because the two required values can be mathematically determined, or at least approximated, with decent accuracy. First, the energy difference between the final state ψ_m and the initial state ψ_i is required. This is the ω_{mi} component, since $\omega_{mi} \equiv (E_m - E_i)/\hbar$. These energies are computed with the time-independent Schrödinger equation, and, in the case of this research with the variation approximation, Equation 3.24. Second, the matrix element $\langle\psi_m|\vec{\mu}|\psi_i\rangle$ is required. States ψ_m and ψ_i must be calculated. In many cases, and in the case of this

research, a solution of $\langle \psi_m | \vec{\mu} | \psi_i \rangle$ can be found without having to know the states explicitly. Equation 4.18 does not, however, relate directly to any specific system. More work is required to get to an equation which relates experimental quantities. The two experiments of interest for this research are absorption and resonance Raman scattering. Before deriving the equations for these experiments, an approximation enabling separation of nuclear and electronic properties is required.

4.2 Born-Oppenheimer Approximation

Spectroscopic experiments, for example, an absorption experiment, show the spectra of many systems to consist of several detail scales. At a wide frequency scale, viewing the result of stimulation with a broad range of incident frequency light, a set of peaks appear and each is consistent with the frequency spacing given by Equation 4.18. However, the peaks do not take the shape of delta functions according to Equation 4.18. Instead they are slowly varying functions of frequency. Some of this smoothing effect is due to environmental effects such as solvent interaction and translational speed variations. When the environmental effects are accounted for, a second set of peaks surrounding the original peaks become visible in the spectral result. Furthermore, at even tighter resolution a third set of peaks surround each of the second set of peaks.

The reason for this phenomenon is atomic nuclei are more massive than electrons by a factor of nearly two thousand. Quantum theory shows that larger mass leads to tighter spaced energy levels. This property simplifies the spectroscopy problem into two problems. First, pretend the nuclei are stationary and calculate the electronic energy

levels. Then, use the electronic energy level information to calculate the energy for nuclear motion. The nuclear energy levels display multiple further resolutions and these are approximated as vibrational and rotational energy, respectively. Separating the problem in this manner is called the Born-Oppenheimer approximation.

Consider the matrix element $\langle \psi_m | \vec{\mu} | \psi_i \rangle$ of Equation 4.18 written using this approximation. The electronic state ψ_m is a function of the electronic coordinates r and depends parametrically on the nuclear coordinates Q_j, with $j = 1,\ldots,3P-6$. A polyatomic molecule with P atoms and $3P-6$ vibrational coordinates is assumed. This state function can be rewritten as the product of a function dependent on the electronic coordinates $\psi_m(r;\{Q_j\})$ and a function dependent on the nuclear coordinates $\chi_{\upsilon_j}^{(m)}(Q_j)$. The notation $\{Q_j\}$ indicates parametric dependence on the complete set of nuclear coordinates $j = 1,\ldots,3P-6$. The subscript υ_j indicates the quantum number associated with coordinate Q_j. Each fixed set of nuclear positions is a different value for the set of Q_k. Writing in terms of nuclear coordinates in this manner is related to the harmonic oscillator approximation for vibrational energy. Drop the vector nature of $\vec{\mu}$ in $\langle \psi_m | \vec{\mu} | \psi_i \rangle$ and treat as one component of the direction.

$$\langle \psi_m | \hat{\mu} | \psi_i \rangle = \left\langle \psi_m(r;\{Q_j\}) \Pi_{k=1}^{3P-6} \chi_{\upsilon_k}^{(m)}(Q_k) \middle| \hat{\mu} \middle| \psi_i(r;\{Q_j\}) \Pi_{k'=1}^{3P-6} \chi_{\upsilon_{k'}}^{(i)}(Q_{k'}) \right\rangle \qquad (4.19)$$

Separate the dipole operator into components along the nuclear coordinates and components along the electronic coordinates.

$$= \left\langle \psi_m(r;\{Q_j\}) \Pi_{k=1}^{3P-6} \chi_{\upsilon_k}^{(m)}(Q_k) \middle| \hat{\mu}(Q_1, Q_2 ... Q_{3P-6}) + \mu(r) \right.$$
$$\left. \middle| \psi_i(r;\{Q_j\})) \Pi_{k'=1}^{3P-6} \chi_{\upsilon_{k'}}^{(i)}(Q_{k'}) \right\rangle \tag{4.20}$$

Consider the nuclear component term first.

$$\left\langle \Pi_{k=1}^{3P-6} \chi_{\upsilon_k}^{(m)}(Q_k) \middle| \left\{ \hat{\mu}(Q_1, Q_2 ... Q_{3P-6}) \left\langle \psi_m(r;\{Q_j\}) \middle| \psi_i(r;\{Q_j\}) \right\rangle \right\} \middle| \Pi_{k'=1}^{3P-6} \chi_{\upsilon_{k'}}^{(i)}(Q_{k'}) \right\rangle \tag{4.21}$$

Because eigenvectors are chosen orthogonal, the inner product is zero.

$$\left\langle \psi_m(r;\{Q_j\}) \middle| \psi_i(r;\{Q_j\}) \right\rangle = 0 \tag{4.22}$$

Now consider the electronic component.

$$\left\langle \psi_m \middle| \hat{\mu} \middle| \psi_i \right\rangle = \left\langle \Pi_{k=1}^{3P-6} \chi_{\upsilon_k}^{(m)}(Q_k) \middle| \left\langle \psi_m(r;\{Q_j\}) \middle| \hat{\mu}(r) \middle| \psi_i(r;\{Q_j\}) \right\rangle \middle| \Pi_{k'=1}^{3P-6} \chi_{\upsilon_{k'}}^{(i)}(Q_{k'}) \right\rangle \tag{4.23}$$

The electronic terms is parametrically a function of the nuclear coordinates and cannot be separated from the nuclear term inner product. Define a nuclear dipole matrix element.

$$\mu_{m,i}(Q_1, Q_2 ... Q_{3P-6}) = \left\langle \psi_m(r;\{Q_j\}) \middle| \hat{\mu}(r) \middle| \psi_i(r;\{Q_j\}) \right\rangle \tag{4.24}$$

Rewrite Equation 4.23 using this new defined term.

$$\left\langle \psi_m \middle| \hat{\mu} \middle| \psi_i \right\rangle = \left\langle \Pi_{k=1}^{3P-6} \chi_{\upsilon_k}^{(m)}(Q_k) \middle| \mu_{a,b}(Q_1, Q_2 ... Q_{3P-6}) \middle| \Pi_{k'=1}^{3P-6} \chi_{\upsilon_{k'}}^{(m)}(Q_{k'}) \right\rangle \tag{4.25}$$

Expand Equation 4.25 with a Taylor series expansion. Define $\mu_{m,i}^{(j)}$ as the partial derivative with respect to the normal coordinate at geometry of interest. So this means $\mu_{m,i}^{(j)} \equiv \left(\partial \mu_{m,i} / \partial Q_j\right)_o$.

$$= \mu^{o}_{m,i} \left\langle \Pi^{3P-6}_{k=1} \chi^{(m)}_{\upsilon_k}(Q_k) \middle| \Pi^{3P-6}_{k'=1} \chi^{(i)}_{\upsilon_{k'}}(Q_{k'}) \right\rangle + \\ \Sigma^{3P-6}_{j=1} \mu^{(j)}_{m,i} \left\langle \Pi^{3P-6}_{k=1} \chi^{(m)}_{\upsilon_k}(Q_k) \middle| Q_j \middle| \Pi^{3P-6}_{k'=1} \chi^{(i)}_{\upsilon_{k'}}(Q_{k'}) \right\rangle + \cdots \tag{4.26}$$

Approximate by keeping the first term. This called the Condon approximation.

$$= \mu^{o}_{m,i} \left\langle \Pi^{3P-6}_{k=1} \chi^{(m)}_{\upsilon_k}(Q_k) \middle| \Pi^{3P-6}_{k'=1} \chi^{(i)}_{\upsilon_{k'}}(Q_{k'}) \right\rangle \tag{4.27}$$

For notational convenience write the product using only the quantum number υ_i. Also, factor the inner products into common coordinates Q_i. Each $\left\langle \upsilon^{(m)}_k \middle| \upsilon^{(i)}_k \right\rangle$ is called a Franck-Condon term.

$$= \mu^{o}_{m,i} \Pi^{3P-6}_{k=1} \left\langle \upsilon^{(m)}_k \middle| \upsilon^{(i)}_k \right\rangle \tag{4.28}$$

Similarly, apply the Born-Oppenheimer approximation to enable separating the energy levels (where $\omega_{mi} = E_{mi}/\hbar$) of Equation 4.18. Approximate the nuclear motion as a solution to the harmonic oscillator potential energy system.

$$E = E^{(electronic)}_{mi} + \sum\nolimits_{k=1}^{3P-6} \left(\upsilon_k + \frac{1}{2} \right) \hbar \omega_k \tag{4.29}$$

Figure 4.1 shows a graphical representation of the Born-Oppenheimer approximation. The energy spacing $E^{(electronic)}_{mi}$ is also known as the 0-0 energy.

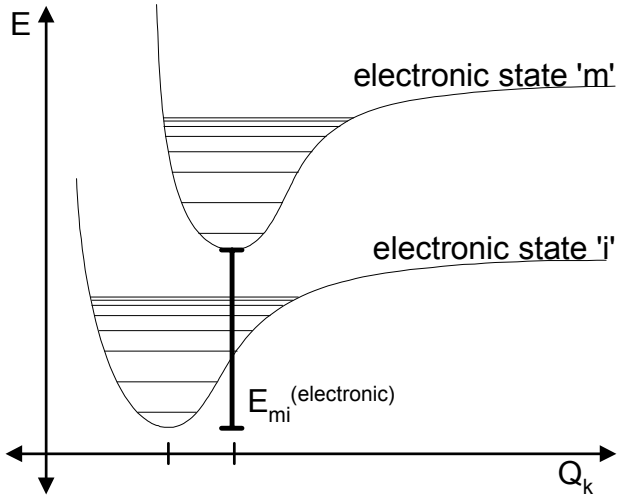

Figure 4.1. Born-Oppenheimer approximation.

The lower curve is the electronic energy E_i and is plotted as a function of the internuclear distances for a particular coordinate Q_k. The upper curve is the electronic energy E_m along the same coordinates. The energy difference $E_{mi}^{(electronic)}$ is spacing of these two curves. The horizontal lines within the electronic potential energy curves are the vibrational energy levels $\left(\upsilon_k + \frac{1}{2}\right)\hbar\omega_k$. Figure 4.1 shows the spacing of these energy levels with the more physically accurate tightening of energy differences for higher energy levels.

Typical vibrational energy level spacing is on the order of 1000 cm^{-1}. Thermal energy is approximately 202 cm^{-1}. Although in a statistical mechanical sense, non-ground vibrational states are populated for the initial state, it is approximated in this research that none are populated. Therefore, vibrational quantum numbers for all normal modes are set to zero for the ground state in this research.

$$\left\langle \psi_m \left| \hat{\mu} \right| \psi_i \right\rangle = \mu_{m,i}^{o} \Pi_{k=1}^{3P-6} \left\langle \upsilon_k^{(m)} = 0 \middle| \upsilon_k^{(i)} \right\rangle \tag{4.30}$$

4.3 Absorption Experiment Relationship

Experiments show the attenuation of an electromagnetic signal when propagating through a liquid material is proportional to the distance d through the material and the concentration C of the material. This is called Beer's law.

$$A = \varepsilon d C \tag{4.31}$$

The molar absorbtivity ε is a unique property of the material. It connects to the dipole matrix element using Equation 4.23 [47].

$$\left|\langle \psi_m | \vec{\mu} | \psi_i \rangle\right|^2 = \frac{6\varepsilon_o \hbar^2 2303c}{N_A h n} \int_{band} \frac{\varepsilon(\nu)}{\rho(\nu)\nu} d\nu \tag{4.32}$$

Approximate the molar absorbtivity as constant over a narrow band of incident frequency light.

$$\rho(\nu)\left|\langle \psi_\nu | \vec{\mu} | \psi_i \rangle\right|^2 = \frac{6\varepsilon_o \hbar^2 2303c}{N_A h n} \frac{\varepsilon(\nu)}{\nu} \tag{4.33}$$

Equation 4.33 provides a useful approximation relating the absorption spectrum to the transition matrix elements $\langle \psi_\nu | \vec{\mu} | \psi_i \rangle$ and density of states $\rho(\nu)$.

4.4 Absorption Experiment with Vibrational Levels Included

An absorption experiment with sufficient resolution to measure the detail of vibrational energy level differences measures the absorption cross-section [47], Equation 4.34. In Equation 4.34 the initial electronic energy level is indicated with a g to denote the ground state. The final electronic energy level is indicated with an e to denote the excited state. Previously the letters used were i (for initial state) and m (for one of many final states) were used, respectively.

$$\sigma_A(\omega_o) = \frac{4\pi^2\left(\mu_{ge}^o\right)^2\omega_o}{3cn\hbar}\sum_m \frac{\Gamma}{\pi}\frac{\Pi_{k=1}^{3P-6}\left|\left\langle 0_k^{(g)}\middle|\upsilon_k^{(e)}(m)\right\rangle\right|^2}{\left(\omega_{eg}+\omega_{\upsilon(m),0}-\omega_o\right)^2+\Gamma^2} \tag{4.34}$$

The initial vibrational state is chosen with all quanta equal to zero. The excited vibrational states are on the excited electronic state potential energy curve, Figure 4.1. The summation over m indicates a summation over a set of quantum numbers, one for each of the $3P-6$ normal modes $\{\upsilon_1(m),\upsilon_2(m),\ldots,\upsilon_{3P-6}(m)\}$. The summation runs from $m=0$, corresponding to quantum numbers $\{0,0,\ldots,0\}$ to $m=\infty$ and therefore corresponding to a summation over all possible values of the quantum numbers. Each vibrational state along the excited state potential energy curve corresponds to an index m.

The denominator term $\omega_{\upsilon(m),0}$ is the radial frequency difference between the vibrational energy level on the excited electronic state potential energy surface and the vibrational energy level on the ground electronic state potential energy surface.

$$\omega_{\upsilon(m),0} = \sum_{k=1}^{3P-6}\left(\upsilon_k(m)+\frac{1}{2}\right)\omega_k^{(e)} - \sum_{k=1}^{3P-6}\frac{1}{2}\omega_k^{(g)} \tag{4.35}$$

It is a reasonable approximation for the molecules of this research that the vibrational frequencies of the excited and ground potential energy surface are equivalent. In this case the $1/2$ scaled quantities cancel.

$$\omega_{\upsilon(m),0} = \sum_{k=1}^{3P-6}\upsilon_k(m)\omega_k^{(e)} \tag{4.36}$$

The Franck-Condon factors in the numerator of Equation 4.34 have an explicit form when the potential energy curves are harmonic, have the same frequency, and the initial state is all normal modes in the ground. These are acceptable approximations for the system studied.

$$\left|\left\langle \upsilon^{(g)}=0\middle|\upsilon^{(e)}\right\rangle\right|^2 = \frac{1}{\upsilon!}\left(\frac{\Delta^2}{2}\right)^{\upsilon} e^{\frac{-\Delta^2}{2}} \tag{4.37}$$

The spacing term Δ is the shift in equilibrium position between the excited and ground electronic potential energy surfaces. This quantity is dimensionless.

$$\Delta \equiv \sqrt{\frac{\mu\omega}{\hbar}}\left|R_{eq,g} - R_{eq,e}\right| \tag{4.38}$$

Substitute Equation 4.37 into Equation 4.34. The resulting equation provides a model of the absorption spectrum due to excitation between a single ground state and a set of vibrational states along a single excited electronic state potential. A spectrum is modeled given the shift in equilibrium position along each normal mode (Δ_k), the vibrational quantum number for each excited vibration state along each normal mode

($\upsilon_k(m)$), the energy of each electronic and vibrational level (ω_{eg} and ω_k), the lifetime parameter (Γ), and the electronic energy Condon term (μ_{ge}^o), along with the incident frequency (ω_o).

$$\sigma_A(\omega_o) = \frac{4\pi^2 \omega_o \left(\mu_{ge}^o\right)^2}{3cn\hbar} \sum_m \frac{\Gamma}{\pi} \frac{\Pi_{k=1}^{3P-6} \frac{1}{\upsilon_k(m)!} \left(\frac{\Delta_k^2}{2}\right)^{\upsilon_k(m)} e^{-\frac{\Delta_k^2}{2}}}{\left(\omega_{eg} + \sum_{k=1}^{3P-6} \upsilon_k(m)\omega_k - \omega_o\right)^2 + \Gamma^2} \tag{4.39}$$

4.5 Resonance Raman Experiment Relationship

Scattering is a phenomenon that results from taking Equation 4.6 one step further. The molecule dynamically polarizes due to the incident electromagnetic field. Scattering is a two-photon effect. The system is excited into a final energy state through an intermediate state with a simultaneous process. A polarizability coupling element for scattering, similar to the dipole coupling element $\langle \psi_m | \vec{\mu} | \psi_i \rangle$ for absorption is required. Derive by utilizing the first order time-dependent state function approximation.

$$\langle \Psi_i(t) | \vec{\mu} | \Psi_f(t) \rangle = e^{-i\omega_{if}t} \left(\mu_{if}(perm) + \mu_{if}(induced)\right) \tag{4.40}$$

For the state function coefficients, start with Equation 4.15 except indicate the initial state k as part of the coefficient notation. Also, the delta function is for the case when $m = k$.

$$a_m^{(k)}(t) = \delta_{mk} + \frac{j\vec{E}_o \cdot \langle \psi_m | \vec{\mu} | \psi_k \rangle}{2\hbar} \int_0^t \left\{ e^{j(\omega_{mk} - \omega)t'} + e^{j(\omega_{mk} + \omega)t'} \right\} dt' \tag{4.41}$$

Substitute Equation 4.41 into Equation 4.3.

$$\Psi_k = e^{-j\omega_k t}\left\{\psi_k + \sum_{m\neq k}\psi_m\left(\frac{j\vec{E}_o\cdot\langle\psi_m|\vec{\mu}|\psi_k\rangle}{2\hbar}e^{-j\omega_{mk}t}\int_0^t\left\{e^{j(\omega_{mk}-\omega)t'}+e^{j(\omega_{mk}+\omega)t'}\right\}dt'\right)\right\} \quad (4.42)$$

Substitute Equation 4.42, with $k = i$ and with $k = f$ into Equation 4.40. The first term is the permanent dipole , $\mu_{if}(perm)$, and is not associated with Raman scattering. The second-order term proportional to the square of the electric field is dropped. The remaining cross terms have two components.

$$\begin{aligned}&\langle\Psi_i(t)|\vec{\mu}|\Psi_f(t)\rangle_{induced} = \\ &\sum_{m\neq f}\langle\psi_i|\vec{\mu}|\psi_m\rangle\frac{j\vec{E}_o\cdot\langle\psi_m|\vec{\mu}|\psi_f\rangle}{2\hbar}e^{-j\omega_{mf}t}\int_0^t\left\{e^{j(\omega_{mf}-\omega)t'}+e^{j(\omega_{mf}+\omega)t'}\right\}dt' + \\ &\sum_{m\neq i}\langle\psi_m|\vec{\mu}|\psi_f\rangle\frac{j\vec{E}_o\cdot\langle\psi_i|\vec{\mu}|\psi_m\rangle}{2\hbar}e^{j\omega_{mi}t}\int_0^t\left\{e^{-j(\omega_{mi}-\omega)t'}+e^{-j(\omega_{mi}+\omega)t'}\right\}dt'\end{aligned} \quad (4.43)$$

Selecting the subset not associated with the electric field results in a form for the induced dipole that can be interpreted as a polarizability value.

$$\begin{aligned}&\langle\Psi_i(t)|\vec{\mu}|\Psi_f(t)\rangle_{induced} = \\ &\sum_{m\neq f}\vec{\mu}_{im}\vec{\mu}_{mf}\frac{j}{2\hbar}e^{-j\omega_{mf}t}\int_0^t\left\{e^{j(\omega_{mf}-\omega)t'}+e^{j(\omega_{mf}+\omega)t'}\right\}dt' + \\ &\sum_{m\neq i}\vec{\mu}_{mf}\vec{\mu}_{im}\frac{j}{2\hbar}e^{j\omega_{mi}t}\int_0^t\left\{e^{-j(\omega_{mi}-\omega)t'}+e^{-j(\omega_{mi}+\omega)t'}\right\}dt'\end{aligned} \quad (4.44)$$

The polarizability is physically observable and therefore must satisfy a Hermitian property, $\alpha_{if} = \alpha_{fi}^{*}$. Selecting the first integral term out of each summation results in a polarizability that satisfies this requirement.

$$\left\langle \Psi_i(t)\left|\vec{\mu}\right|\Psi_f(t)\right\rangle_{(induced,subset)} = \sum_{m\neq f}\vec{\mu}_{im}\vec{\mu}_{mf}\frac{j}{2\hbar}e^{-j\omega_{mf}t}\int_0^t e^{j(\omega_{mf}+\omega)t'}dt' + \sum_{m\neq i}\vec{\mu}_{mf}\vec{\mu}_{im}\frac{j}{2\hbar}e^{j\omega_{mi}t}\int_0^t e^{-j(\omega_{mi}-\omega)t'}dt' \tag{4.45}$$

Integrate Equation 4.45. Drop the portion that depends on $e^{\pm j\omega_{mk}t}$ since only the electric field portion is important. Define the polarizability.

$$\vec{\alpha}_{if} \equiv \frac{1}{2\hbar}\sum_{m\neq f}\frac{\vec{\mu}_{im}\vec{\mu}_{mf}}{\omega_{mf}+\omega} + \frac{1}{2\hbar}\sum_{m\neq i}\frac{\vec{\mu}_{mf}\vec{\mu}_{im}}{\omega-\omega_{mi}} \tag{4.46}$$

Now compute the three dimensional matrix dot product with the electric field. The result is written in matrix notation.

$$\begin{bmatrix} \mu_x^{in}\mu_x^{nf} & \mu_x^{in}\mu_y^{nf} & \mu_x^{in}\mu_z^{nf} \\ \mu_y^{in}\mu_x^{nf} & \mu_y^{in}\mu_y^{nf} & \mu_y^{in}\mu_z^{nf} \\ \mu_z^{in}\mu_x^{nf} & \mu_z^{in}\mu_y^{nf} & \mu_z^{in}\mu_z^{nf} \end{bmatrix}\begin{bmatrix} E_x \\ E_y \\ E_z \end{bmatrix} \equiv \left(\mu_{in}\mu_{nf}\right)\cdot\overline{E}_o \tag{4.47}$$

The Raman [47] cross section is shown in Equation 4.48

$$\sigma_R = \frac{8\pi}{3}\left(\frac{1+2\rho}{1+\rho}\right)\left(\left(\frac{d\sigma}{d\Omega}\right)_{//} + \left(\frac{d\sigma}{d\Omega}\right)_{\perp}\right)_{90^o} \tag{4.48}$$

The measured cross section is related to theory by projecting the polarizability along the incident and scattered directions.

$$\left(\frac{d\sigma}{d\Omega}\right)_{s,i} = \frac{\omega_s^3\omega_o}{c^4}\left|\hat{e}_s\cdot\vec{\alpha}_{if\,s,o}(T,\omega_o)\cdot\hat{e}_o\right|^2 \tag{4.49}$$

The polarizability in Equation 4.49 is the Equation 4.46 result. The subscript s,o indicates the orientation terms from Equation 4.47: scattered (s) and incident (o) directions. The unit vectors select the component in the incident and scattered direction.

Direct the incident radiation in the z-direction, and measure the parallel scattering is along the same direction.

$$\left(\frac{d\sigma}{d\Omega}\right)_{//} = \frac{\omega_s^3\omega_o}{c^4}\left|\begin{bmatrix}0 & 0 & 1\end{bmatrix}\begin{bmatrix}\alpha_{XX} & \alpha_{XY} & \alpha_{XZ}\\ \alpha_{YX} & \alpha_{YY} & \alpha_{YZ}\\ \alpha_{ZX} & \alpha_{ZY} & \alpha_{ZZ}\end{bmatrix}\begin{bmatrix}0\\0\\1\end{bmatrix}\right|^2 = \frac{\omega_s^3\omega_o}{c^4}\left|\alpha_{ZZ}\right|^2 \tag{4.50}$$

Measure the perpendicular direction along the x-axis.

$$\left(\frac{d\sigma}{d\Omega}\right)_{\perp} = \frac{\omega_s^3\omega_o}{c^4}\left|\begin{bmatrix}1 & 0 & 0\end{bmatrix}\begin{bmatrix}\alpha_{XX} & \alpha_{XY} & \alpha_{XZ}\\ \alpha_{YX} & \alpha_{YY} & \alpha_{YZ}\\ \alpha_{ZX} & \alpha_{ZY} & \alpha_{ZZ}\end{bmatrix}\begin{bmatrix}0\\0\\1\end{bmatrix}\right|^2 = \frac{\omega_s^3\omega_o}{c^4}\left|\alpha_{XZ}\right|^2 \tag{4.51}$$

Define a depolarization ratio and substitute with Equation 4.50 and Equation 4.51.

$$\rho = \left(\frac{d\sigma}{d\Omega}\right)_{\perp} \Big/ \left(\frac{d\sigma}{d\Omega}\right)_{//} = \frac{\left|\alpha_{XZ}\right|^2}{\left|\alpha_{ZZ}\right|^2} \tag{4.52}$$

The resulting cross section from using Equation 4.48, Equation 4.50, and Equation 4.52 in Equation 4.43.

$$\sigma_R = (1+2\rho)\frac{8\pi}{3c^4}\left|\alpha_{ZZ}\right|^2 \tag{4.53}$$

These directions are in the lab frame but theory can only give polarizability in the molecule frame of reference [47].

$$\sigma_R = (1+2\rho)\frac{8\pi\omega_s^3\omega_o}{3c^4}\left\{\begin{array}{l}\frac{1}{9}\left|\alpha_{xx}+\alpha_{yy}+\alpha_{zz}\right|^2 + \\ \frac{2}{15}\left[\frac{1}{2}\left(\left|\alpha_{xy}+\alpha_{yx}\right|^2+\left|\alpha_{xz}+\alpha_{zx}\right|^2+\left|\alpha_{yz}+\alpha_{zy}\right|^2\right)+\right. \\ \left.\frac{1}{3}\left(\left|\alpha_{xx}-\alpha_{yy}\right|^2+\left|\alpha_{xx}-\alpha_{zz}\right|^2+\left|\alpha_{yy}-\alpha_{zz}\right|^2\right)\right]\end{array}\right\} \tag{4.54}$$

Assume that the α_{yy} polarization in the molecule frame is active. This results in $\rho = \frac{1}{3}$ and simplifies the terms on the right of Equation 4.54.

$$\sigma_R = \frac{8\pi\omega_s^3\omega_o}{9c^4}\left|\alpha_{yy}\right|^2 \tag{4.55}$$

Substitute into Equation 4.54. Transition dipoles are no longer vectors because they are in the molecule y-direction only.

$$\sigma_R = \frac{4\pi\omega_s^3\omega_o}{9\hbar c^4}\left|\sum_{m\neq f}\frac{\mu_{im}\mu_{mf}}{\omega_{mf}+\omega_o}+\sum_{m\neq i}\frac{\mu_{mf}\mu_{im}}{\omega_o-\omega_{mi}}\right|^2 \tag{4.56}$$

The Born-Oppenheimer approximation provides further simplification. Let the initial and final states be on the same electronic potential energy curve. The intermediate state is at an excited electronic potential energy curve. For resonance Raman, just keep the second term in Equation 4.56 since it is large in comparison to the first term. Also, take the term which is due to the Condon approximation in the Born-Oppenheimer approximation. This is called the Albrecht A term. The subscripts on the cross section, $\sigma_{R,A}$, indicate Raman cross section and for Albrecht A term only. The summation over

m indicates a summation over a set of quantum numbers, one for each of the $3P-6$ normal modes: $\{\upsilon_1(m),\upsilon_2(m),\ldots,\upsilon_{3P-6}(m)\}$.

$$\sigma_{R,A}=\frac{4\pi\omega_s^3\omega_o}{9\hbar c^4}\left(\mu_{ge}^o\right)^4\left|\sum_{m\neq f}\frac{\Pi_{k=1}^{3P-6}\left|\left\langle\upsilon_k^{(g)}(m)\middle|\upsilon_k^{(e)}(m)\right\rangle\right|^2}{\omega_o-\omega_{mg}+j\Gamma}\right|^2 \tag{4.57}$$

Note that $\omega_{mg}=\omega_{eg}+\sum_{k=1}^{3P-6}\upsilon_k(m)\omega_k$ because the excited and ground potential energy surfaces are approximated to have the same fundamental frequency and the initial ground electronic vibrational state is the all zero state. All vibrational quantum numbers for the vibrational state of the initial state are zero.

Substitute Equation 4.37 into Equation 4.57. Multiply by -1 to cast the denominator in the same form as for the absorption case, Equation 4.39. This makes no difference because the quantity is squared.

$$\sigma_{R,A}(\omega_o)=\frac{4\pi\omega_s^3\omega_o}{9\hbar c^4}\left(\mu_{ge}^o\right)^4\left|\sum_{m\neq f}\frac{\Pi_{k=1}^{3P-6}\frac{1}{\upsilon_k(m)!}\left(\frac{\Delta_k^2}{2}\right)^{\upsilon_k(m)}e^{\frac{-\Delta_k^2}{2}}}{\left(\omega_{eg}+\sum_{k=1}^{3P-6}\upsilon_k(m)\omega_k-\omega_o\right)-j\Gamma}\right|^2 \tag{4.58}$$

Equation 4.39 and Equation 4.58 are the key results of this section. These equations provide a means to mathematically calculate the spectra for comparison against experiment, after the new energy levels and transition dipole moments are modeled according to theory derived in the next several sections. The equations differ from each other in several ways. Absorption scales linearly with frequency. Resonance Raman includes a cubic term of the scattered frequency. Absorption follows the second power of

μ_{ge}^{o} whereas resonance Raman follows the fourth power of μ_{ge}^{o}. Resonance Raman squares the sum of the vibrational scattering terms. Therefore, multiple cross-terms appear in the spectrum. Absorption includes each term only once, with no additional terms appearing due to the squaring operation.

Equation 4.39 is applied later in the thesis to explore the impact of vibrational states on the energy and spread of an absorption experiment. Equation 4.58 is not as useful because of the many approximations required to get this simple form. Raman effects can be characterized qualitatively.

5.0 System Description and Deconstruction

The investigated system is a small molecule in close proximity to a relatively large semiconducting material. Notation is defined in Figure 5.1. The semiconductor is represented by sixteen nuclei and sixteen electrons in this figure. The actual studied semiconductor nanoparticle contains millions of nuclei and electrons. The molecule is represented by four nuclei and four electrons. The actual studied molecules have anywhere from ten to hundreds of nuclei and perhaps an order of magnitude more electrons. A small number of particles are shown in Figure 5.1 so that key equations are easy to introduce and define notation. The theory derived in this thesis uses the full number of electrons and nuclei in the system.

A position vector points from an arbitrary origin to one of the particles. Figure 5.1 shows four representative position vectors connecting the origin to each type of particle. Semiconductor nuclei are indexed with the symbol 'α'. Molecule nuclei are index with the symbol 'β'. Semiconductor electrons are indexed with the letter 'a'. Molecule electrons are index with the letter 'b'.

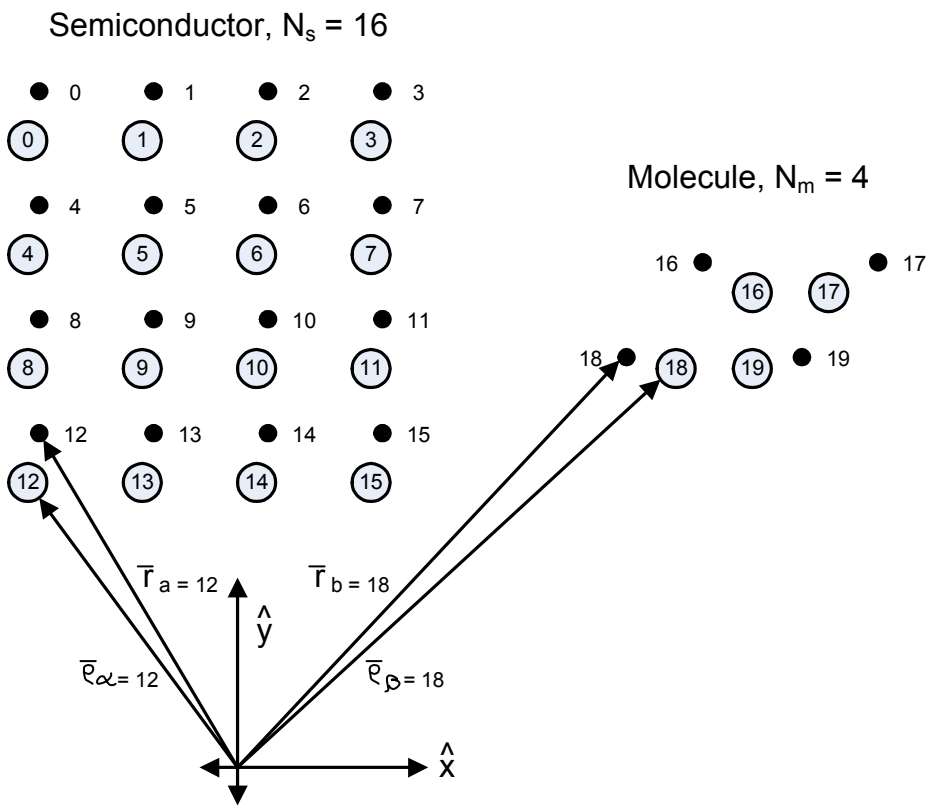

Figure 5.1. Representative geometry of system.

The system Hamiltonian provides a means to find all physically measurable properties according to Equation 3.12 and Equation 3.24. The Hamiltonian shown in Equation 3.14 is for a single particle in one-dimensional space. The system of Figure 5.1, and, furthermore, the full system studied, consists of many particles. Organize the resulting Hamiltonian into common sets, according to how each set operates on the state function coordinates.

1. Semiconductor electronic energy.
2. Molecule electronic energy.
3. Semiconductor and molecule nuclei energy.
4. Electronic coupling energy.

This partition organizes the Hamiltonian into parts that operate individually on the molecule and semiconductor and parts that operate collectively on the semiconductor and molecule. The first two sets are the individual semiconductor and molecule Hamiltonians. The third set is justified based on the Born-Oppenheimer approximation. Semiconductor and molecule nuclear energy are separated so they can be initially neglected. The coupling investigated in this research is in the fourth set. Each is described next.

The first set, semiconductor electronic energy, itself consists of three subsets of terms. The first subset term, $\hat{H}_{SE}$, is the kinetic energy of the electrons. The summation in Equation 5.1 runs over all electrons in the semiconductor.

$$\hat{H}_{SE} = -\frac{\hbar}{2}\frac{1}{m_{electron}}\sum_{a}\nabla_a^2 \tag{5.1}$$

The second subset term, $\hat{H}_{SE-SN}$, is the potential energy connecting each semiconductor nuclei to each semiconductor electron. The potential energy is weighted by the charge of each nucleus, Z_α.

$$\hat{H}_{SE-SN} = -e^2/4\pi\varepsilon_o \sum_{\alpha}\sum_{a}\frac{Z_\alpha}{|\bar{r}_a - \bar{\rho}_\alpha|} \tag{5.2}$$

The third subset term, $\hat{H}_{SE-SE}$, is the electron coupling energy.

$$\hat{H}_{SE-SE} = e^2/4\pi\varepsilon_o \sum_{a}\sum_{a'>a}\frac{1}{|\bar{r}_a - \bar{r}_{a'}|} \tag{5.3}$$

Similarly, the molecule set also is separated into three subset terms: kinetic energy of electrons, potential energy connecting electrons to nuclei, and electron coupling energy.

$$\hat{H}_{ME} = -\frac{\hbar}{2}\frac{1}{m_{electron}}\sum_{b}\nabla_{b}^{2} \tag{5.4}$$

$$\hat{H}_{ME-MN} = -e^{2}/4\pi\varepsilon_{o}\sum_{\beta}\sum_{b}\frac{Z_{\beta}}{\left|\bar{r}_{b}-\bar{\rho}_{\beta}\right|} \tag{5.5}$$

$$\hat{H}_{ME-ME} = e^{2}/4\pi\varepsilon_{o}\sum_{b}\sum_{b'>b}\frac{1}{\left|\bar{r}_{b}-\bar{r}_{b'}\right|} \tag{5.6}$$

Terms for the kinetic and potential energy of the molecule and semiconductor nuclei are treated separately. It is a reasonable approximation to initially ignore these terms during theoretical development and then add them back into the solution as vibrational energy. This is the Born-Oppenheimer approximation.

$$\hat{H}_{SN} = -\frac{\hbar}{2}\sum_{\alpha}\frac{1}{m_{\alpha}}\nabla_{\alpha}^{2} \tag{5.7}$$

$$\hat{H}_{MN} = -\frac{\hbar}{2}\sum_{\beta}\frac{1}{m_{\beta}}\nabla_{\beta}^{2} \tag{5.8}$$

$$\hat{H}_{SN-SN} = \sum_{\alpha}\sum_{\alpha'>\alpha}\frac{Z_{\alpha}Z_{\alpha'}\,e^{2}/4\pi\varepsilon_{o}}{\left|\bar{\rho}_{\alpha}-\bar{\rho}_{\alpha'}\right|} \tag{5.9}$$

$$\hat{H}_{MN-MN} = \sum_{\beta}\sum_{\beta'>\beta}\frac{Z_{\beta}Z_{\beta'}\,e^{2}/4\pi\varepsilon_{o}}{\left|\bar{\rho}_{\beta}-\bar{\rho}_{\beta'}\right|} \tag{5.10}$$

Finally, four sets of Hamiltonian terms are the coupling energy. The semiconductor nuclei couple to the molecule nuclei through $\hat{H}_{SN-MN}$, the semiconductor electrons couple to the molecule electrons through $\hat{H}_{SE-ME}$, the molecule electrons couple to the semiconductor electrons through $\hat{H}_{ME-SN}$, and the semiconductor electrons couple to the molecule electrons through $\hat{H}_{SE-MN}$.

$$\hat{H}_{SN-MN} = \sum_{\alpha}\sum_{\beta} \frac{Z_\alpha Z_\beta \, e^2/4\pi\varepsilon_o}{\left|\bar{\rho}_\alpha - \bar{\rho}_\beta\right|} \tag{5.11}$$

$$\hat{H}_{SE-ME} = \sum_{a}\sum_{b} \frac{e^2/4\pi\varepsilon_o}{\left|\bar{r}_a - \bar{r}_b\right|} \tag{5.12}$$

$$\hat{H}_{ME-SN} = -\sum_{\alpha}\sum_{b} \frac{Z_\alpha \, e^2/4\pi\varepsilon_o}{\left|\bar{r}_b - \bar{\rho}_\alpha\right|} \tag{5.13}$$

$$\hat{H}_{SE-MN} = -\sum_{\beta}\sum_{a} \frac{Z_\beta \, e^2/4\pi\varepsilon_o}{\left|\bar{r}_a - \bar{\rho}_\beta\right|} \tag{5.14}$$

In summary, the total Hamiltonian is separated into four sets of terms. The individual semiconductor Hamiltonian consists of Equation 5.1, Equation 5.2, and Equation 5.3: $\hat{H}_S = \hat{H}_{SE} + \hat{H}_{SE-SN} + \hat{H}_{SE-SE}$. The individual molecule Hamiltonian consists of Equation 5.4, Equation 5.5, and Equation 5.6: $\hat{H}_M = \hat{H}_{ME} + \hat{H}_{ME-MN} + \hat{H}_{ME-ME}$. The nuclei energy of the individual systems is collected

into a Hamiltonian consisting of Equation 5.7 through Equation 5.10: $\hat{H}_N = \hat{H}_{SN} + \hat{H}_{MN} + \hat{H}_{SN-SN} + \hat{H}_{MN-MN}$. The coupling set is $\hat{V} = \hat{H}_{SN-MN} + \hat{H}_{SE-ME} + \hat{H}_{ME-SN} + \hat{H}_{SE-MN}$

A solution to the Schrödinger equation consisting of either $\hat{H}_S$ in isolation or $\hat{H}_M$ in isolation has well-known approximations. The third Hamiltonian set, $\hat{H}_N$, is initially neglected. The final Hamiltonian set, $\hat{V}$, is responsible for the coupling effects under consideration by this research. It is initially ignored and then treated as a perturbation on the individual semiconductor and molecule electronic energies. A summation of each individual collection of terms results in the total Hamiltonian.

$$\hat{H}_{TOTAL} = \hat{H}_S + \hat{H}_M + \hat{H}_N + \hat{V} \tag{5.15}$$

As much as possible, the letter M represents a quantity related to the molecule and the letter S represents a quantity related to the semiconductor. Summation indices over molecule quantities use a lower-case letter m. Summation indices over semiconductor quantities often use a lower-case letter s. However, other letters, such as the lower-case n, are sometimes also required for semiconductor summation indices.

Next, derive the energy of the molecule and the semiconductor in isolation using $\hat{H}_M$ and $\hat{H}_S$ respectively. These energy levels are the foundation of the model because energy levels for the coupled system utilize individual energies.

5.1 Molecular Electronic Energy

Consider the molecule Hamiltonian $\hat{H}_M$ and temporarily ignore the electron coupling term $\hat{H}_{ME-ME}$ in $\hat{H}_M$.

$$\hat{H}_M^{(ele,0)} = -\frac{\hbar}{2}\frac{1}{m_{electron}}\sum_b \nabla_b^2 - \frac{e^2}{4\pi\varepsilon_o}\sum_\beta\sum_b \frac{Z_\beta}{\left|\bar{r}_b - \bar{\rho}_\beta\right|} \tag{5.16}$$

Factor the summation over electronic coordinates.

$$\hat{H}_M^{(ele,0)} = \sum_b \left[-\frac{\hbar}{2}\frac{1}{m_{electron}}\nabla_b^2 + \sum_\beta \frac{e^2/4\pi\varepsilon_o\, Z_\beta}{\left|\bar{r}_b - \bar{\rho}_\beta\right|} \right] \tag{5.17}$$

The result is a sum of independent terms. The benefit of this factorization is a summation of individual Schrödinger equations. The resulting state function consists of a product of Hamiltonian solutions and each solution is called an orbital. An orbital is a function of the molecule coordinates. Each electron in Equation 5.17 is represented by a different orbital function. For example, $\xi_i^{1181999}$ represents a function ξ_i over the coordinates of electron number 1,181,999. The model developed in this thesis does not require computing the actual orbital functions. These are introduced here and also in Equation 5.30 and Equation 5.31 to demonstrate important simplifications of the model. Subsequently the individual orbitals are not required.

An important property of electrons is that they are indistinguishable. So, although it is mathematically convenient to find and identify electron number 1,181,999, in practice this is an impossible task. Electrons do not appear with numbers attached to

them. For example, exchanging two electrons has no effect on physically measurable properties. Therefore, a product of orbitals is not the correct system solution because the product is sensitive to exchanging electrons. The product $\xi_i^5 \xi_j^{27}$ is not equivalent to the product $\xi_i^{27} \xi_j^5$.

The solution is to include a spin coordinate with the orbital, and write the state function as a Slater determinant of spin-orbitals. Equation 5.18 is a solution in Slater determinant form to a Schrödinger equation with Equation 5.17 as the Hamiltonian. The Slater determinant forms a summation of every electron attached to every spin-orbital, with the sign of each term determined according to the rules of matrix determinant evaluation. In Equation 5.18, a curved overbar indicates a spin-orbital with spin in the opposite direction as a spin-orbital without a curved overbar. The total number of electrons in the system is P.

$$\left|\widetilde{M}\right\rangle = \left|\xi_0^0 \breve{\xi}_0^1 \xi_1^2 \breve{\xi}_1^3 \xi_2^4 \breve{\xi}_2^5 \cdots \xi_{P/2}^{P-2} \breve{\xi}_{P/2}^{P-1}\right| \tag{5.18}$$

The tilde on the state function $\left|\widetilde{M}\right\rangle$ is required to distinguish individual molecule or semiconductor state functions from combined state functions which include both molecule and semiconductor state functions. A tilde always indicates an individual state function or an individual energy.

Equation 5.18 is representative of the molecule state function $\left|\widetilde{M}\right\rangle$. An actual molecule has a very large number of state functions available and they are indexed with a subscript. The state $\left|\widetilde{M}_m\right\rangle$ is one of many state functions. State functions are constructed

by sorting the molecule electrons into various collections of spin-orbitals. For example, the Aufbau procedure of filling spin-orbitals starts with the lowest energy spin-orbital and moves monotonically up through higher energy spin-orbitals.

When electron-electron potential energy, $\hat{H}_{ME-ME}$, is included with Equation 5.16 the spin-orbital solution of Equation 5.18 is not exact. A variety of methods to resolving this problem are available. The exact nature of the method is not important to the present research work. What is necessary is that some method is available. The specific form is not relevant, all that is important is that a molecule state function, or a sufficiently good approximation, is available.

In any case, a set of solutions for $\hat{H}_M$ results in a set of molecule state functions $\left|\widetilde{M}_m\right\rangle$, each with energy $\widetilde{E}_m$. The molecules under consideration in this research absorb visible light for proper solar cell operation. According to Equation 4.16, the molecules must have a set of energy levels separated by energy equal to the source light energy. Figure 5.2 shows typical form of the electronic energy levels for the class of molecules under consideration.

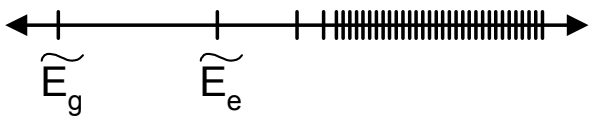

Figure 5.2. Molecule electronic energy level spacing.

In the ground state, $\widetilde{E}_g$, all spin-orbitals are filled with electrons. The energy $\widetilde{E}_g$ is the total molecule energy, not the energy of an individual spin-orbital. The

immediately adjacent energy state is an excited state with one electron excited into the next highest energy spin-orbital. This state has energy defined as $\widetilde{E}_e$. During an absorption process, the energy difference $\widetilde{E}_e - \widetilde{E}_g$ equals the energy of an incident photon. The result is an excitation of the molecule from the ground state $\left|\widetilde{M}_g\right\rangle$ with energy $\widetilde{E}_g$ to an excited state $\left|\widetilde{M}_e\right\rangle$ with energy $\widetilde{E}_e$.

At energies above $\widetilde{E}_e$ many excited states are available. Collect a subset of these states into a set close enough to $\widetilde{E}_e$ such that they also can be excited by the visible spectrum. This collection is denoted $\widetilde{E}_{e_m}$ where $m \in \{1,2,\cdots M\}$. If the incident light spectrum is broad enough to include photons with energy $\widetilde{E}_{e_m} - \widetilde{E}_g$ then these additional states participate in an absorption experiment. Figure 5.2 shows the electronic energy levels for the class of molecules under consideration. In Figure 5.2 a single excited energy level $\widetilde{E}_e$ is available and the next highest energy level is significantly larger in energy. Therefore, the physical model of the molecule approximates a single excited energy level is available to the photon absorption experiment.

5.2 Molecular Vibronic Energy

The terms previously selected for $\hat{H}_M$ are related to electronic interaction. Nuclei interaction is neglected according to the Born-Oppenheimer approximation. So the energy levels shown in Figure 5.2 are electronic energy levels. When the molecule nuclei motion is reintroduced, using Equation 5.8 and Equation 5.10, additional energy levels appear. These energies are small compared to the molecule electronic energy.

Notice in Equation 5.17 the summation over the nuclear coordinates $\sum_{\beta} \frac{e^2/4\pi\varepsilon_o \, Z_\beta}{\left|\bar{r}_b - \bar{\rho}_\beta\right|}$. Although the nuclei are treated as stationary, each set of nuclear coordinates results in a different set of molecule state functions $\left|\widetilde{M}_m\right\rangle$ and energies $\widetilde{E}_m$. So, these quantities are best written as a function of the electronic coordinates, and a parametric function of the nuclear coordinates. Temporarily write the full form of these quantities $\left|\widetilde{M}_m\left(\{\bar{r}_b\};\{\bar{\rho}_\beta\}\right)\right\rangle$ and $\widetilde{E}_m\left(\{\bar{\rho}_\beta\}\right)$ to show the nuclear component explicitly. Vectors in curly brackets denote the complete set of appropriate coordinates.

Nuclear motion is included by solving Equation 5.17 for each possible nuclei position. Calculate the energy. Then, use the electronic energy as a potential energy for a Schrödinger equation over the nuclear coordinates.

$$\hat{H}_M^{(nuc)} = -\frac{\hbar}{2}\sum_{\beta}\frac{1}{m_\beta}\nabla_\beta^2 + \left[\sum_{\beta}\sum_{\beta'>\beta}\frac{Z_\beta Z_{\beta'}\, e^2/4\pi\varepsilon_o}{\left|\bar{\rho}_\beta - \bar{\rho}_{\beta'}\right|} + \widetilde{E}_m\left(\{\bar{\rho}_\beta\}\right)\right] \tag{5.19}$$

The terms in square brackets in Equation 5.19 are treated as a total potential energy for nuclear motion. The internuclear repulsion increases as the nuclei approach each other. The electronic energy increases as the nuclei separate. The combination can sometimes result in a potential energy with minima. Figure 4.1 shows an example potential, $E_{nuc-potential} = \frac{Z_{\beta=0} Z_{\beta=1} e^2 / 4\pi\varepsilon_o}{\left|\overline{\rho}_{\beta=0} - \overline{\rho}_{\beta=1}\right|} + \widetilde{E}_m\left(\{\overline{\rho}_0, \overline{\rho}_1\}\right)$, as a function of the internuclear distance for a single normal coordinate.

Because the shapes of the curves in Figure 4.1 are nearly parabolic around the equilibrium position, an approximate solution to a Schrödinger equation with Equation 4.1 as the Hamiltonian is a harmonic oscillator. The result is additional energy levels near each electronic energy level. These are vibrational energies. Each normal mode contributes a quantum of energy.

The system energy including nuclear motion is a set of energy levels per Equation 4.29. This set of vibronic energy levels is denoted $\widetilde{E}_{e_m}$ where $m \in \{1,2,\cdots M\}$. No notational distinction is made between $m \in \{1,2,\cdots M\}$ for electronic energy levels or $m \in \{1,2,\cdots M\}$ for vibronic energy levels. However, the focus of the research is primarily either a single electronic energy level, $m \in \{1\}$, or a single electronic energy level with a set of vibronic energy levels, $m \in \{1,2,\cdots M\}$. Therefore, the meaning is clear from context.

5.3 Semiconductor Electronic Energy

The other significant subset of the system in Figure 5.1 is the semiconductor. Consider the semiconductor electronic states and energy. When all of the atoms in a semiconductor are widely separated in space, the energy levels are independent. As these isolated atoms converge in space and interact, forming the final structure, the individual energy levels split. Figure 5.3 shows this effect for a silicon crystal [48].

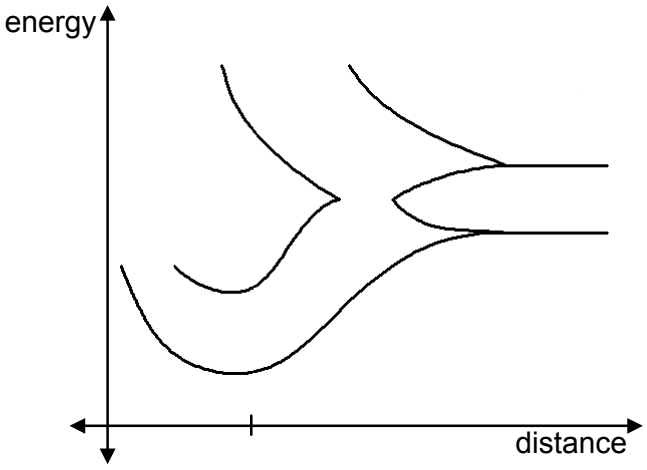

Figure 5.3. Splitting of energy bands in a pure silicon semiconductor.

At the equilibrium distance splitting results in at least two bands of energy. The difference in energy between the highest energy of the lower band and the lowest energy of the upper band is called the bandgap energy. The material is a semiconductor because electrons mostly reside in the lower band of energy. Thermal excitation results in a relatively small number of electrons in the upper band of energy. Electrons in the upper band are available for electrical conduction. The upper band is called the conduction

band. In a solar cell electromagnetic radiation excites electrons into the upper conduction band. For that application a material with a bandgap close to the wavelength of natural sunlight is chosen.

In general, approximations for solving the Schrödinger equation such as separating electron from nuclear motion (Born-Oppenheim approximation), limiting the nature of the electron-to-electron correlation, and separating time and space domains help. For large crystals typical of semiconductors the resulting equation is still intractable. One difficulty is the form of the potential energy in Equation 5.2 for such a large system. This potential energy can be approximated, as shown in Figure 5.4 for the single dimensional case. The potential of Figure 5.4 is called the Kronig-Penny model. It approximates the exact potential with a periodic boxcar function.

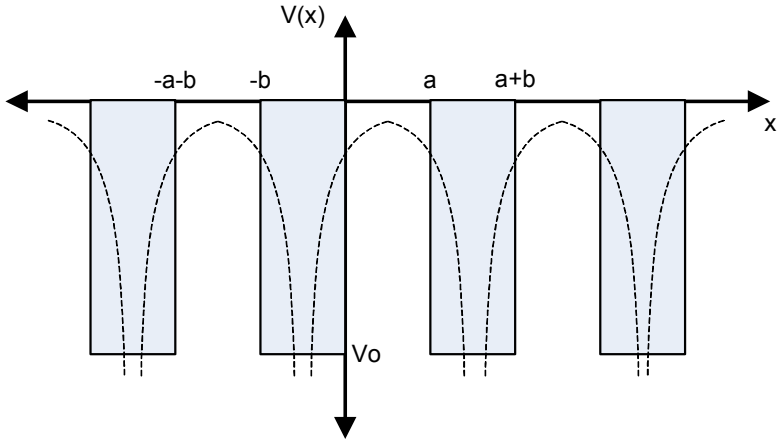

Figure 5.4. Kronig-Penny potential energy model in one dimension.

Substitute the Kronig-Penny potential into the time-independent Schrödinger equation. The resulting solution has a general form called the Bloch state function.

Equation 5.20 shows the form of the resulting state function for a one-dimensional crystal.

$$\left|\widetilde{S}_k\right\rangle = u_k(x)e^{jk\cdot x} \tag{5.20}$$

The function $u(x)$ is periodic and is loosely dependent on parameter k.

$$u_k(x) = u_k(x + n(a+b)) \tag{5.21}$$

The traveling wave portion, $e^{jk\cdot x}$, represents delocalized electron motion. The state function Equation 5.20 is a solution to the Schrödinger equation if certain boundary conditions are met. These lead to a constraint on the electron energy, as a function of k, V_o, a, and b (see Figure 5.4 for a definition of these parameters). Equation 5.22 shows this constraint as b goes to zero and V_o goes to infinity. The parameter χ is defined equal to $\sqrt{\frac{2mE}{\hbar^2}}$.

$$\cos(ka) = \cos(\chi a) + \frac{mV_0 ba}{\hbar^2}\frac{\sin(\chi a)}{\chi a} \tag{5.22}$$

Physical insight can be gained if Equation 5.22 is considered for the case when $V_o = 0$ [49]. This corresponds to a free particle. Then k is proportional to the momentum p.

$$k = \sqrt{\frac{2mE}{\hbar^2}} = \frac{p}{\hbar} \tag{5.23}$$

Although k is related to momentum only for the free particle case, the parameter $\hbar k$ is often referred to as the crystal momentum and k is called the crystal wave number.

The model developed in this thesis does not require analytically solving for semiconductor state functions or energies. The important concept for this research is that the semiconductor has two bands of energy and the bandgap energy is much larger than thermal energy spacing. Also, a density of states is required. For a three dimensional crystal, the state function is extended.

$$\psi(\vec{k},\vec{r}) = u_{\vec{k}}(r)e^{j\vec{k}\cdot\vec{r}} \tag{5.24}$$

A phenomenon of the multidimensional case is degeneracy of the energy as a function of k. This leads to a density of states per unit energy per unit volume. For example, the three dimensional corollary to Equation 5.23 is Equation 5.25.

$$\frac{2mE}{\hbar^2} = \left|\vec{k}\right|^2 \tag{5.25}$$

For states near the lowest energy of the conduction band, the density of states is approximated.

$$\rho(E) = \left(\frac{8\sqrt{2}\pi}{h^3}\right)(m^*)^{\frac{3}{2}}V\sqrt{E-E_c}, \quad E > E_c \tag{5.26}$$

The lowest energy of the conduction band is E_c. Volume V is included because the research requires density of states to have units per energy. The effective mass m^* is a parameter that compensates for curvature of the potential energy curve given by Equation 5.23. This accounts for the electron interacting with the crystal instead of moving in free space.

5.4 Combined Electronic Energy

Now that the molecule and semiconductor have been treated separately, consider the effect of coupling, $\hat{V}$. First write Equation 5.15 without the nuclei energy.

$$\hat{H} = \hat{H}_M + \hat{H}_S + \hat{V} \tag{5.27}$$

If the coupling Hamiltonian $\hat{V}$ is set to zero, then the molecule and semiconductor Hamiltonians $\hat{H}_M + \hat{H}_S$ have no coordinates in common. They are independent. In this approximation all properties of the system are summations of the properties of the individual systems. For example, the combined absorption spectrum is the sum of the individual spectra. Write the combined state function as a product and the combined energy as a sum.

$$\psi^{(0)} = \left|\tilde{M}\right\rangle\left|\tilde{S}\right\rangle \tag{5.28}$$

$$E^{(0)} = \tilde{E}_M + \tilde{E}_S \tag{5.29}$$

The superscript "zero" denotes a zeroth order approximation. The tilde symbol on the molecule and semiconductor indicate individual system state function or energy.

One issue with Equation 5.28 is the state function is not anti-symmetric. Experimental evidence shows all state functions must be anti-symmetric with respect to electron coordinate exchange. Consider, for example, Equation 5.28 written as a product of three spin-orbitals on each of the molecule and semiconductor. The spin-orbital ξ_a^i is defined to be a solution to the Schrödinger equation with $\hat{H}_M$ as the Hamiltonian and is a

function of coordinates for electron i. The spin-orbital σ_a^j is defined to be a solution to the Schrödinger equation with $\hat{H}_S$ as the Hamiltonian and is a function of coordinates for electron j.

$$\begin{aligned}\psi^{(0)} = &\left\{\xi_a^3\xi_b^4\xi_c^5 - \xi_a^3\xi_b^5\xi_c^4 + \xi_a^4\xi_b^5\xi_c^3 - \xi_a^4\xi_b^3\xi_c^5 + \xi_a^5\xi_b^3\xi_c^4 - \xi_a^5\xi_b^4\xi_c^3\right\}\times \\ &\left\{\sigma_a^0\sigma_b^1\sigma_c^2 - \sigma_a^0\sigma_b^2\sigma_c^1 + \sigma_a^1\sigma_b^2\sigma_c^0 - \sigma_a^1\sigma_b^0\sigma_c^2 + \sigma_a^2\sigma_b^0\sigma_c^1 - \sigma_a^2\sigma_b^1\sigma_c^0\right\}\end{aligned} \tag{5.30}$$

Exchanging electrons, for example, electron three and electron two, results in a completely different state function. The correct anti-symmetrized combination is written as a product of all molecule and semiconductor spin-orbitals.

$$\psi_n^{(0)} = \sum_{i,j,k,l,m,n} p_{i,j,k,l,m,n}\sigma_a^i\sigma_b^j\sigma_c^k\xi_a^l\xi_b^m\xi_c^n \tag{5.31}$$

While Equation 5.31 is more correct, unfortunately the individual molecule and semiconductor state functions are not separated. This is a problem for the theory developed later in this thesis. A solution is to remember that anti-symmetry is a consequence of the identical nature of electrons. They cannot be distinguished. However, if the molecule and semiconductor are weakly coupled then it is reasonable to approximate the individual electrons as distinguishable by their proximity to the original molecule or semiconductor nuclei cluster. Therefore, the combined state function is approximated in product form without a combined anti-symmetric property.

In an absorption experiment, the system changes energy between a ground and an excited state. If the electromagnetic energy is within the molecule energy range, and not within the semiconductor energy range, and if the systems are separated, then the excitation energy difference does not include the semiconductor energy.

$$\Delta E = \left(\widetilde{E}_{M,excited} + \widetilde{E}_S\right) - \left(\widetilde{E}_{M,ground} + \widetilde{E}_S\right) \tag{5.32}$$

$$= \widetilde{E}_{M,excited} - \widetilde{E}_{M,ground} \tag{5.33}$$

The individual molecule and semiconductor systems have been well studied. What is interesting to this research is what happens when they couple. Add the coupling Hamiltonian back into Equation 5.27. Now the combined state function is no longer a separate product of the individual state functions. The strategy for treating the combined system is variation theory. This requires additional product states. These states are listed here and utilized later in the thesis.

First, the ground and excited individual molecule state.

$$\left|\widetilde{M}_{ground}\right\rangle \equiv \left|\widetilde{\varphi}_g\right\rangle \tag{5.34}$$

The ground state is represented by $\left|\widetilde{\varphi}_g\right\rangle$. Approximate the molecule as having either one available excited state, or M available excited states, Figure 5.2. For one excited state.

$$\left|\widetilde{M}_{excited}\right\rangle \equiv \left|\widetilde{\varphi}_e\right\rangle \tag{5.35}$$

When $\hat{H}_M$ includes nuclear motion then multiple excited states are possible. For M excited states write the state function with an additional subscript.

$$\left|\widetilde{M}_{excited-m}\right\rangle \equiv \left|\widetilde{\varphi}_{e_m}\right\rangle \tag{5.36}$$

Similar to the molecule case, the semiconductor ground and excited state functions are required. The semiconductor is approximated with a two-band structure. In the ground state all electrons are within the lower band.

$$\left|\widetilde{S}_{ground}\right\rangle \equiv \left|\widetilde{\psi}_{o}\right\rangle \tag{5.37}$$

Unlike the molecule, the semiconductor has many available excited states. In the model it is approximated that all subsets of electrons are within the upper band, called the conduction band. At the lower edge of the conduction band, semiconductor states may extend into lower energies in the bandgap. These states are treated separately because of their special impact on the model. States with energy completely in the semiconductor conduction band are called bulk states. States extending into the bandgap are termed surface states. This is because for an infinitely large semiconductor, no states exist with energy within the bandgap. For a semiconductor nanoparticle, the discontinuity at the surface diminishes the applicability of a bandgap model.

$$\left|\widetilde{S}_{excited,bulk}\right\rangle \equiv \left|\widetilde{\psi}_{s}\right\rangle \tag{5.38}$$

Defects within the semiconductor bulk also cause localized states. These are not treated explicitly. While the bulk states are effectively continuous, surface states are approximated as discrete. Surface states are indexed by n and this index ranges from one to N.

$$\left|\widetilde{S}_{excited,surface}\right\rangle \equiv \left|\widetilde{\theta}_{n}\right\rangle \tag{5.39}$$

The product of molecule and semiconductor states for the uncoupled case, Equation 5.28, is applied to all combinations of Equations 5.34 through 5.39. These are listed next, along with the symbol identifying each combination.

First, the total ground state is the molecule and semiconductor both in the ground state.

$$\left|\varphi_{TG}\right\rangle \equiv \left|\widetilde{\varphi}_{g}\right\rangle \left|\widetilde{\psi}_{o}\right\rangle \tag{5.40}$$

The excited molecule state is the molecule in one of its M available excited states while the semiconductor remains in its ground state.

$$\left|\varphi_{m}\right\rangle \equiv \left|\widetilde{\varphi}_{e_m}\right\rangle \left|\widetilde{\psi}_{o}\right\rangle \tag{5.41}$$

In many cases there is only one available excited state for the molecule. In this case Equation 5.41 is written with simpler notation.

$$\left|\varphi\right\rangle \equiv \left|\widetilde{\varphi}_{e}\right\rangle \left|\widetilde{\psi}_{o}\right\rangle \tag{5.42}$$

The semiconductor surface state is identified separately from the semiconductor bulk states. While all semiconductor states arise from the same Hamiltonian, it is useful to treat the surface states separately because energy difference to the semiconductor ground state $\left|\widetilde{\psi}_{o}\right\rangle$ is close to the molecule ground $\left|\widetilde{\varphi}_{g}\right\rangle$ to excited $\left|\widetilde{\varphi}_{e}\right\rangle$ energy difference.

$$\left|\theta_{n}\right\rangle \equiv \left|\widetilde{\varphi}_{g}\right\rangle \left|\widetilde{\theta}_{n}\right\rangle \tag{5.43}$$

The semiconductor surface state can also be paired with an excited molecule state. The index n' encompasses both indexes e_m and n: $n' = f(m,n)$. This slightly complicated notation is temporary because later Equation 5.44 is neglected in the model.

$$\left|\chi_{n'}\right\rangle \equiv \left|\widetilde{\varphi}_{e_m}\right\rangle \left|\widetilde{\theta}_n\right\rangle \tag{5.44}$$

Finally, the semiconductor bulk state is paired with molecule ground and excited states.

$$\left|\psi_s\right\rangle \equiv \left|\widetilde{\varphi}_g\right\rangle \left|\widetilde{\psi}_s\right\rangle \tag{5.45}$$

$$\left|\chi_{s'}\right\rangle \equiv \left|\widetilde{\varphi}_{e_m}\right\rangle \left|\widetilde{\psi}_{s'}\right\rangle \tag{5.46}$$

With coupling neglected, the energy of each combination is the sum of the individual energies.

$$E_{TG} = \widetilde{E}_g + \widetilde{E}_o \tag{5.47}$$

$$E_{\varphi_m} = \widetilde{E}_{e_m} + \widetilde{E}_o \tag{5.48}$$

$$E_{\theta_n} = \widetilde{E}_g + \widetilde{E}_{\theta_n} \tag{5.49}$$

$$E_{e_m,n'} = \widetilde{E}_{e_m} + \widetilde{E}_{\theta_n} \tag{5.50}$$

$$E_s = \widetilde{E}_g + \widetilde{E}_s \tag{5.51}$$

$$E_{e_m,s'} = \widetilde{E}_{e_m} + \widetilde{E}_{s'} \tag{5.52}$$

The order of the energy values is important for the model developed. Equation 5.53 lists the combined energies in order from highest energy to lowest energy. The doubly excited states have the highest energies. Next are the combined with semiconductor excited states, both surface and bulk. The surface excited states are separated because the combined energy with surface excited states is approximately equal to the combined energy with molecule excited states. The total ground energy is lowest.

$$E_{e_m,s'} > E_{e_m,n'} >> E_s > E_{\theta_n} \approx E_{\varphi_m} >> E_{TG} \tag{5.53}$$

The four combined states $|\varphi_{TG}\rangle$, $|\varphi_m\rangle$, $|\theta_n\rangle$, and $|\psi_s\rangle$ have energies somewhat similar in value. The higher energy states $|\chi_{n'}\rangle$ and $|\chi_{s'}\rangle$ are later neglected.

Table 5.1 summarizes the contribution to each energy level, and orders according to energy.

Combined State Energy	Molecule Energy	Semiconductor Energy
E_{TG}	$\tilde{E}_g$	$\tilde{E}_o$
E_{φ_m}	$\tilde{E}_{e_m}$	$\tilde{E}_o$
E_{θ_n}	$\tilde{E}_g$	$\tilde{E}_{\theta_n}$
E_s	$\tilde{E}_g$	$\tilde{E}_s$
$E_{e_m,n'}$	$\tilde{E}_{e_m}$	$\tilde{E}_{\theta_n}$
$E_{e_m,s'}$	$\tilde{E}_{e_m}$	$\tilde{E}_{s'}$

Table 5.1. Energy of each combined state.

When a single excited molecule state is available then simplify Equation 5.48.

$$E_{\varphi_1} \equiv E_{\varphi} = \tilde{E}_{e_1} + \tilde{E}_o \tag{5.54}$$

6.0 Coupling Model

Although a coupling term in the total Hamiltonian is identified (Equations 5.11, 5.12, 5.13, and 5.14) $\hat{V} = \hat{H}_{SN-MN} + \hat{H}_{SE-ME} + \hat{H}_{ME-SN} + \hat{H}_{SE-MN}$, it is much too complicated an expression and therefore useless to contribute to further theoretical progress, at the level of theory attempted in this research. A simple approximation of the coupling is required. This section derives a simple model for $\hat{V}$.

6.1 Goals of Model

According to the goals of this research, the overall coupling model should include experimentally measurable quantities as parameters. This requirement enables comparing theory to experiment using simple absorption spectroscopy. If the model contains non-measurable parameters then the comparison is difficult. This is a problem often encountered when developing theoretical models with quantum mechanics. While quantum mechanics can yield *ab-initio* results, such a level of calculation is well beyond the scope of this thesis. Typically full quantum mechanical calculations are performed on systems involving only a few atoms. The proposed molecule and semiconductor interaction model involves thousands of atoms.

The spectroscopic approach of this thesis leads to a model which includes dipole operators. As shown in Chapter 4, a first-order approximation of spectroscopy includes

the dipole operator. So it is intended that the coupling model include the quantum mechanical dipole operator.

Another goal of the model is separation of the molecule and semiconductor coordinates. In Equations 5.11, 5.12, 5.13, and 5.14 the coordinates are combined together and this significantly complicates mathematics. Separating the coordinates enables a mathematically tractable result.

The model must also include a defined region of applicability. Approximations often trade accuracy for simplicity. This is acceptable when the model boundaries are clearly defined. Finally, a physically realistic approximation is required. Even with loss of accuracy when applied to the physical system of interest, at least the model must correspond to something physical. Whatever simplified physical system it is that the final model corresponds, it is important to define this physical system and how it differs from the desired physical system.

The theories of intermolecular forces are a place to investigate in looking for a model. These forces are weak interactions between stable molecules. Such forces include electrostatic effects, van der Waals interactions, dipole-dipole forces, and hydrogen bonding. Approximating Equations 5.11, 5.12, 5.13, and 5.14 with this class of interaction has several drawbacks. One is that the intermolecular forces are not necessarily stable. This is in contrast to the studied system in which the molecules are connected with some stable mechanism to the semiconductor surface. For intermolecular forces, when the interactions are stable, it is often only in a transient sense because the forces are influenced by a multitude of time-dependent effects in the environment. However, these limitations are acceptable because of the advantage of a simple model,

which directly includes the useful dipole interaction for spectroscopy investigations. Therefore the approach is to approximate molecule to semiconductor coupling as an electronic dipole interaction.

6.2 Dipole-Dipole Interaction

Derive a quantum mechanical operator for the coupling based on a dipole interaction by starting with the potential energy equation of a dipole. This energy is inversely proportional to the distance from the dipole.

$$V(\vec{r}) = \frac{\vec{\mu} \cdot \vec{r}}{4\pi\varepsilon_o r^3} \tag{6.1}$$

The electric field due to a dipole is the negative divergence of the potential.

$$\vec{E}(\vec{r}) = -\nabla V(\vec{r}) = -\frac{1}{4\pi\varepsilon_o} \nabla\left(\frac{\vec{\mu} \cdot \vec{r}}{r^3}\right) \tag{6.2}$$

Calculate the divergence.

$$\vec{E}(\vec{r}) = \frac{1}{4\pi\varepsilon_o}\left[\frac{3(\vec{\mu} \cdot \vec{r})\vec{r}}{r^5} - \frac{\vec{\mu}}{r^3}\right] \tag{6.3}$$

The molecule and semiconductor system is approximated as the coupling being related to a dipole interaction from each. Therefore there are two dipoles involved. The potential energy of two dipoles is given by the dot product of the first dipole with the electric field of the second [50].

$$V = -\vec{\mu}_1 \cdot \vec{E}_2 \tag{6.4}$$

Substitute for the electric field, Equation 6.3.

$$V = -\vec{\mu}_1 \cdot \left\{ \frac{1}{4\pi\varepsilon_o} \left[\frac{3(\vec{\mu}_2 \cdot \vec{r})\vec{r}}{r^5} - \frac{\vec{\mu}_2}{r^3} \right] \right\} \tag{6.5}$$

Expand the dot product.

$$V = \frac{1}{4\pi\varepsilon_o} \left[\frac{\vec{\mu}_1 \cdot \vec{\mu}_2}{r^3} - \frac{3(\vec{\mu}_1 \cdot \vec{r})(\vec{\mu}_2 \cdot \vec{r})}{r^5} \right] \tag{6.6}$$

Write the individual position vectors as unit position vectors divided by the magnitude of the position vector.

$$V = \frac{1}{4\pi\varepsilon_o} \frac{\left[\vec{\mu}_1 \cdot \vec{\mu}_2 - 3(\vec{\mu}_1 \cdot \hat{r})(\vec{\mu}_2 \cdot \hat{r}) \right]}{r^3} \tag{6.7}$$

6.3 Quantum Mechanical Dipole-Dipole Operator

Convert Equation 6.7 to a quantum mechanical operator as follows. First let the coordinates of one dipole be over the molecule coordinates and the second dipole over the semiconductor coordinates. Treat each position as a position operator; $\hat{x} \equiv x$, $\hat{y} \equiv y$, and $\hat{z} \equiv z$ [45]. The dipole becomes an operator over the electronic and nuclear coordinates. For example, the dipole for the semiconductor has the following form.

$$\hat{\vec{\mu}}_S = e\sum\nolimits_\alpha Z_\alpha \hat{\vec{\rho}}_\alpha - e\sum\nolimits_a \hat{\vec{r}}_a \tag{6.8}$$

Replace the lower-case position vector $\vec{r}$ with an upper case $\vec{R}$. The vector represents distance between the centers of the dipole of each individual system.

$$\hat{V} = \frac{1}{4\pi\varepsilon_o R^3}\left[\hat{\vec{\mu}}_M \cdot \hat{\vec{\mu}}_S - 3\left(\hat{\vec{\mu}}_M \cdot \hat{R}\right)\left(\hat{\vec{\mu}}_S \cdot \hat{R}\right)\right] \tag{6.9}$$

Equation 6.9 is the simplified model of the coupling Hamiltonian. Note $\hat{R}$ indicates a unit vector connecting the two systems. This should not be confused with the ^ symbol to indicate an operator. The use of unit vectors is confined to this section. Temporary to this section the ^ simultaneously indicates either an operator or a unit vector, depending on the context. Also, the subscript on the dipole, for example, $\vec{\mu}_M$ or $\vec{\mu}_S$, indicates the coordinates of the molecule or semiconductor and not a molecular or semiconductor state.

Motivated by Section 3, and anticipating the variation theory based model of the next section, the matrix elements of the coupling potential are required. Each matrix element consists of two combined state functions, each as shown in Section 5, and integrated over all particle coordinates.

$$\left\langle M_a S_a \left| \hat{V} \right| M_b S_b \right\rangle = \left\langle M_a S_a \left| \frac{1}{4\pi\varepsilon_o R^3}\left[\hat{\vec{\mu}}_M \cdot \hat{\vec{\mu}}_S - 3\left(\hat{\vec{\mu}}_M \cdot \hat{R}\right)\left(\hat{\vec{\mu}}_S \cdot \hat{R}\right)\right] M_b S_b \right\rangle \right. \tag{6.10}$$

Separate the summed terms.

$$= \frac{\left\langle M_a S_a \left| \hat{\vec{\mu}}_M \cdot \hat{\vec{\mu}}_S \right| M_b S_b \right\rangle - 3\left\langle M_a S_a \left| \left(\hat{\vec{\mu}}_M \cdot \hat{R}\right)\left(\hat{\vec{\mu}}_S \cdot \hat{R}\right) \right| M_b S_b \right\rangle}{4\pi\varepsilon_o R^3} \tag{6.11}$$

Because the molecule and semiconductor state functions used in the combined product terms have no coordinates in common, separate the integrals behind the matrix elements.

$$= \frac{\langle M_a | \hat{\tilde{\mu}}_M | M_b \rangle \cdot \langle S_a | \hat{\tilde{\mu}}_S | S_b \rangle - 3\left(\langle M_a | \hat{\tilde{\mu}}_M | M_b \rangle \cdot \hat{R}\right)\left(\langle S_a | \hat{\tilde{\mu}}_S | S_b \rangle \cdot \hat{R}\right)}{4\pi\varepsilon_o R^3} \tag{6.12}$$

Following the Born-Oppenheimer approximation, write each matrix element in terms of nuclear and electronic coordinates and write each state function in terms of nuclear and electronic coordinates. Neglect semiconductor nuclear motion.

$$= \frac{\left\{\begin{array}{l}\left\langle M_a^{(nuc)} M_a^{(ele)} \left| \hat{\tilde{\mu}}_M^{(nuc)} + \hat{\tilde{\mu}}_M^{(ele)} \right| M_b^{(nuc)} M_b^{(ele)} \right\rangle \cdot \left\langle S_a^{(ele)} \left| \hat{\tilde{\mu}}_S^{(ele)} \right| S_b^{(ele)} \right\rangle - \\ 3\left[\left\langle M_a^{(nuc)} M_a^{(ele)} \left| \hat{\tilde{\mu}}_M^{(nuc)} + \hat{\tilde{\mu}}_M^{(ele)} \right| M_b^{(nuc)} M_b^{(ele)} \right\rangle \cdot \hat{R}\right]\left[\left\langle S_a^{(ele)} \left| \hat{\tilde{\mu}}_S^{(ele)} \right| S_b^{(ele)} \right\rangle \cdot \hat{R}\right]\end{array}\right\}}{4\pi\varepsilon_o R^3} \tag{6.13}$$

Remember the nuclear state function is independent of electronic coordinates under the Born-Oppenheimer approximation. Therefore, terms with nuclear coordinate dipole operators are eliminated because the separated inner product of electronic state functions are zero. They are orthogonal. Rewrite Equation 6.13 with the nuclear terms removed and with the electronic dipole operators included within the nuclear because the electronic dipole operator depends parametrically on the nuclear coordinates.

$$= \frac{\left\{\begin{array}{l}\left\langle M_a^{(nuc)} \left| \left\langle M_a^{(ele)} \left| \hat{\tilde{\mu}}_M^{(ele)} \right| M_b^{(ele)} \right\rangle \right| M_b^{(nuc)} \right\rangle \cdot \left\langle S_a^{(ele)} \left| \hat{\tilde{\mu}}_S^{(ele)} \right| S_b^{(ele)} \right\rangle - \\ 3\left[\left\langle M_a^{(nuc)} \left| \left\langle M_a^{(ele)} \left| \hat{\tilde{\mu}}_M^{(ele)} \right| M_b^{(ele)} \right\rangle \right| M_b^{(nuc)} \right\rangle \cdot \hat{R}\right]\left[\left\langle S_a^{(ele)} \left| \hat{\tilde{\mu}}_S^{(ele)} \right| S_b^{(ele)} \right\rangle \cdot \hat{R}\right]\end{array}\right\}}{4\pi\varepsilon_o R^3} \tag{6.14}$$

Following Equation 4.26, expand the electronic dipole operators in a Taylor series and approximate higher order terms as zero. Approximate semiconductor vibrational coupling as zero. Write the molecule vibrational states in terms of the molecule normal coordinates and use the notation of Equation 4.28 for the molecule vibrational states.

$$= \frac{\left\{ \begin{array}{l} \left[\begin{array}{l} \vec{\mu}^{o}_{MaMb} \Pi_{k=1}^{3P-6} \left\langle \upsilon_k^{(a)} \middle| \upsilon_k^{(b)} \right\rangle + \\ \Sigma_{j=1}^{3P-6} \vec{\mu}^{(j)}_{MaMb} \left\langle \Pi_{k=1}^{3P-6} \upsilon_k^{(a)} \middle| Q_j \middle| \Pi_{k=1}^{3P-6} \upsilon_k^{(b)} \right\rangle \end{array} \right] \cdot \left\langle S_a^{(ele)} \middle| \hat{\vec{\mu}}_S^{(ele)} \middle| S_b^{(ele)} \right\rangle - \\ 3 \left[\left(\begin{array}{l} \vec{\mu}^{o}_{MaMb} \Pi_{k=1}^{3P-6} \left\langle \upsilon_k^{(a)} \middle| \upsilon_k^{(b)} \right\rangle + \\ \Sigma_{j=1}^{3P-6} \vec{\mu}^{(j)}_{MaMb} \left\langle \Pi_{k=1}^{3P-6} \upsilon_k^{(a)} \middle| Q_j \middle| \Pi_{k=1}^{3P-6} \upsilon_k^{(b)} \right\rangle \end{array} \right) \cdot \hat{R} \right] \left[\left\langle S_a^{(ele)} \middle| \hat{\vec{\mu}}_S^{(ele)} \middle| S_b^{(ele)} \right\rangle \cdot \hat{R} \right] \end{array} \right\}}{4\pi\varepsilon_o R^3} \tag{6.15}$$

Note $\mu^{(j)}_{Ma,Mb} \equiv \left(\partial \mu_{Ma,Mb} / \partial Q_j \right)_o$. Distribute the multiplication and define $\vec{\mu}_{SaSb} \equiv \left\langle S_a^{(ele)} \middle| \hat{\vec{\mu}}_S^{(ele)} \middle| S_b^{(ele)} \right\rangle$.

$$= \frac{\left\{ \begin{array}{l} \left(\vec{\mu}^{o}_{MaMb} \cdot \vec{\mu}_{SaSb} - 3 \left(\vec{\mu}^{o}_{MaMb} \cdot \hat{R} \right) \left(\vec{\mu}_{SaSb} \cdot \hat{R} \right) \right) \Pi_{k=1}^{3P-6} \left\langle \upsilon_k^{(a)} \middle| \upsilon_k^{(b)} \right\rangle + \\ \Sigma_{j=1}^{3P-6} \left(\vec{\mu}^{(j)}_{MaMb} \cdot \vec{\mu}_{SaSb} - 3 \left(\vec{\mu}^{(j)}_{MaMb} \cdot \hat{R} \right) \left(\vec{\mu}_{SaSb} \cdot \hat{R} \right) \right) \left\langle \Pi_{k=1}^{3P-6} \upsilon_k^{(a)} \middle| Q_j \middle| \Pi_{k=1}^{3P-6} \upsilon_k^{(b)} \right\rangle \end{array} \right\}}{4\pi\varepsilon_o R^3} \tag{6.16}$$

6.4 Further Model Simplifications

As defined by Equation 6.16, the coupling model is too complicated. A simpler expression is needed. Three levels of approximation are possible. First, neglect all vibrational motion. The molecule is treated as stationary over the nuclear coordinates.

$$\left\langle M_a S_a \middle| \hat{V} \middle| M_b S_b \right\rangle = \frac{\vec{\mu}_{MaMb} \cdot \vec{\mu}_{SaSb} - 3 \left(\vec{\mu}_{MaMb} \cdot \hat{R} \right) \left(\vec{\mu}_{SaSb} \cdot \hat{R} \right)}{4\pi\varepsilon_o R^3} \tag{6.17}$$

Figure 6.1 shows the geometric arrangement of the two vectors.

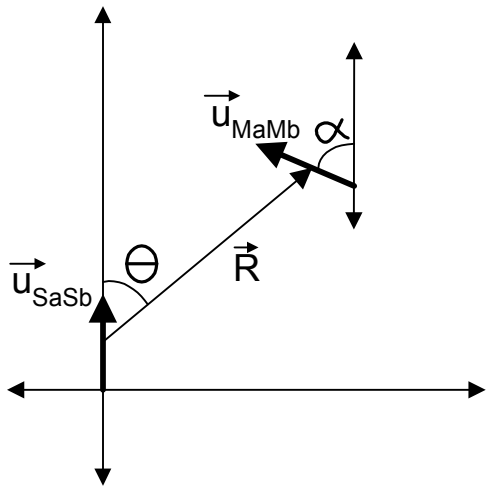

Figure 6.1. Arrangement of the two dipoles.

Using simple geometry, convert the dot product to polar coordinates. While Figure 6.1 shows a single value of α and a single value of θ, in general there is a separate dipole orientation for each quantum mechanical state. Equation 6.18 expresses these angles on a per state basis. For example, θ_{SaSb} is the orientation for states $|S_a\rangle$ and $|S_b\rangle$.

$$= |\vec{\mu}_{MaMb}||\vec{\mu}_{SaSb}|\left\{\frac{2\cos(\theta_{SaSb})\sin(\alpha_{MaMb})+\sin(\theta_{SaSb})\cos(\alpha_{MaMb})}{4\pi\varepsilon_o R^3}\right\} \tag{6.18}$$

Show the matrix element explicitly and define the geometric term as $G(R,\theta_{SaSb},\alpha_{MaMb})$.

$$\langle M_a S_a|\hat{V}|M_b S_b\rangle = |\vec{\mu}_{MaMb}||\vec{\mu}_{SaSb}|G(R,\theta_{SaSb},\alpha_{MaMb}) \tag{6.19}$$

Figure 6.2 shows the orientation, $2\cos(\theta_{SaSb})\sin(\alpha_{MaMb})+\sin(\theta_{SaSb})\cos(\alpha_{MaMb})$, portion of $G(R,\theta,\alpha)$ for a few dipole arrangements. The horizontal axis is the angle of the molecule dipole, α. Four curves are shown, one for $\theta = 0$, one for $\theta = 45^o$, one for

$\theta = 90^o$ and one for $\theta = 180^o$. The term $G(R,\theta,\alpha)$ is based on simple geometry and therefore applies both to the classical and quantum mechanical system. A pair of fixed dipoles treated with classical mechanics results in a more stable system for negative $G(R,\theta,\alpha)$. The dipoles attract. Positive values of $G(R,\theta,\alpha)$ indicate a dipole repelling arrangement. In the quantum mechanical sense, when treating the system as transition dipoles, such an interpretation is not possible.

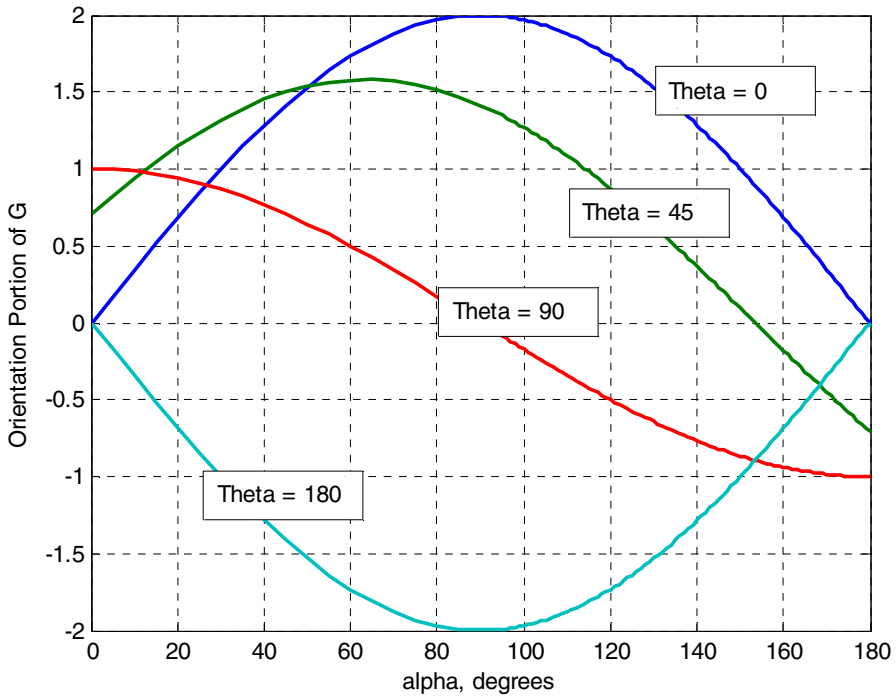

Figure 6.2. Plot of $2\cos(\theta_{SaSb})\sin(\alpha_{MaMb})+\sin(\theta_{SaSb})\cos(\alpha_{MaMb})$. Angle between dipoles (horizontal axis) is α.

A second approximation is keeping nuclear motion and the first term of the Taylor series. This is the Condon approximation. Equation 6.16 simplifies to a form very similar to Equation 6.17, except scaled by the Franck-Condon factor.

$$= \frac{\vec{\mu}^{o}_{MaMb} \cdot \vec{\mu}_{SaSb} - 3\left(\vec{\mu}^{o}_{MaMb} \cdot \hat{R}\right)\left(\vec{\mu}_{SaSb} \cdot \hat{R}\right)}{4\pi\varepsilon_o R^3} \Pi_{k=1}^{3P-6} \left\langle \upsilon_k^{(a)} \middle| \upsilon_k^{(b)} \right\rangle \tag{6.20}$$

Then the resulting equation, including the geometric term is similar to Equation 6.19. An important difference is that the first term, $\vec{\mu}^{o}_{MaMb}$, is the result of a Taylor series expansion and is not equal to $\langle M_a | \vec{\mu}_M | M_b \rangle$ as in Equation 6.19.

$$= \left|\vec{\mu}^{o}_{MaMb}\right| \left|\vec{\mu}_{SaSb}\right| G^{(o)}\left(R, \theta_{SaSb}, \alpha_{MaMb}\right) \Pi_{k=1}^{3P-6} \left\langle \upsilon_k^{(a)} \middle| \upsilon_k^{(b)} \right\rangle \tag{6.21}$$

The final level of approximation is keeping all terms in Equation 6.16.

$$= \frac{\left\{ \begin{array}{l} \left(\vec{\mu}^{o}_{MaMb} \cdot \vec{\mu}_{SaSb} - 3\left(\vec{\mu}^{o}_{MaMb} \cdot \hat{R}\right)\left(\vec{\mu}_{SaSb} \cdot \hat{R}\right)\right) \Pi_{k=1}^{3P-6} \left\langle \upsilon_k^{(a)} \middle| \upsilon_k^{(b)} \right\rangle + \\ \Sigma_{j=1}^{3P-6} \left(\vec{\mu}^{(j)}_{MaMb} \cdot \vec{\mu}_{SaSb} - 3\left(\vec{\mu}^{(j)}_{MaMb} \cdot \hat{R}\right)\left(\vec{\mu}_{SaSb} \cdot \hat{R}\right)\right) \left\langle \Pi_{k=1}^{3P-6} \upsilon_k^{(a)} \middle| Q_j \middle| \Pi_{k=1}^{3P-6} \upsilon_k^{(b)} \right\rangle \end{array} \right\}}{4\pi\varepsilon_o R^3} \tag{6.22}$$

The first term of Equation 6.22 reduces identically to the Equation 6.21 result, with the understanding that $G^{(o)}\left(R, \theta_{SaSb}, \alpha_{MaMb}\right)$ relates to the geometry of $\vec{\mu}^{o}_{MaMb}$.

$$\begin{array}{l} = \left|\vec{\mu}^{o}_{MaMb}\right| \left|\vec{\mu}_{SaSb}\right| G^{(o)}\left(R, \theta_{SaSb}, \alpha_{MaMb}\right) \Pi_{k=1}^{3P-6} \left\langle \upsilon_k^{(a)} \middle| \upsilon_k^{(b)} \right\rangle + \\ \frac{1}{4\pi\varepsilon_o R^3} \Sigma_{j=1}^{3P-6} \left(\vec{\mu}^{(j)}_{MaMb} \cdot \vec{\mu}_{SaSb} - 3\left(\vec{\mu}^{(j)}_{MaMb} \cdot \hat{R}\right)\left(\vec{\mu}_{SaSb} \cdot \hat{R}\right)\right) \left\langle \Pi_{k=1}^{3P-6} \upsilon_k^{(a)} \middle| Q_j \middle| \Pi_{k=1}^{3P-6} \upsilon_k^{(b)} \right\rangle \end{array} \tag{6.23}$$

Define a second geometry term for each of the Condon and non-Condon coefficients.

$$= \left|\vec{\mu}^{o}_{MaMb}\right|\left|\vec{\mu}_{SaSb}\right|G^{(o)}\left(R,\theta_{SaSb},\alpha_{MaMb}\right)\Pi_{k=1}^{3P-6}\left\langle \upsilon_k^{(a)}\middle|\upsilon_k^{(b)}\right\rangle + \\ \left|\vec{\mu}_{SaSb}\right|\Sigma_{j=1}^{3P-6}\left|\vec{\mu}^{(j)}_{MaMb}\right|G^{(j)}\left(R,\theta_j,\alpha_j\right)\left\langle \Pi_{k=1}^{3P-6}\upsilon_k^{(a)}\middle|Q_j\middle|\Pi_{k=1}^{3P-6}\upsilon_k^{(b)}\right\rangle \tag{6.24}$$

Separate the Franck-Condon elements and factor common terms.

$$= \left|\vec{\mu}_{SaSb}\right|\left\{\begin{matrix}\left|\vec{\mu}^{o}_{MaMb}\right|G^{(o)}\left(R,\theta_{SaSb},\alpha_{MaMb}\right)\Pi_{k=1}^{3P-6}\left\langle \upsilon_k^{(a)}\middle|\upsilon_k^{(b)}\right\rangle + \\ \Sigma_{j=1}^{3P-6}\left|\vec{\mu}^{(j)}_{MaMb}\right|G^{(j)}\left(R,\theta_j,\alpha_j\right)\left\langle \upsilon_j^{(a)}\middle|Q_j\middle|\upsilon_j^{(b)}\right\rangle\Pi_{k=1,k\neq j}^{3P-6}\left\langle \upsilon_k^{(a)}\middle|\upsilon_k^{(b)}\right\rangle\end{matrix}\right\} \tag{6.25}$$

The quantum mechanical matrix element $\left\langle M_a S_a\middle|\hat{V}\middle|M_b S_b\right\rangle$ formed with the dipole operator does not have the energy property of the classical system. The result of $\left\langle M_a S_a\middle|\hat{V}\middle|M_b S_b\right\rangle$ is complex valued and for at least this reason cannot represent a stabilization energy. For example, the quantum mechanical dipoles $\vec{\mu}_{MaMb}$ and $\vec{\mu}_{SaSb}$ depend on the state function phase. The sign of each is based on something that is not measurable.

Equation 6.19 with vibrational motion neglected, Equation 6.21 using the Condon approximation, and Equation 6.25 with the first two Taylor series terms included represent three levels of coupling matrix element approximation. An additional simplification applied later in the thesis is to define the orientation term as independent of the molecule state. For the molecule this approximation is perhaps reasonable given the existing simplifications such as the Condon approximation. A constant orientation term provides significant benefit to the mathematical development at the expense of separating the theory from physical reality. Therefore, after the mathematical model is developed, a subsequent adjustment to the model is necessary.

6.5 Comparison of Dipole-Dipole for Limiting Case

It is instructive to compare the dipole-dipole quantum mechanical operator, Equation 6.9, to the correct quantum mechanical coupling Hamiltonian, Equations 5.11 through 5.14, for a limiting case. The "semiconductor" consists of a single positive particle and a single negative particle. Similarly, the "molecule" consists of a single positive particle and a single negative particle. The resulting Hamiltonian is similar to an H_2 molecule system. Models of small atomic or molecular hydrogen systems often provide sufficient simplicity to allow more exact calculations [51]. So, this analysis provides some physical understanding of the model and helps provide applicability boundaries.

Write each term of Equation 5.15, $\hat{H}_{TOTAL} = \hat{H}_S + \hat{H}_M + \hat{H}_N + \hat{V}$, for the case of $N_S = 1$, $N_M = 1$, and two electrons. Use atomic units. Place the origin at the center point of the vector connecting nucleus α and electron a. This choice of origin enables direct comparison to the dipole-dipole approximation because of the dipole center definition. The vector connecting the two nuclei is $\overline{R}$ and is selected such that it always is aligned with the x-axis. Figure 6.3 shows the arrangement along with two electron position vectors.

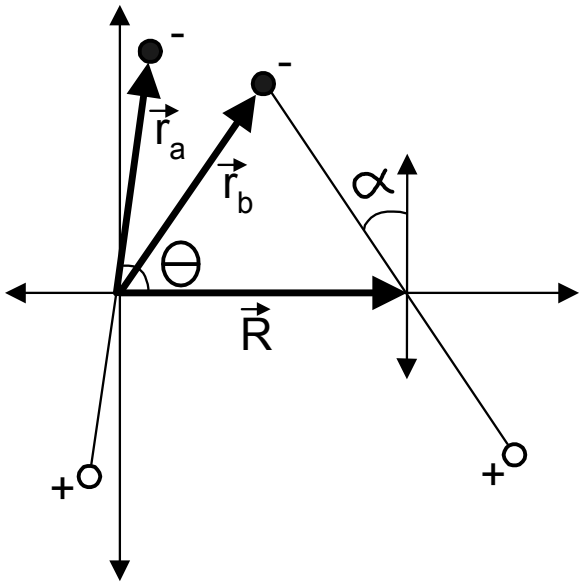

Figure 6.3. Geometry of limiting system.

The equations for $\hat{H}_S$ and $\hat{H}_M$ are identical and equivalent to two separated hydrogen molecules.

$$\hat{H}_S = -\frac{1}{2}\nabla_a^2 - \frac{1}{|\bar{r}_a - \bar{\rho}_\alpha|} \tag{6.26}$$

$$\hat{H}_M = -\frac{1}{2}\nabla_b^2 - \frac{1}{|\bar{r}_b - \bar{\rho}_\beta|} \tag{6.27}$$

The coupling operator includes all terms connecting the two dipoles. Write as a function. It is important to keep the internuclear potential term because a dipole includes both the positive and negative charged quantities.

$$V_h = \frac{1}{\left|\bar{\rho}_\alpha - \bar{\rho}_\beta\right|} + \frac{1}{\left|\bar{r}_a - \bar{r}_b\right|} - \frac{1}{\left|\bar{r}_b - \bar{\rho}_\alpha\right|} - \frac{1}{\left|\bar{r}_a - \bar{\rho}_\beta\right|} \tag{6.28}$$

Compare Equation 6.28 with Equation 6.7. Equation 6.29 shows Equation 6.7 with atomic units and the notation of Figure 6.3. By definition $R \equiv \left|\bar{R}\right|$.

$$V_{dd} = \frac{\left(\bar{r}_a - \bar{\rho}_\alpha\right)\cdot\left(\bar{r}_b - \bar{\rho}_\beta\right) - 3\left(\left(\bar{r}_a - \bar{\rho}_\alpha\right)\cdot\hat{R}\right)\left(\left(\bar{r}_b - \bar{\rho}_\beta\right)\cdot\hat{R}\right)}{R^3} \tag{6.29}$$

Sweep the ranges $R \in \{4,\ldots,25\}$ and $\alpha \in \{0^o,\ldots,180^o\}$. Set $\left|\bar{r}_a - \bar{\rho}_\alpha\right| = \left|\bar{r}_b - \bar{\rho}_\beta\right| = 1$. Normalizing $\left|\bar{r}_a - \bar{\rho}_\alpha\right|$ and $\left|\bar{r}_b - \bar{\rho}_\beta\right|$ means the plot versus R indicates separation of the two individual dipoles as a ratio to the individual hydrogen atom proton electron distance.

The result is displayed as percent error of the dipole-dipole approximation compared to the original Hamiltonian coupling function. The comparison is only in terms of the mathematical form of the Hamiltonian itself. This is not comparing the result of applying the Hamiltonian for quantum mechanical calculations.

$$Error \equiv \left(\frac{V_{dd}}{V_h} - 1\right)\cdot 100\% \tag{6.30}$$

When the result is negative this indicates $V_{dd} < V_h$. Similarly when the result is positive $V_{dd} > V_h$. Figure 6.4 shows the result for $\theta = 90^o$. Notice that as R increases, the dipole-dipole approximation becomes accurate, in the sense that the Hamiltonians treated as functions produce the same result, and the error is relatively independent of α. Although only the $\theta = 90^o$ case is shown, the results are similar for all values of θ.

In general the error is less than 1% by $R > 10 \cdot \left(\left| \bar{r}_a - \bar{\rho}_\alpha \right| = \left| \bar{r}_b - \bar{\rho}_\beta \right| \right)$. This is when the distance between the two dipoles is larger than ten times the individual dipole distances.

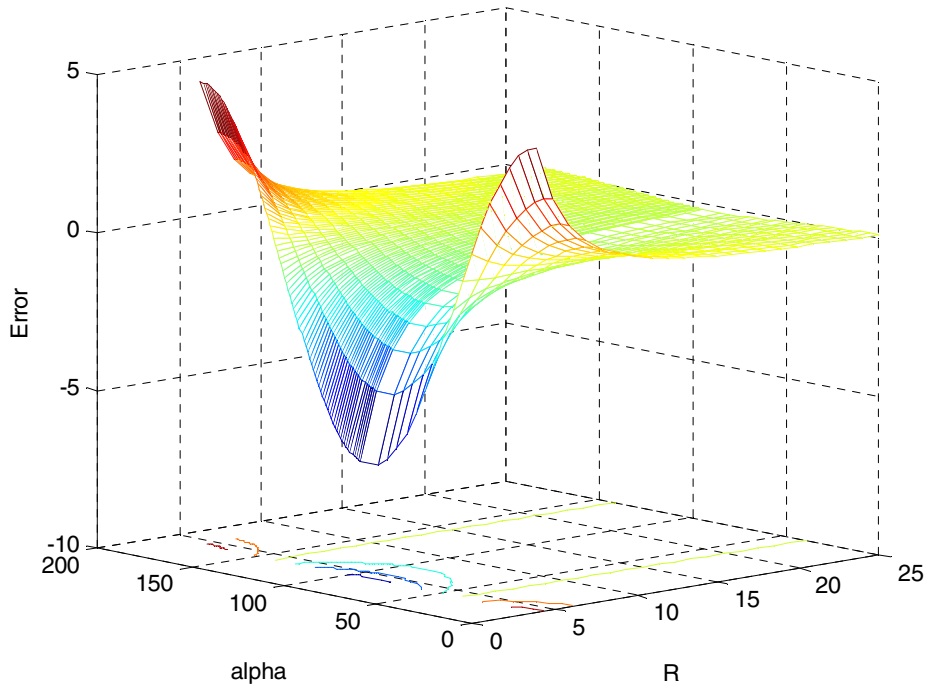

Figure 6.4. Equation 6.30 as a function of R and α for $\theta = 90^o$.

Figure 6.5 compares the individual functions as a function of R, for $R \geq 10$. The approximation becomes reasonably accurate as the distance increases.

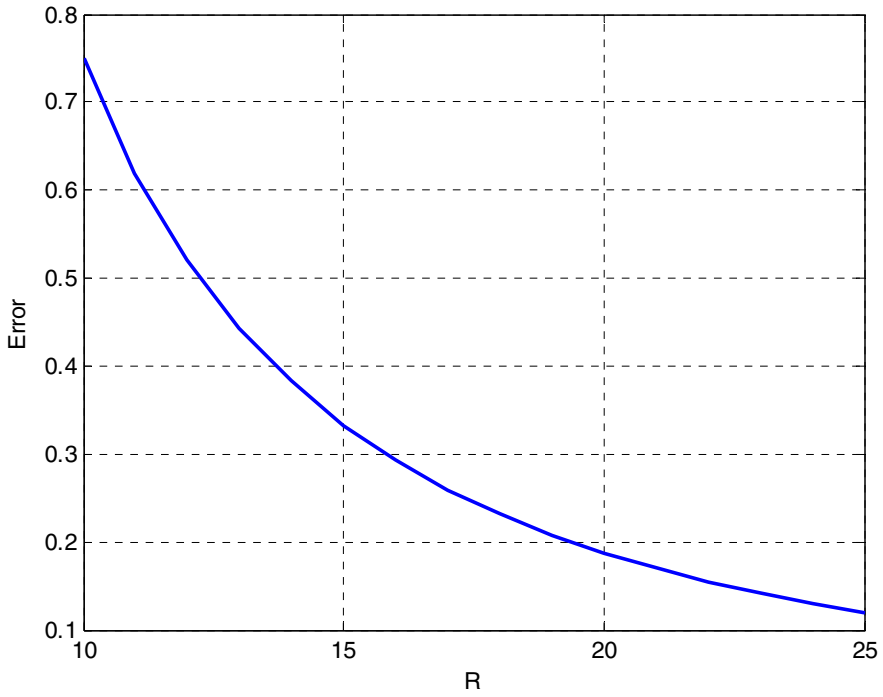

Figure 6.5. Equation 6.30 as a function of R and for $\alpha = 0^o$ for $\theta = 90^o$.

7.0 Variational Theory Foundation of Model

The foundation of the model for semiconductor effect on molecule energy states, through the coupling Hamiltonian $\hat{V}$ derived in the previous section, is variation theory. Start with one of the uncoupled product states, such as Equation 5.40 for $|\varphi_{TG}\rangle$ or Equation 5.41 for $|\varphi_m\rangle$. Construct a new state by adding a weighted sum of the other uncoupled product states $|\varphi_m\rangle$, $|\theta_n\rangle$, $|\psi_s\rangle$, $|\chi_{n'}\rangle$, and $|\chi_{s'}\rangle$. Find the coefficients of the sum and the energy of the new state according to the variation theory described in Equations 3.19 and Equation 3.24. Equations 7.1 and 7.2 show the new states that start with the excited $|\varphi_m\rangle$ and total ground $|\varphi_{TG}\rangle$ states respectively. A separate symbol is used (E and ε) to help distinguish between the new excited energy, E, and ground state energy, ε.

$$\Psi_E = \sum_{m=1}^{M} a_m(E)\varphi_m + \sum_{n=1}^{N} c_n(E)\theta_n + \sum_s b_s(E)\psi_s + \sum_{n=1}^{N} c'_{n'}(E)\chi_{n'} + \sum_{s'} b'_{s'}(E)\chi_{s'} \qquad (7.1)$$

$$\Psi_\varepsilon = a(\varepsilon)\varphi_{TG} + \sum_{n=1}^{N} c_n(\varepsilon)\theta_n + \sum_s b_s(\varepsilon)\psi_s + \sum_{n=1}^{N} c'_{n'}(\varepsilon)\chi_{n'} + \sum_{s'} b'_{s'}(\varepsilon)\chi_{s'} \qquad (7.2)$$

The coefficients are functions of the energy because the linear equations have a number of solutions equal to the number of states in the summation. The semiconductor bulk states are effectively continuous and therefore a very large number of solutions are possible.

An initial simplification of Equation 7.1 and 7.2 is to neglect the doubly excited terms. This is because the energy of these terms is so much larger than the energy of the

other terms. For example, consider the energy difference between the combined state with molecule excited $|\varphi\rangle$ and the combined state with semiconductor excited $|\psi_s\rangle$.

$$E_s - E_\varphi = \left(\widetilde{E}_g + \widetilde{E}_s\right) - \left(\widetilde{E}_e + \widetilde{E}_o\right) = \left(\widetilde{E}_s - \widetilde{E}_o\right) - \left(\widetilde{E}_e - \widetilde{E}_g\right) \tag{7.3}$$

In the physical systems considered, the energy difference between the individual molecule excited and ground state is slightly smaller than the energy difference of the semiconductor bandgap. Therefore, E_s and E_φ have approximately the same energy, although probably $E_s > E_\varphi$ in many cases. However, the doubly excited terms $|\chi_{n'}\rangle$ and $|\chi_{s'}\rangle$ are composed of a molecule excited state, instead of a molecule ground state. Therefore, the energy difference does not have the $\widetilde{E}_e - \widetilde{E}_g$ factor to lower the energy and these states are much higher in energy than $|\varphi\rangle$. Because of these energy differences, all doubly excited terms are neglected.

$$\Psi_E = \sum_{m=1}^{M} a_m(E)\varphi_m + \sum_{n=1}^{N} c_n(E)\theta_n + \sum_s b_s(E)\psi_s \tag{7.4}$$

For the ground states, the semiconductor surface states are also neglected because of the relatively large energy difference to the ground energy levels.

$$\Psi_\varepsilon = a(\varepsilon)\varphi_{TG} + \sum_s b_s(\varepsilon)\psi_s \tag{7.5}$$

Next, use Equation 3.24 to find the coefficients of Equations 7.4 and 7.5, along with the energy for each set of coefficients. Equation 7.6 applies to the case for Equation 7.4. The case for Equation 7.5 follows trivially by setting $M = 1$, $N = 0$, and replacing $|\varphi\rangle$ with $|\varphi_{TG}\rangle$.

$$\begin{vmatrix}
\langle\varphi_1|\hat{H}|\varphi_1\rangle - W & \cdots & \langle\varphi_1|\hat{H}|\varphi_M\rangle & \langle\varphi_1|\hat{H}|\theta_1\rangle & \cdots & \langle\varphi_1|\hat{H}|\theta_N\rangle & \langle\varphi_1|\hat{H}|\psi_1\rangle & \cdots \\
\vdots & \ddots & \vdots & \vdots & \ddots & \vdots & \vdots & \cdots \\
\langle\varphi_M|\hat{H}|\varphi_1\rangle & \cdots & \langle\varphi_M|\hat{H}|\varphi_M\rangle - W & \langle\varphi_M|\hat{H}|\theta_1\rangle & \cdots & \langle\varphi_M|\hat{H}|\theta_N\rangle & \langle\varphi_M|\hat{H}|\psi_1\rangle & \cdots \\
\langle\theta_1|\hat{H}|\varphi_1\rangle & \cdots & \langle\theta_1|\hat{H}|\varphi_M\rangle & \langle\theta_1|\hat{H}|\theta_1\rangle - W & \cdots & \langle\theta_1|\hat{H}|\theta_N\rangle & \langle\theta_1|\hat{H}|\psi_1\rangle & \cdots \\
\vdots & \ddots & \vdots & \vdots & \ddots & \vdots & \vdots & \cdots \\
\langle\theta_N|\hat{H}|\varphi_1\rangle & \cdots & \langle\theta_N|\hat{H}|\varphi_M\rangle & \langle\theta_N|\hat{H}|\theta_1\rangle & \cdots & \langle\theta_N|\hat{H}|\theta_N\rangle - W & \langle\theta_N|\hat{H}|\psi_1\rangle & \cdots \\
\langle\psi_1|\hat{H}|\varphi_1\rangle & \cdots & \langle\psi_1|\hat{H}|\varphi_M\rangle & \langle\psi_1|\hat{H}|\theta_1\rangle & \cdots & \langle\psi_1|\hat{H}|\theta_N\rangle & \langle\psi_1|\hat{H}|\psi_1\rangle - W & \cdots \\
\vdots & \vdots & \vdots & \vdots & \vdots & \vdots & \vdots & \vdots
\end{vmatrix} = 0 \qquad (7.6)$$

7.1 Electronic Energy Levels

Next, derive an equation for each matrix element in Equation 7.6 with the molecule and semiconductor state functions as separated as possible. This maximizes experimentally accessible data. Use the Hamiltonian from Equation 5.27 and coupling model from Equation 6.19 for the result of applying the coupling operator $\hat{V}$. First, matrix elements for combined states with the molecule excited.

$$\langle\varphi_k|\hat{H}|\varphi_m\rangle = \langle\widetilde{\varphi}_{e_k}\widetilde{\psi}_o|\hat{H}_M + \hat{H}_S + \hat{V}|\widetilde{\varphi}_{e_m}\widetilde{\psi}_o\rangle \qquad (7.7)$$

$$= \langle\widetilde{\varphi}_{e_k}\widetilde{\psi}_o|\hat{H}_M|\widetilde{\varphi}_{e_m}\widetilde{\psi}_o\rangle + \langle\widetilde{\varphi}_{e_k}\widetilde{\psi}_o|\hat{H}_S|\widetilde{\varphi}_{e_m}\widetilde{\psi}_o\rangle + \langle\widetilde{\varphi}_{e_k}\widetilde{\psi}_o|\hat{V}|\widetilde{\varphi}_{e_m}\widetilde{\psi}_o\rangle \qquad (7.8)$$

Apply the first simplified model, Equation 6.19. This model neglects vibrational motion. The full state-dependent form of the orientation term G is kept in Equation 7.9. The approximation of constant G, $G\left(R,\theta_{\widetilde{\psi}_o,\widetilde{\psi}_o},\alpha_{\widetilde{\varphi}_{e_k},\widetilde{\varphi}_{e_m}}\right) = G$, is reserved for later. Notice that while previously G was defined in terms of orientations θ_{SaSb} and α_{MaMb}, now the

specific state symbol is used. So, for example, $|S_a\rangle$ is selected as $|\tilde{\psi}_o\rangle$ and this is why the notation for θ_{SaSb} is now written $\theta_{\tilde{\psi}_o,\tilde{\psi}_o}$.

$$\begin{aligned} &= \langle \tilde{\varphi}_{e_k} | \hat{H}_M | \tilde{\varphi}_{e_m} \rangle \langle \tilde{\psi}_o | \tilde{\psi}_o \rangle + \langle \tilde{\varphi}_{e_k} | \tilde{\varphi}_{e_m} \rangle \langle \tilde{\psi}_o | \hat{H}_S | \tilde{\psi}_o \rangle + \\ &| \vec{\mu}(\tilde{\varphi}_{e_k}, \tilde{\varphi}_{e_m}) \| \vec{\mu}(\tilde{\psi}_o, \tilde{\psi}_o) | G\left(R, \theta_{\tilde{\psi}_o,\tilde{\psi}_o}, \alpha_{\tilde{\varphi}_{e_k},\tilde{\varphi}_{em}}\right) \end{aligned} \tag{7.9}$$

The states are normalized and orthogonal. Therefore $\langle \tilde{\psi}_o | \tilde{\psi}_o \rangle = 1$ and $\langle \tilde{\varphi}_{e_k} | \tilde{\varphi}_{e_m} \rangle = \delta(k-m)$. Also define the ground state dipoles: $\mu(\tilde{\varphi}_{e_k}, \tilde{\varphi}_{e_m}) \equiv |\vec{\mu}(\tilde{\varphi}_{e_k}, \tilde{\varphi}_{e_m})|$ and $\mu(\tilde{\psi}_o, \tilde{\psi}_o) \equiv |\vec{\mu}(\tilde{\psi}_o, \tilde{\psi}_o)|$.

$$= \tilde{E}_{e_m} \langle \tilde{\varphi}_{e_k} | \tilde{\varphi}_{e_m} \rangle + \delta(k-m) \tilde{E}_o \langle \tilde{\psi}_o | \tilde{\psi}_o \rangle + G\left(R, \theta_{\tilde{\psi}_o,\tilde{\psi}_o}, \alpha_{\tilde{\varphi}_{e_k},\tilde{\varphi}_{e_m}}\right) \mu(\tilde{\psi}_o, \tilde{\psi}_o) \mu(\tilde{\varphi}_{e_k}, \tilde{\varphi}_{e_m}) \tag{7.10}$$

$$= \left(\tilde{E}_{e_m} + \tilde{E}_o\right) \delta(k-m) + G\left(R, \theta_{\tilde{\psi}_o,\tilde{\psi}_o}, \alpha_{\tilde{\varphi}_{e_k},\tilde{\varphi}_{e_m}}\right) \mu(\tilde{\psi}_o, \tilde{\psi}_o) \mu(\tilde{\varphi}_{e_k}, \tilde{\varphi}_{e_m}) \tag{7.11}$$

If the ground state dipole of the semiconductor is approximated as zero then Equation 7.12 is simply the combined excited energy from Equation 5.48. A vanishing ground state dipole provides an important simplification and is one of the approximations which later enable a simple closed form energy solution. Adjustments to the theory when the dipole is not zero are also provided in a later section.

$$\langle \varphi_k | \hat{H} | \varphi_m \rangle = E_{\varphi_m} \delta(k-m) \tag{7.12}$$

Simplify when only one excited molecule state is available.

$$\langle \varphi | \hat{H} | \varphi \rangle = E_\varphi \tag{7.13}$$

Next derive matrix elements for combined states with the semiconductor excited into energy below the lower energy of the conduction band.

$$\left\langle \theta_k \left| \hat{H} \right| \theta_n \right\rangle = \left\langle \widetilde{\varphi}_g \widetilde{\theta}_k \left| \hat{H}_M + \hat{H}_S + \hat{V} \right| \widetilde{\varphi}_g \widetilde{\theta}_n \right\rangle \tag{7.14}$$

$$= \left\langle \widetilde{\varphi}_g \widetilde{\theta}_k \left| \hat{H}_M \right| \widetilde{\varphi}_g \widetilde{\theta}_n \right\rangle + \left\langle \widetilde{\varphi}_g \widetilde{\theta}_k \left| \hat{H}_S \right| \widetilde{\varphi}_g \widetilde{\theta}_n \right\rangle + \left\langle \widetilde{\varphi}_g \widetilde{\theta}_k \left| \hat{V} \right| \widetilde{\varphi}_g \widetilde{\theta}_n \right\rangle \tag{7.15}$$

$$\begin{aligned} &= \left\langle \widetilde{\varphi}_g \left| \hat{H}_M \right| \widetilde{\varphi}_g \right\rangle \left\langle \widetilde{\theta}_k \left| \widetilde{\theta}_n \right\rangle + \left\langle \widetilde{\varphi}_g \left| \widetilde{\varphi}_g \right\rangle \left\langle \widetilde{\theta}_k \left| \hat{H}_S \right| \widetilde{\theta}_n \right\rangle + \right. \\ &\left. G\left(R, \theta_{\widetilde{\theta}_k, \widetilde{\theta}_n}, \alpha_{\widetilde{\varphi}_g, \widetilde{\varphi}_g}\right) \mu\left(\widetilde{\theta}_k, \widetilde{\theta}_n\right) \mu\left(\widetilde{\varphi}_g, \widetilde{\varphi}_g\right) \right. \end{aligned} \tag{7.16}$$

Approximate the dipole for the molecule ground state as sufficiently small to neglect. Similar to the semiconductor dipole approximation leading to Equation 7.12, the molecule dipole approximation is only accurate for certain systems. For example, in the limiting H_2 case, this approximation is not correct. However, the mathematical simplification resulting from this approximation is valuable.

$$= \widetilde{E}_g \left\langle \widetilde{\varphi}_g \left| \widetilde{\varphi}_g \right\rangle \delta(k-n) + \widetilde{E}_{\theta_n} \left\langle \widetilde{\theta}_k \left| \widetilde{\theta}_n \right\rangle \right. \tag{7.17}$$

$$= \left(\widetilde{E}_g + \widetilde{E}_{\theta_n}\right) \delta(k-n) \tag{7.18}$$

$$\left\langle \theta_k \left| \hat{H} \right| \theta_n \right\rangle = E_{\theta_n} \delta(k-n) \tag{7.19}$$

Next matrix elements for combined states with the semiconductor excited into one of the continuum states.

$$\left\langle \psi_k \left| \hat{H} \right| \psi_s \right\rangle = \left\langle \widetilde{\varphi}_g \widetilde{\psi}_k \left| \hat{H}_M + \hat{H}_S + \hat{V} \right| \widetilde{\varphi}_g \widetilde{\psi}_s \right\rangle \tag{7.20}$$

$$= \left\langle \widetilde{\varphi}_g \widetilde{\psi}_k \left| \hat{H}_M \right| \widetilde{\varphi}_g \widetilde{\psi}_s \right\rangle + \left\langle \widetilde{\varphi}_g \widetilde{\psi}_k \left| \hat{H}_S \right| \widetilde{\varphi}_g \widetilde{\psi}_s \right\rangle + \left\langle \widetilde{\varphi}_g \widetilde{\psi}_k \left| \hat{V} \right| \widetilde{\varphi}_g \widetilde{\psi}_s \right\rangle \tag{7.21}$$

$$\begin{aligned} &= \left\langle \widetilde{\varphi}_g \left| \hat{H}_M \right| \widetilde{\varphi}_g \right\rangle \left\langle \widetilde{\psi}_k \left| \widetilde{\psi}_s \right\rangle + \left\langle \widetilde{\varphi}_g \left| \widetilde{\varphi}_g \right\rangle \left\langle \widetilde{\psi}_k \left| \hat{H}_S \right| \widetilde{\psi}_s \right\rangle + \right. \right. \\ &\left. \left. G\left(R, \theta_{\widetilde{\psi}_k, \widetilde{\psi}_s}, \alpha_{\widetilde{\varphi}_g, \widetilde{\varphi}_g}\right) \mu\left(\widetilde{\psi}_k, \widetilde{\psi}_s\right) \mu\left(\widetilde{\varphi}_g, \widetilde{\varphi}_g\right) \right. \right. \end{aligned} \tag{7.22}$$

Approximate the dipole for the molecule ground state as small enough to neglect.

$$= \widetilde{E}_g \left\langle \widetilde{\varphi}_g \left| \widetilde{\varphi}_g \right\rangle \delta(k-s) + \widetilde{E}_s \left\langle \widetilde{\psi}_k \left| \widetilde{\psi}_s \right\rangle \right. \right. \tag{7.23}$$

$$= \left(\widetilde{E}_g + \widetilde{E}_s\right) \delta(k-s) \tag{7.24}$$

$$\left\langle \psi_k \left| \hat{H} \right| \psi_s \right\rangle = E_s \delta(k-s) \tag{7.25}$$

Now compute cross-coupling matrix elements between each of the combined states. First, coupling between combined states with the semiconductor excited into one of the surface states and combined states with the molecule excited.

$$\left\langle \theta_n \left| \hat{H} \right| \varphi_m \right\rangle = \left\langle \widetilde{\varphi}_g \widetilde{\theta}_n \left| \hat{H}_M + \hat{H}_S + \hat{V} \right| \widetilde{\varphi}_{e_m} \widetilde{\psi}_o \right\rangle \tag{7.26}$$

$$= \left\langle \widetilde{\varphi}_g \widetilde{\theta}_n \left| \hat{H}_M \right| \widetilde{\varphi}_{e_m} \widetilde{\psi}_o \right\rangle + \left\langle \widetilde{\varphi}_g \widetilde{\theta}_n \left| \hat{H}_S \right| \widetilde{\varphi}_{e_m} \widetilde{\psi}_o \right\rangle + \left\langle \widetilde{\varphi}_g \widetilde{\theta}_n \left| \hat{V} \right| \widetilde{\varphi}_{e_m} \widetilde{\psi}_o \right\rangle \tag{7.27}$$

$$\begin{aligned} &= \left\langle \widetilde{\varphi}_g \left| \hat{H}_M \right| \widetilde{\varphi}_{e_m} \right\rangle \left\langle \widetilde{\theta}_n \left| \widetilde{\psi}_o \right\rangle + \left\langle \widetilde{\varphi}_g \left| \widetilde{\varphi}_{e_m} \right\rangle \left\langle \widetilde{\theta}_n \left| \hat{H}_S \right| \widetilde{\psi}_o \right\rangle + \right. \right. \\ &\left. \left. G\left(R, \theta_{\widetilde{\theta}_n, \widetilde{\psi}_o}, \alpha_{\widetilde{\varphi}_g, \widetilde{\varphi}_{e_m}}\right) \mu\left(\widetilde{\theta}_n, \widetilde{\psi}_o\right) \mu\left(\widetilde{\varphi}_g, \widetilde{\varphi}_{e_m}\right) \right. \right. \end{aligned} \tag{7.28}$$

All semiconductor states are orthogonal, even surface to bulk.

$$= G\left(R, \theta_{\tilde{\theta}_n, \tilde{\psi}_o}, \alpha_{\tilde{\varphi}_g, \tilde{\varphi}_{e_m}}\right)\mu\left(\tilde{\theta}_n, \tilde{\psi}_o\right)\mu\left(\tilde{\varphi}_g, \tilde{\varphi}_{e_m}\right) \tag{7.29}$$

Define a coupling term $W_{n,m}$.

$$W_{n,m} \equiv \left\langle \theta_n \left| \hat{H} \right| \varphi_m \right\rangle = G_W\left(R, \theta_{\tilde{\theta}_n, \tilde{\psi}_o}, \alpha_{\tilde{\varphi}_g, \tilde{\varphi}_{e_m}}\right)\mu\left(\tilde{\theta}_n, \tilde{\psi}_o\right)\mu\left(\tilde{\varphi}_g, \tilde{\varphi}_{e_m}\right) \tag{7.30}$$

The orientation portion of the coupling, G, is written with a subscript to keep the theory general by treating surface state phenomena separate from bulk states. Simplify the notation for a single excited molecule state.

$$W_n \equiv \left\langle \theta_n \left| \hat{H} \right| \varphi_e \right\rangle = G_W\left(R, \theta_{\tilde{\theta}_n, \tilde{\psi}_o}, \alpha_{\tilde{\varphi}_g, \tilde{\varphi}_e}\right)\mu\left(\tilde{\theta}_n, \tilde{\psi}_o\right)\mu\left(\tilde{\varphi}_g, \tilde{\varphi}_e\right) \tag{7.31}$$

Next compute the cross-coupling between combined states with the semiconductor excited into one of the bulk states and combined states with the molecule excited.

$$\left\langle \psi_s \left| \hat{H} \right| \varphi_m \right\rangle = \left\langle \tilde{\varphi}_g \tilde{\psi}_s \left| \hat{H}_M + \hat{H}_S + \hat{V} \right| \tilde{\varphi}_{e_m} \tilde{\psi}_o \right\rangle \tag{7.32}$$

$$= \left\langle \tilde{\varphi}_g \tilde{\psi}_s \left| \hat{H}_M \right| \tilde{\varphi}_{e_m} \tilde{\psi}_o \right\rangle + \left\langle \tilde{\varphi}_g \tilde{\psi}_s \left| \hat{H}_S \right| \tilde{\varphi}_{e_m} \tilde{\psi}_o \right\rangle + \left\langle \tilde{\varphi}_g \tilde{\psi}_s \left| \hat{V} \right| \tilde{\varphi}_{e_m} \tilde{\psi}_o \right\rangle \tag{7.33}$$

$$\begin{aligned} &= \left\langle \tilde{\varphi}_g \left| \hat{H}_M \right| \tilde{\varphi}_{e_m} \right\rangle \left\langle \tilde{\psi}_s \middle| \tilde{\psi}_o \right\rangle + \left\langle \tilde{\varphi}_g \middle| \tilde{\varphi}_{e_m} \right\rangle \left\langle \tilde{\psi}_s \left| \hat{H}_S \right| \tilde{\psi}_o \right\rangle + \\ &G\left(R, \theta_{\tilde{\psi}_s, \tilde{\psi}_o}, \alpha_{\tilde{\varphi}_g, \tilde{\varphi}_{e_m}}\right)\mu\left(\tilde{\psi}_s, \tilde{\psi}_o\right)\mu\left(\tilde{\varphi}_g, \tilde{\varphi}_{e_m}\right) \end{aligned} \tag{7.34}$$

$$= G\left(R, \theta_{\tilde{\psi}_s, \tilde{\psi}_o}, \alpha_{\tilde{\varphi}_g, \tilde{\varphi}_{e_m}}\right)\mu\left(\tilde{\psi}_s, \tilde{\psi}_o\right)\mu\left(\tilde{\varphi}_g, \tilde{\varphi}_{e_m}\right) \tag{7.35}$$

Define a coupling term $V_{s,m}$.

$$V_{s,m} \equiv \left\langle \psi_s \left| \hat{H} \right| \varphi_m \right\rangle = G\left(R, \theta_{\tilde{\psi}_s, \tilde{\psi}_o}, \alpha_{\tilde{\varphi}_g, \tilde{\varphi}_{e_m}}\right)\mu\left(\tilde{\psi}_s, \tilde{\psi}_o\right)\mu\left(\tilde{\varphi}_g, \tilde{\varphi}_{e_m}\right) \tag{7.36}$$

Simplify the notation for a single excited molecule state.

$$V_s \equiv \langle \psi_s | \hat{H} | \varphi \rangle = G\left(R, \theta_{\tilde{\psi}_s, \tilde{\psi}_o}, \alpha_{\tilde{\varphi}_g, \tilde{\varphi}_e}\right) \mu(\tilde{\psi}_s, \tilde{\psi}_o) \mu(\tilde{\varphi}_g, \tilde{\varphi}_e) \tag{7.37}$$

Finally, compute the cross-coupling between combined states with the semiconductor excited into one of the bulk states and combined states with the semiconductor excited into one of the surface states. The states are solutions to the same Hamiltonian and therefore are orthogonal and the result should be zero. The following derivation verifies this expectation.

$$\langle \psi_s | \hat{H} | \theta_n \rangle = \langle \tilde{\varphi}_g \tilde{\psi}_s | \hat{H}_M + \hat{H}_S + \hat{V} | \tilde{\varphi}_g \tilde{\theta}_n \rangle \tag{7.38}$$

$$= \langle \tilde{\varphi}_g \tilde{\psi}_s | \hat{H}_M | \tilde{\varphi}_g \tilde{\theta}_n \rangle + \langle \tilde{\varphi}_g \tilde{\psi}_s | \hat{H}_S | \tilde{\varphi}_g \tilde{\theta}_n \rangle + \langle \tilde{\varphi}_g \tilde{\psi}_s | \hat{V} | \tilde{\varphi}_g \tilde{\theta}_n \rangle \tag{7.39}$$

$$\begin{aligned} &= \langle \tilde{\varphi}_g | \hat{H}_M | \tilde{\varphi}_g \rangle \langle \tilde{\psi}_s | \tilde{\theta}_n \rangle + \langle \tilde{\varphi}_g | \tilde{\varphi}_g \rangle \langle \tilde{\psi}_s | \hat{H}_S | \tilde{\theta}_n \rangle + \\ &G\left(R, \theta_{\tilde{\psi}_s, \tilde{\theta}_n}, \alpha_{\tilde{\varphi}_g, \tilde{\varphi}_g}\right) \mu(\tilde{\psi}_s, \tilde{\theta}_n) \mu(\tilde{\varphi}_g, \tilde{\varphi}_g) \end{aligned} \tag{7.40}$$

Approximate the dipole for the molecule ground state as small enough to neglect.

$$= \left[\tilde{E}_g + \tilde{E}_{\theta_n}\right] \langle \tilde{\psi}_s | \tilde{\theta}_n \rangle \tag{7.41}$$

$$\langle \psi_s | \hat{H} | \theta_n \rangle = 0 \tag{7.42}$$

Substitute Equation 7.12, 7.19, 7.25, 7.30, 7.36, and 7.42 into Equation 7.6.

$$\overline{H} = \begin{bmatrix} E_{\varphi_1} & \cdots & 0 & W^*_{1,1} & \cdots & W^*_{N,1} & V^*_{1,1} & \cdots \\ \vdots & \ddots & \vdots & \vdots & \ddots & \vdots & \vdots & \cdots \\ 0 & \cdots & E_{\varphi_M} & W^*_{1,M} & \cdots & W^*_{N,M} & V^*_{1,M} & \cdots \\ W_{1,1} & \cdots & W_{1,M} & E_{\theta_1} & \cdots & 0 & 0 & \cdots \\ \vdots & \ddots & \vdots & \vdots & \ddots & \vdots & \vdots & \cdots \\ W_{N,1} & \cdots & W_{N,M} & 0 & \cdots & E_{\theta_N} & 0 & \cdots \\ V_{1,1} & \cdots & V_{1,M} & 0 & \cdots & 0 & E_1 & \cdots \\ \vdots & \vdots & \vdots & \vdots & \vdots & \vdots & \vdots & \ddots \end{bmatrix} \tag{7.43}$$

Notice that that large matrix of Equation 7.43 can be simplified into several smaller submatrices. Treating the problem with each submatrix simplifies future computations and helps to visualize the nature of the solution.

$$\overline{H} = \begin{bmatrix} \overline{E}_{\varphi} & \overline{W}^{*T} & \overline{V}^{*T} \\ \overline{W} & \overline{E}_{\theta} & \overline{0} \\ \overline{V} & \overline{0} & \overline{E}_i \end{bmatrix} \tag{7.44}$$

Each of the matrices $\overline{E}_{\varphi}$, $\overline{E}_{\theta}$, and $\overline{E}_i$ are diagonal. The submatrix $\overline{E}_{\varphi}$ is MxM. The submatrix $\overline{E}_{\theta}$ is NxN. The submatrix $\overline{E}_i$ is square but without defined size. The number of semiconductor excited states in the conduction band is very large and the exact number of states is not a necessary parameter of the theory, as will be shown later.

When the semiconductor ground state dipole is nonzero and cannot be neglected then the matrix $\overline{E}_{\varphi}$ is full and conjugate symmetric. When the molecule ground state dipole is nonzero and cannot be neglected then the matrices $\overline{E}_{\theta}$, $\overline{E}_i$, and $\overline{0}$ become full and conjugate symmetric.

Remember all state functions are chosen orthonormal therefore Equation 3.23 is the identity matrix.

$$\bar{S} = \bar{I} \tag{7.45}$$

Because of orthonormal states, the energy solutions to Equation 3.24 are the eigenvalues of Equation 7.44.

7.2 Vibronic Energy Levels

For vibronic energy levels, define φ_m with the molecular portion $\tilde{\varphi}_m$ including vibronic states. The index 'm' indicates some set of vibrational quantum numbers. For example, the ground vibrational state has the following meaning: $m = 0 \Rightarrow \{\upsilon_1 = 0, \upsilon_2 = 0, \ldots \upsilon_{3P-6} = 0,\}$. For this analysis a single excited electronic state is considered and $M > 1$ due to vibronic levels, not due to electronic levels.

Vibrational states are associated with a single state potential energy curve, as shown in Figure 4.1. An example is the vibrational states on the excited potential energy curve. A product form is applicable when the vibrational coordinates are separated into normal coordinates based on symmetry of the molecule.

$$\tilde{\varphi}_{e_m} \equiv \tilde{\varphi}_e \Pi_{i=1}^{3P-6} \chi_{\upsilon_i} \tag{7.46}$$

Compute the matrix elements. Include Equation 5.19 for the nuclear Hamiltonian. First, compute $\langle \varphi_k | \hat{H} | \varphi_m \rangle$.

$$\langle \varphi_k | \hat{H} | \varphi_m \rangle = \left\langle \tilde{\varphi}_e \Pi_{i=1}^{3P-6} \chi_{\upsilon'_i} \tilde{\psi}_o \middle| \hat{H}_M + \hat{H}_S + \hat{V} + \hat{H}_M^{(nuc)} \middle| \tilde{\varphi}_e \Pi_{j=1}^{3P-6} \chi_{\upsilon_j} \tilde{\psi}_o \right\rangle \tag{7.47}$$

Expand the summation.

$$
\begin{aligned}
&= \left\langle \widetilde{\varphi}_e \Pi_{i=1}^{3P-6} \chi_{\upsilon'_i} \widetilde{\psi}_o \left| \hat{H}_M \right| \widetilde{\varphi}_e \Pi_{j=1}^{3P-6} \chi_{\upsilon_j} \widetilde{\psi}_o \right\rangle + \\
&\left\langle \widetilde{\varphi}_e \Pi_{i=1}^{3P-6} \chi_{\upsilon'_i} \widetilde{\psi}_o \left| \hat{H}_S \right| \widetilde{\varphi}_e \Pi_{j=1}^{3P-6} \chi_{\upsilon_j} \widetilde{\psi}_o \right\rangle + \\
&\left\langle \widetilde{\varphi}_e \Pi_{i=1}^{3P-6} \chi_{\upsilon'_i} \widetilde{\psi}_o \left| \hat{V} \right| \widetilde{\varphi}_e \Pi_{j=1}^{3P-6} \chi_{\upsilon_j} \widetilde{\psi}_o \right\rangle + \\
&\left\langle \widetilde{\varphi}_e \Pi_{i=1}^{3P-6} \chi_{\upsilon'_i} \widetilde{\psi}_o \left| \hat{H}_M^{(nuc)} \right| \widetilde{\varphi}_e \Pi_{j=1}^{3P-6} \chi_{\upsilon_j} \widetilde{\psi}_o \right\rangle
\end{aligned}
\tag{7.48}
$$

Separate according to common coordinates. For the coupling term, use the Condon approximation. This is the first term of the Taylor series approximation.

$$
\begin{aligned}
&= \left\langle \widetilde{\varphi}_e \left| \hat{H}_M \right| \widetilde{\varphi}_e \right\rangle \left\langle \Pi_{i=1}^{3P-6} \chi_{\upsilon'_i} \left| \Pi_{j=1}^{3P-6} \chi_{\upsilon_j} \right\rangle \left\langle \widetilde{\psi}_o \left| \widetilde{\psi}_o \right\rangle \right. \right. + \\
&\left\langle \widetilde{\varphi}_e \left| \widetilde{\varphi}_e \right\rangle \left\langle \Pi_{i=1}^{3P-6} \chi_{\upsilon'_i} \left| \Pi_{j=1}^{3P-6} \chi_{\upsilon_j} \right\rangle \left\langle \widetilde{\psi}_o \left| \hat{H}_S \right| \widetilde{\psi}_o \right\rangle \right. \right. + \\
&G\left(R, \theta_{\widetilde{\psi}_o, \widetilde{\psi}_o}, \alpha_{\widetilde{\varphi}_e, \widetilde{\varphi}_e}\right) \mu\left(\widetilde{\varphi}_e, \widetilde{\varphi}_e\right) \left\langle \Pi_{i=1}^{3P-6} \chi_{\upsilon'_i} \left| \Pi_{j=1}^{3P-6} \chi_{\upsilon_j} \right\rangle \mu\left(\widetilde{\psi}_o, \widetilde{\psi}_o\right) + \right. \\
&\left\langle \widetilde{\varphi}_e \left| \widetilde{\varphi}_e \right\rangle \left\langle \Pi_{i=1}^{3P-6} \chi_{\upsilon'_i} \left| \hat{H}_M^{(nuc)} \right| \Pi_{j=1}^{3P-6} \chi_{\upsilon_j} \right\rangle \left\langle \widetilde{\psi}_o \left| \widetilde{\psi}_o \right\rangle \right. \right.
\end{aligned}
\tag{7.49}
$$

The vibrational states are associated with the same excited state potential energy curve, therefore they are orthogonal. The $\delta(k-m)$ function indicates all vibrational states are the same on both sides of the matrix element.

$$
= \left(\widetilde{E}_e + \widetilde{E}_o + \sum\nolimits_{i=1}^{3P-6} \left(\upsilon_i(m) + \frac{1}{2} \right) \hbar \omega_i \right) \delta(k-m) \tag{7.50}
$$

Equation 7.50 is identical to Equation 7.11, with the addition of vibronic energy levels. Notice that it is not necessary to approximate the ground state semiconductor dipole as zero. The coupling term is eliminated by vibrational state orthogonality. This is a consequence of the Born-Oppenheimer approximation.

Next consider the coupling matrix element between the molecule excited states and the semiconductor continuum states. In this case the vibrational levels are for two different potential energy surfaces, one for the ground electronic state and one for the excited electronic state. Therefore they are not orthogonal. Also, the continuum state is now defined as the total ground including vibrational energy.

$$\left|\psi_s\right\rangle \equiv \left|\widetilde{\varphi}_g\right\rangle \left|\Pi_{i=1}^{3P-6}\chi_{\upsilon'_i=0}\right\rangle \left|\widetilde{\psi}_s\right\rangle \tag{7.51}$$

$$\left\langle\psi_s\left|\hat{H}\right|\varphi_m\right\rangle = \left\langle\widetilde{\varphi}_g\Pi_{i=1}^{3P-6}\chi_{\upsilon'_i=0}\widetilde{\psi}_s\left|\hat{H}_M+\hat{H}_S+\hat{V}+\hat{H}_M^{(nuc)}\right|\widetilde{\varphi}_e\Pi_{i=1}^{3P-6}\chi_{\upsilon'_i}\widetilde{\psi}_o\right\rangle \tag{7.52}$$

Separate each term in the summation.

$$\begin{aligned}
&= \left\langle\widetilde{\varphi}_g\left|\hat{H}_M\right|\widetilde{\varphi}_e\right\rangle\left\langle\Pi_{i=1}^{3P-6}\chi_{\upsilon'_i=0}\left|\Pi_{j=1}^{3P-6}\chi_{\upsilon_j}\right\rangle\right\langle\widetilde{\psi}_s\left|\widetilde{\psi}_o\right\rangle + \\
&\left\langle\widetilde{\varphi}_g\left|\widetilde{\varphi}_e\right\rangle\left\langle\Pi_{i=1}^{3P-6}\chi_{\upsilon'_i=0}\left|\Pi_{j=1}^{3P-6}\chi_{\upsilon_j}\right\rangle\right\langle\widetilde{\psi}_s\left|\hat{H}_S\right|\widetilde{\psi}_o\right\rangle + \\
&G\left(R,\theta_{\widetilde{\psi}_s,\widetilde{\psi}_o},\alpha_{\widetilde{\varphi}_g,\widetilde{\varphi}_e}\right)\mu\left(\widetilde{\varphi}_g,\widetilde{\varphi}_e\right)\left\langle\Pi_{i=1}^{3P-6}\chi_{\upsilon'_i=0}\left|\Pi_{j=1}^{3P-6}\chi_{\upsilon_j}\right\rangle\mu\left(\widetilde{\psi}_s,\widetilde{\psi}_o\right)\right. \\
&\left\langle\widetilde{\varphi}_g\left|\widetilde{\varphi}_e\right\rangle\left\langle\widetilde{\psi}_s\left|\widetilde{\psi}_o\right\rangle\right\langle\Pi_{i=1}^{3P-6}\chi_{\upsilon'_i=0}\left|\hat{H}_M^{(nuc)}\right|\Pi_{j=1}^{3P-6}\chi_{\upsilon_j}\right\rangle
\end{aligned} \tag{7.53}$$

All terms are zero due to orthogonality, except the third term.

$$= G\left(R,\theta_{\widetilde{\psi}_s,\widetilde{\psi}_o},\alpha_{\widetilde{\varphi}_g,\widetilde{\varphi}_e}\right)\mu\left(\widetilde{\psi}_s,\widetilde{\psi}_o\right)\mu\left(\widetilde{\varphi}_g,\widetilde{\varphi}_e\right)\left\langle\Pi_{i=1}^{3P-6}\chi_{\upsilon'_i=0}\left|\Pi_{j=1}^{3P-6}\chi_{\upsilon_j}\right\rangle\right. \tag{7.54}$$

Define a coupling term which includes vibrational motion, $U_{s,m}$. Again, the index number m represents a set of vibrational quantum numbers.

$$\begin{aligned}
&U_{s,m} \equiv \left\langle\psi_s\left|\hat{H}\right|\varphi_m\right\rangle = \\
&G\left(R,\theta_{\widetilde{\psi}_s,\widetilde{\psi}_o},\alpha_{\widetilde{\varphi}_g,\widetilde{\varphi}_e}\right)\mu\left(\widetilde{\psi}_s,\widetilde{\psi}_o\right)\mu\left(\widetilde{\varphi}_g,\widetilde{\varphi}_e\right)\left\langle\Pi_{i=1}^{3P-6}\chi_{\upsilon'_i=0}\left|\Pi_{j=1}^{3P-6}\chi_{\upsilon_j(m)}\right\rangle\right.
\end{aligned} \tag{7.55}$$

Similar to the case for electronic energy levels, Equation 7.50 and Equation 7.55 are the matrix elements for solving Equation 7.6. The coupling term includes the Franck-Condon factors $\left\langle \Pi_{i=1}^{3P-6} \chi_{\upsilon'_i=0} \middle| \Pi_{j=1}^{3P-6} \chi_{\upsilon_j(m)} \right\rangle$. This is a new effect when including vibronic energies. Similar calculations for the surface state matrix elements $\langle \theta_n | \hat{H} | \varphi_m \rangle$.

$$W_{s,m} \equiv \langle \theta_n | \hat{H} | \varphi_m \rangle = G\left(R, \theta_{\tilde{\theta}_n, \tilde{\psi}_o}, \alpha_{\tilde{\varphi}_g, \tilde{\varphi}_e}\right) \mu\left(\tilde{\theta}_n, \tilde{\psi}_o\right) \mu\left(\tilde{\varphi}_g, \tilde{\varphi}_e\right) \left\langle \Pi_{i=1}^{3P-6} \chi_{\upsilon'_i=0} \middle| \Pi_{j=1}^{3P-6} \chi_{\upsilon_j(m)} \right\rangle \tag{7.56}$$

The final form of $\overline{H}$ for the case with vibronic levels is similar to Equation 7.44.

$$\overline{H} = \begin{bmatrix} \overline{E}_\varphi & \overline{W}^{*T} & \overline{U}^{*T} \\ \overline{W} & \overline{E}_\theta & \overline{0} \\ \overline{U} & \overline{0} & \overline{E}_i \end{bmatrix} \tag{7.57}$$

Equation 7.57 is different from Equation 7.44 in the following ways. First, $\overline{E}_\varphi$ is always diagonal, even if the semiconductor ground dipole moment is nonzero. Also, $\overline{V}$ is written as $\overline{U}$ and includes the Franck-Condon terms $\left\langle \Pi_{i=1}^{3P-6} \chi_{\upsilon'_i=0} \middle| \Pi_{j=1}^{3P-6} \chi_{\upsilon_j(m)} \right\rangle$ in each submatrix element. The submatrix letter for $\overline{W}$ is left unchanged because later in the thesis surface states are neglected in the vibronic level analysis. However, similar to the case for $\overline{V}$, the only difference between $\overline{W}$ with vibronic levels and $\overline{W}$ without vibronic levels is the inclusion of the terms $\left\langle \Pi_{i=1}^{3P-6} \chi_{\upsilon'_i=0} \middle| \Pi_{j=1}^{3P-6} \chi_{\upsilon_j(m)} \right\rangle$. The submatrices $\overline{E}_\theta$ and $\overline{E}_i$ are identical as the case without vibronic levels and become full conjugate symmetric if the molecule ground electronic state dipole moment is nonzero.

At this stage of the derivation, all terms of Equation 7.43 have a defined form. Equation 7.43 (as either Equation 7.44 or Equation 7.57) is the mathematical equation useful to determine the new combined system energy levels and transition dipole matrix elements. Solving this equation is the subject of the next section.

8.0 Energy Shift Prediction of Model

Now that a model has been created, and many simplifying assumptions explained, the next step is to apply the model to derive a mathematical expression for calculating new energy levels due to semiconductor coupling. The combined molecule and semiconductor energy, without coupling $E_{\varphi} = \left(\widetilde{E}_e + \widetilde{E}_o\right)$, is modified by the mixing of states in the variation theory summation. Then, based on the new energy levels, determine if any experimental trends are predicted.

Before proceeding, it is useful to stop and summarize all approximations at this point in the model development.

1. Born-Oppenheimer approximation which separates nuclear and electronic energy level models
2. Zero-order model of combined system, representing combined state function as product of molecule and semiconductor states and without the property of antisymmetry under electron exchange.
3. Weak coupling. This is achieved with a bridge-anchor molecular spacer, spatially separating the initially excited state function from the semiconductor.
4. Harmonic oscillator Hamiltonian with normal coordinate approximation for molecule vibrational energy analysis.
5. Semiconductor vibrational energy neglected.

6. Hamiltonian terms for energy interaction between molecule and semiconductor is approximated as a dipole-dipole interaction.
7. Neglect semiconductor vibrational motion.
8. Either neglect molecule vibrational motion or apply Condon approximation (first term in Taylor series expansion).
9. Approximate orientation term in dipole-dipole model as constant, independent of state. This approximation has been discussed but not yet included in the mathematics. Part of the justification for constant G when treating vibrational levels is consistency with the use of the Condon approximation. This section will demonstrate where and why this approximation is required.
10. Combined system state function approximated with variational theory linear superposition of higher energy system excited states.
11. Most system excited states neglected in variation equation.
12. Approximate molecule ground state dipole as zero.
13. Approximate semiconductor ground state dipole as zero ($M = 1$ case).

These approximations are necessary to obtain a simple, closed-form mathematical expression of the semiconductor coupling effect on the molecule. It is shown later that certain predictions of the resulting mathematical model are not physically realistic. This is because of the approximations. The most radical approximations, such as constant orientation term, and neglecting the ground state dipoles, require further adjustments to the theory in order to alleviate certain nonphysical predictions.

8.1 Coupled Energy Levels

Find the energy due to semiconductor coupling by substituting Equation 7.44 and Equation 7.45 into Equation 3.24. Solve for the energy E, with the understanding that this is an approximation to the correct combined total energy. Each of the submatrics $\bar{I}'$, $\bar{I}''$, and $\bar{I}'''$ are square identity matrices. The size of $\bar{I}'$ is MxM and the size of $\bar{I}''$ is NxN. The submatrix $\bar{I}'''$ presently has no defined size.

$$\begin{vmatrix} \overline{E}_{\varphi} - E\bar{I}' & \overline{W}^{*T} & \overline{V}^{*T} \\ \overline{W} & \overline{E}_{\theta} - E\bar{I}'' & \overline{0} \\ \overline{V} & \overline{0} & \overline{E}_{i} - E\bar{I}''' \end{vmatrix} = 0 \tag{8.1}$$

Solutions to Equation 8.1 provide a set of new energies for the system composed of a linear combination of states according to Equation 7.4 and Equation 7.5. The determinant of Equation 8.1 is solved with an identity derived in the Appendix.

$$\begin{vmatrix} \overline{A} & \overline{B} & \overline{C} \\ \overline{B}^{T} & \overline{D} & \overline{0} \\ \overline{C}^{T} & \overline{0} & \overline{E} \end{vmatrix} = \left| \overline{D} \right\| \overline{E} \left\| \overline{A} - \overline{B}\overline{D}^{-1}\overline{B}^{T} - \overline{C}\overline{E}^{-1}\overline{C}^{T} \right| \tag{8.2}$$

Equation 8.2 simplifies Equation 8.1.

$$\left| \overline{E}_{\theta} - \overline{E} \middle| \overline{E}_{i} - \overline{E} \right\| \left(\overline{E}_{\varphi} - \overline{E} \right) - \overline{W}^{*T} \left(\overline{E}_{\theta} - \overline{E} \right)^{-1} \overline{W} - \overline{V}^{*T} \left(\overline{E}_{i} - \overline{E} \right)^{-1} \overline{V} \right| = 0 \tag{8.3}$$

In Equation 8.3 the matrices have the following property and size.

Submatrix	Size and properties
$\left(\overline{E}_{\varphi} - \overline{E}\right)$	MxM diagonal matrix
$\left(\overline{E}_{\theta} - \overline{E}\right)^{-1}$	NxN diagonal matrix
$\left(\overline{E}_{i} - \overline{E}\right)^{-1}$	Square diagonal matrix – size not specified
$\overline{W}$	NxM
$\overline{V}$	Number of rows not specified, M columns

Table 8.1. Submatrix sizes.

When $W = V = 0$ then the roots are the original energies, as expected. This is because the original separated semiconductor and molecule energies are unchanged when the semiconductor and molecule do not interact. Now define a quantity called $J(E)$.

$$J(E) \equiv \left(\overline{E}_{\varphi} - \overline{E}\right) - \overline{W}^{*T}\left(\overline{E}_{\theta} - \overline{E}\right)^{-1}\overline{W} - \overline{V}^{*T}\left(\overline{E}_{i} - \overline{E}\right)^{-1}\overline{V} \tag{8.4}$$

The two determinants on the left side of Equation 8.3 can be divided out of the equation. The reason for this is because their roots are completely contained within $J(E)$. Specifically, setting $J(E)$ equal to zero and solving for the roots results in identical roots as are found by solving Equation 8.3. However, care must be taken with $J(E)$. The issue is that when Equation 8.3 is multiplied, no inverse terms remain. The fractional terms cancel. In contrast, $J(E)$ has roots in the denominator terms and this is an issue when solving for E in regions where E can equal one of E_n or E_i. This is not a problem for E_n because the states associated with these energies are modeled discrete and relatively separated in energy. Then E can be constrained to not equal one of the

E_n. The states associated with E_i however are effectively continuous. Therefore, when a solution E is in the range of E_i care must be taken in handling the inverse terms. This is addressed later.

The benefit of working with Equation 8.4, $J(E)$ directly, instead of Equation 8.3 is that the energies are localized to each corresponding coupling matrix element. This is seen by expanding Equation 8.4. $J(E)$ is an M x M matrix. First, consider diagonal terms of the $J(E)$ matrix.

$$J_{a,a} = \left(E_{\varphi_a} - E\right) - \sum_{n=1}^{N} \frac{\left|W_{na}\right|^2}{E_{\theta_n} - E} - \sum_s \frac{\left|V_{sa}\right|^2}{E_s - E} \tag{8.5}$$

The diagonal terms have the convenient property that all coupling elements are magnitude squared. This is important because physically measurable properties correspond to the magnitude squared of these elements. The off-diagonal terms retain cross correlated products.

$$J_{a,b} = J_{b,a}^* = -\sum_{n=1}^{N} \frac{W_{na}^* W_{nb}}{E_{\theta_n} - E} - \sum_s \frac{V_{na}^* V_{nb}}{E_s - E} \tag{8.6}$$

The energy roots of $J(E)$ are real because of the complex conjugate transpose nature of the matrix $J(E)$.

8.2 Single Excited State

When $M = 1$, then $J(E)$ is no longer a matrix (see Table 8.1). The systems under investigation in this thesis do not have more than a single excited molecule state. When vibrational energies are neglected, the $M = 1$ case is a nice approximation.

$$J(E) = (E_\varphi - E) - \sum_{n=1}^{N} \frac{|W_{nn}|^2}{E_{\theta_n} - E} - \sum_s \frac{|V_{ss}|^2}{E_s - E} \tag{8.7}$$

Equation 8.7 is approaching an equation that can yield solutions for E. However the very large summation over the semiconductor bulk states presents a problem. An approach to simplifying Equation 8.7 starts by substituting for the coupling elements from Equation 7.31 and Equation 7.37. At this point G_W and G must be written as independent of the state. This approximation enables factoring them out of the summation.

$$J(E) = (E_\varphi - E) - \sum_{n=1}^{N} \frac{\left| G_W \langle \tilde{\theta}_n | \hat{\mu}_S | \tilde{\psi}_o \rangle \langle \tilde{\varphi}_g | \hat{\mu}_M | \tilde{\varphi}_e \rangle \right|^2}{E_{\theta_n} - E} - \sum_s \frac{\left| G \langle \tilde{\varphi}_g | \hat{\mu}_M | \tilde{\varphi}_e \rangle \langle \tilde{\psi}_s | \hat{\mu}_S | \tilde{\psi}_o \rangle \right|^2}{E_s - E} \tag{8.8}$$

Factor molecule terms not depending on a summation index.

$$J(E) = (E_\varphi - E) - \left| \langle \tilde{\varphi}_g | \hat{\mu}_M | \tilde{\varphi}_e \rangle \right|^2 \left\{ G_W^2 \sum_{n=1}^{N} \frac{\left| \langle \tilde{\theta}_n | \hat{\mu}_S | \tilde{\psi}_o \rangle \right|^2}{E_{\theta_n} - E} + G^2 \sum_s \frac{\left| \langle \tilde{\psi}_s | \hat{\mu}_S | \tilde{\psi}_o \rangle \right|^2}{E_s - E} \right\} \tag{8.9}$$

Define a term for the summation over the semiconductor bulk continuum states. The subscript on Z_D indicates a discrete summation over all states.

$$Z_D(E) = \sum_s \frac{\left|\langle \tilde{\psi}_s | \hat{\mu}_S | \tilde{\psi}_o \rangle\right|^2}{E - E_s} \tag{8.10}$$

Substitute and rearrange terms. Multiplication by -1 has no effect because $J(E)$ is set to zero when solving for the energy.

$$J(E) = E - E_\varphi - \left|\langle \tilde{\varphi}_g | \hat{\mu}_M | \tilde{\varphi}_e \rangle\right|^2 \left\{ G_W^2 \sum_{n=1}^{N} \frac{\left|\langle \tilde{\theta}_n | \hat{\mu}_S | \tilde{\psi}_o \rangle\right|^2}{E - E_{\theta_n}} + G^2 Z_D(E) \right\} \tag{8.11}$$

Equation 8.11 has a number of roots (solutions for E). The roots are independent of the sign of G. This is important because the sign of G cannot be experimentally measured. The total number of roots is equal to the order of $J(E)$. Count the number of possible roots as follows. First, one root is possible due to the E_φ energy. Next, N roots are possible due to the summation over the surface states. Finally, an undefined number of roots are possible due to the summation $Z_D(E)$ because the limits of this summation have not yet been defined. The conclusion is that a very large number of solutions to $J(E) = 0$ are possible.

It is expected that the lowest energy roots of Equation 8.11 contain large contribution from the energy of states $|\varphi\rangle$ and $|\theta_n\rangle$. The higher energy roots are for states having the largest energy contribution from $|\psi_s\rangle$. The research is investigating the effect of the semiconductor on the molecule and not the molecule on the semiconductor. So the roots related to perturbation of $|\psi_s\rangle$ are not interesting. What is needed is an

approach to eliminate the additional roots created by including $Z_D(E)$ corresponding to the semiconductor, while simultaneously keeping the effect of the semiconductor $Z_D(E)$ on the roots associated with $|\varphi\rangle$ and $|\theta_n\rangle$. If such an approach is found then the problem becomes more tractable.

The solution: reduce the order of $Z_D(E)$ in E by approximating it as a lower order function. Consider that these discrete energy levels are approximately a continuum of energy levels. Finding a continuous approximation to $Z_D(E)$ provides a mathematical convenience and is also physically justifiable. The semiconductor bulk has closely spaced energy levels compared to the thermal energy KT, where K is Boltzmann's constant and T is temperature in Kelvin. For example, translational energy is approximated with a particle-in-a-box potential. The energy levels decrease as the side of the "box" increases. The relatively large size of the semiconductor particle ensures tightly spaced energy levels. The number of states in an infinitesimal energy range $E + dE$ is later defined as the density of the states.

Define a summation, similar to Equation 8.10, but weighted by the energy difference between each state. This is shown in Equation 8.12. It is very similar to a summation which gives the Rieman integral in the limit of the spacing between energy levels going to zero. However, in Equation 8.12 the difference between increments of E_s are not constant and furthermore degeneracy could lead to some increments being zero.

$$Z_A(E) \equiv \sum_{s=s'}^{s''} (E_{s+1} - E_s) \frac{\left|\langle \tilde{\psi}_s | \hat{\mu}_S | \tilde{\psi}_o \rangle\right|^2}{E - E_s} \tag{8.12}$$

Select a fixed increment , Δ, which is equal to the largest energy spacing in the summation. This is a very small spacing because of the nearly continuous nature of the energy levels. Define a term σ_d equal to the number of states within the increment for each summation index. The summation is now over energy levels instead of states, with the approximation that $\langle \tilde{\psi}_s | \hat{\mu}_S | \tilde{\psi}_o \rangle$ is equal to $\langle \tilde{\psi}_d | \hat{\mu}_S | \tilde{\psi}_o \rangle$ for all $\tilde{\psi}_s$ with the same E_d.

$$Z_A(E) \approx \sum_{d=d'}^{d''} \Delta \cdot \sigma_d \frac{\left| \langle \tilde{\psi}_d | \hat{\mu}_S | \tilde{\psi}_o \rangle \right|^2}{E - E_d} \tag{8.13}$$

Equation 8.13 is the discrete definition of a Rieman integral and from basic theorems of calculus can be written as an integral in the limit as $\Delta \to 0$.

$$\lim_{\Delta \to 0} \Delta \sum_{d=d'}^{d''} \sigma_d \frac{\left| \langle \tilde{\psi}_d | \hat{\mu}_S | \tilde{\psi}_o \rangle \right|^2}{E - E_d} = \int_{E_{d'}}^{E_{d''}} \sigma(E') \frac{\left| \langle \tilde{\psi}_{E'} | \hat{\mu}_S | \tilde{\psi}_o \rangle \right|^2}{E - E'} dE' \tag{8.14}$$

Divide both sides by delta and define $\lim_{\Delta \to 0} \left\{ \frac{\sigma(E')}{\Delta} \right\}$ as the density of states.

$$\rho(E') \equiv \lim_{\Delta \to 0} \left\{ \frac{\sigma(E')}{\Delta} \right\} \tag{8.15}$$

This represents the number of states in a given energy increment. This definition is justified by the common density of states definition $\rho(E) \equiv dN/dE$, where N is the number of states per unit volume. Equation 8.15 is simply the definition of an integral. Now a term approximately equal to the original $Z_D(E)$, as defined in Equation 8.10, is available.

$$Z_D(E) \approx \int_{E_{d'}}^{E_{d''}} \rho(E') \frac{\left|\langle \tilde{\psi}_{E'} | \hat{\mu}_S | \tilde{\psi}_o \rangle\right|^2}{E - E'} dE' \tag{8.16}$$

Care must be taken because this integral has singularity problems if E is in the range of the integral. So, Equation 8.16 requires $E < E_{d'}$. Physically this means that the energy under consideration is below the lower limit of the semiconductor continuum states. Cases when $E > E_{d'}$ are covered with further approximations to the integral later in the thesis. Define a new function, $Z(E)$, equal to the right side of Equation 8.16. This function is an approximation of $Z_D(E)$.

$$Z(E) \equiv \int_{E_{d'}}^{E_{d''}} \frac{\rho(\tilde{E}') \left|\langle \tilde{\psi}_{E'} | \hat{\mu}_S | \tilde{\psi}_o \rangle\right|^2}{E - (\tilde{E}_g + \tilde{E}')} d\tilde{E}' \tag{8.17}$$

The advantage of Equation 8.17 is in reducing the dimensionality of $J(E)$. The term $Z_D(E)$ in Equation 8.11 presents a problem because of the uncounted number of terms in the summation over the bulk semiconductor states. If Equation 8.17 either is solvable or can be approximated, and if the order of the solution is anything less than the number of terms in the summation $\sum_s \frac{\left|\langle \tilde{\psi}_s | \hat{\mu}_S | \tilde{\psi}_o \rangle\right|^2}{E - E_s}$, then the number of roots which must be computed is reduced. Also, the form of Equation 8.17 suggests that its value as a function of energy can be measured by an absorption experiment. Substitute $Z(E)$ into Equation 8.11. This presents the opportunity of experimentally measuring a value which contributes to a prediction of new energy values due to coupling. Setting Equation 8.18

to zero enables solving for the roots which are new energy values E due to the coupling effect of the semiconductor on the molecule.

$$J(E) \approx E - E_{\varphi} - \left|\left\langle \tilde{\varphi}_g \left| \hat{\mu}_M \right| \tilde{\varphi}_e \right\rangle\right|^2 \left\{ G_W^2 \sum_{n=1}^{N} \frac{\left|\left\langle \tilde{\theta}_n \left| \hat{\mu}_S \right| \tilde{\psi}_o \right\rangle\right|^2}{E - E_{\theta_n}} + G^2 Z(E) \right\} = 0 \qquad (8.18)$$

8.3 Multiple Excited States

Although the system typically has only a single available excited electronic state, it does have multiple excited vibrational states. Therefore, a solution to Equation 8.4 for $M > 1$ is necessary to properly model the absorption spectrum. Simplify the derivation by neglecting surface states. These can be included with the bulk states later but it is helpful to not single them out in the derivation.

To measure the energy shift, start again with Equation 8.4. Rewrite Equation 8.4 without surface states and with the coupling between the semiconductor and the molecule which includes vibrational states. In this case, the symbol $U_{s,m}$ from Equation 7.55 is used instead of the symbol $V_{s,m}$ from Equation 7.36. The matrix element $U_{s,m}$ indicates inclusion of the vibration states. Therefore, for Equation 8.4, in place of matrix $\overline{V}$ the matrix $\overline{U}$ is substituted.

$$\bar{J}(E) \equiv \left(\overline{E}_{\varphi} - \overline{E}\right) - \overline{U}^{*T} \left(\overline{E}_i - \overline{E}\right)^{-1} \overline{U} \qquad (8.19)$$

Solving this equation is challenging because the simplification for $M = 1$ no longer applies. Both Equation 8.5 and Equation 8.6 must be accounted for in the solution.

Substitute Equation 7.55 into Equation 8.5 and Equation 8.6 (while using the symbol U_{sa} in place of V_{sa}). The indexes represent a set of vibrational quantum numbers, for example, $a = 1 \Rightarrow \{\upsilon_1 = 1, \upsilon_2 = 0, \ldots \upsilon_{3P-6} = 0,\}$. Surface states are not directly identified and are applicable to the following derivation for the cases when the coupling to surface states is the same as to bulk states. Notice that G is approximated as a constant, independent of the vibrational state.

$$J_{a,a} = \left(E_{\varphi_a} - E\right) + \sum_s \frac{\left|G\langle\widetilde{\psi}_s|\hat{\mu}_S|\widetilde{\psi}_o\rangle\langle\widetilde{\varphi}_g|\hat{\mu}_M|\widetilde{\varphi}_e\rangle\Pi_{k=1}^{3P-6}\langle 0_k|\upsilon_k(a)\rangle\right|^2}{E - E_s} \tag{8.20}$$

$$J_{a,b} = J_{b,a}^* = \sum_s \frac{\left[G\langle\widetilde{\psi}_s|\hat{\mu}_S|\widetilde{\psi}_o\rangle\langle\widetilde{\varphi}_g|\hat{\mu}_M|\widetilde{\varphi}_e\rangle\Pi_{k=1}^{3P-6}\langle 0_k|\upsilon_k(a)\rangle\right]^* G\langle\widetilde{\psi}_s|\hat{\mu}_S|\widetilde{\psi}_o\rangle\langle\widetilde{\varphi}_g|\hat{\mu}_M|\widetilde{\varphi}_e\rangle\Pi_{k=1}^{3P-6}\langle 0_k|\upsilon_k(b)\rangle}{E - E_s} \tag{8.21}$$

Factor terms independent of the bulk semiconductor state index and then use the definition of $Z_D(E)$ from Equation 8.10.

$$J_{a,a} = \left(E_{\varphi_a} - E\right) + G^2\left|\langle\widetilde{\varphi}_g|\hat{\mu}_M|\widetilde{\varphi}_e\rangle\right|^2 \Pi_{k=1}^{3P-6}\left|\langle 0_k|\upsilon_k(a)\rangle\right|^2 Z_D(E) \tag{8.22}$$

$$J_{a,b} = J_{b,a}^* = G^2\left|\langle\widetilde{\varphi}_g|\hat{\mu}_M|\widetilde{\varphi}_e\rangle\right|^2 \Pi_{k=1}^{3P-6}\langle 0_k|\upsilon_k(a)\rangle^*\langle 0_k|\upsilon_k(b)\rangle Z_D(E) \tag{8.23}$$

As an example, write the resulting $\bar{J}(E)$ matrix for the case $M = 3$.

$$\bar{J}(E)=\begin{bmatrix} E_{\varphi_1}-E & 0 & 0 \\ 0 & E_{\varphi_2}-E & 0 \\ 0 & 0 & E_{\varphi_3}-E \end{bmatrix}+$$
$$G^2\left|\left\langle\tilde{\varphi}_g\left|\hat{\mu}_M\right|\tilde{\varphi}_e\right\rangle\right|^2 Z_D(E)$$
$$\begin{bmatrix} \Pi_{k=1}^{3P-6}\left|\langle 0_k|\upsilon_k(1)\rangle\right|^2 & \Pi_{k=1}^{3P-6}\langle 0_k|\upsilon_k(1)\rangle^*\langle 0_k|\upsilon_k(2)\rangle & \Pi_{k=1}^{3P-6}\langle 0_k|\upsilon_k(1)\rangle^*\langle 0_k|\upsilon_k(3)\rangle \\ \Pi_{k=1}^{3P-6}\langle 0_k|\upsilon_k(2)\rangle^*\langle 0_k|\upsilon_k(1)\rangle & \Pi_{k=1}^{3P-6}\left|\langle 0_k|\upsilon_k(2)\rangle\right|^2 & \Pi_{k=1}^{3P-6}\langle 0_k|\upsilon_k(2)\rangle^*\langle 0_k|\upsilon_k(3)\rangle \\ \Pi_{k=1}^{3P-6}\langle 0_k|\upsilon_k(3)\rangle^*\langle 0_k|\upsilon_k(1)\rangle & \Pi_{k=1}^{3P-6}\langle 0_k|\upsilon_k(3)\rangle^*\langle 0_k|\upsilon_k(2)\rangle & \Pi_{k=1}^{3P-6}\left|\langle 0_k|\upsilon_k(3)\rangle\right|^2 \end{bmatrix} \quad (8.24)$$

The new energy levels are equal to the roots of $\left|\bar{J}(E)\right|=0$. Rewrite Equation 8.24 with $T\equiv G^2\left|\left\langle\tilde{\varphi}_g\left|\hat{\mu}_M\right|\tilde{\varphi}_e\right\rangle\right|^2 Z_D(E)$ and $c_i\equiv\Pi_{k=1}^{3P-6}\langle 0_k|\upsilon_k(i)\rangle$ when calculating the determinant.

$$\left|\bar{J}(E)\right|=\begin{vmatrix} E_{\varphi_1}-E+Tc_1*c_1 & Tc_1*c_2 & Tc_1*c_3 \\ Tc_2*c_1 & E_{\varphi_2}-E+Tc_2*c_2 & Tc_2*c_3 \\ Tc_3*c_1 & Tc_3*c_2 & E_{\varphi_3}-E+Tc_3*c_3 \end{vmatrix}=0 \quad (8.25)$$

Calculate the determinant.

$$\begin{aligned} &E^3-\left(E_{\varphi_1}+E_{\varphi_2}+E_{\varphi_3}+T\left(c_1^2+c_2^2+c_3^2\right)\right)E^2+ \\ &\left(\begin{aligned} &E_{\varphi_1}E_{\varphi_3}+E_{\varphi_2}E_{\varphi_3}+E_{\varphi_1}E_{\varphi_2}+ \\ &T\left[\left(c_2^2+c_3^2\right)E_{\varphi_1}+\left(c_1^2+c_3^2\right)E_{\varphi_2}+\left(c_1^2+c_2^2\right)E_{\varphi_3}\right] \end{aligned}\right)E- \\ &\left(E_{\varphi_1}E_{\varphi_2}E_{\varphi_3}+T\left(c_1^2E_{\varphi_2}E_{\varphi_3}+c_2^2E_{\varphi_1}E_{\varphi_3}+c_3^2E_{\varphi_1}E_{\varphi_2}\right)\right)=0 \end{aligned} \quad (8.26)$$

Move the terms without c_i to one side.

$$\begin{aligned} &E^3-\left(E_{\varphi_1}+E_{\varphi_2}+E_{\varphi_3}\right)E^2+\left(E_{\varphi_1}E_{\varphi_3}+E_{\varphi_2}E_{\varphi_3}+E_{\varphi_1}E_{\varphi_2}\right)E-E_{\varphi_1}E_{\varphi_2}E_{\varphi_3}= \\ &T\left\{\begin{aligned} &\left(c_1^2+c_2^2+c_3^2\right)E^2-\left[\left(c_2^2+c_3^2\right)E_{\varphi_1}+\left(c_1^2+c_3^2\right)E_{\varphi_2}+\left(c_1^2+c_2^2\right)E_{\varphi_3}\right]E+ \\ &\left(c_1^2E_{\varphi_2}E_{\varphi_3}+c_2^2E_{\varphi_1}E_{\varphi_3}+c_3^2E_{\varphi_1}E_{\varphi_2}\right) \end{aligned}\right\} \end{aligned} \quad (8.27)$$

The term on the left is easy to simplify.

$$\begin{aligned}&\left(E-E_{\varphi_1}\right)\left(E-E_{\varphi_2}\right)\left(E-E_{\varphi_3}\right)= \\ &T\left\{\begin{array}{l}\left(c_1^2+c_2^2+c_3^2\right)E^2-\left[\left(c_2^2+c_3^2\right)E_{\varphi_1}+\left(c_1^2+c_3^2\right)E_{\varphi_2}+\left(c_1^2+c_2^2\right)E_{\varphi_3}\right]E+ \\ \left(c_1^2E_{\varphi_2}E_{\varphi_3}+c_2^2E_{\varphi_1}E_{\varphi_3}+c_3^2E_{\varphi_1}E_{\varphi_2}\right)\end{array}\right\}\end{aligned} \tag{8.28}$$

Manipulate the right side of Equation 8.28 into the form shown in Equation 8.29.

$$\begin{aligned}&\left(E-E_{\varphi_1}\right)\left(E-E_{\varphi_2}\right)\left(E-E_{\varphi_3}\right)= \\ &T\left\{c_1^2\left(E-E_{\varphi_2}\right)\left(E-E_{\varphi_3}\right)+c_2^2\left(E-E_{\varphi_1}\right)\left(E-E_{\varphi_3}\right)+c_3^2\left(E-E_{\varphi_1}\right)\left(E-E_{\varphi_2}\right)\right\}\end{aligned} \tag{8.29}$$

Divide both sides by the left side.

$$1=T\left\{\frac{c_1^2}{\left(E-E_{\varphi_1}\right)}+\frac{c_2^2}{\left(E-E_{\varphi_2}\right)}+\frac{c_3^2}{\left(E-E_{\varphi_3}\right)}\right\} \tag{8.30}$$

Using the definition of $Z_D(E)$ from Equation 8.10, and substituting $c_i \equiv \Pi_{k=1}^{3P-6}\langle 0_k \,|\, \upsilon_k(i)\rangle$, the result is an equation relating $Z_D(E)$ to the Franck-Condon terms.

$$Z_D(E)=\frac{1}{G^2\left|\left\langle\tilde{\varphi}_g\left|\hat{\mu}_M\right|\tilde{\varphi}_e\right\rangle\right|^2\sum_{m=1}^{M}\frac{\Pi_{k=1}^{3P-6}\left|\langle 0_k\,|\,\upsilon_k(m)\rangle\right|^2}{E-E_{\varphi_m}}} \tag{8.31}$$

It is clear that while the derivation of Equation 8.30 used M = 3, the result is applicable to any positive integer value of M. Equation 8.31 is not a definition of $Z_D(E)$. The function $Z_D(E)$ remains as defined in Equation 8.10. What Equation 8.31 shows is a relationship useful for calculating the new energy E when the molecule is coupled to the semiconductor.

Notice that because $Z(E) \approx Z_D(E)$, it is valid to substitute $Z(E)$ for $Z_D(E)$ in Equation 8.31. This is done in the experimental comparison section of the thesis. Also, as a check on the accuracy of Equation 8.31, it is easy to see that for $M = 1$, Equation 8.31 reduces to the Equation 8.11 form.

$$G^2 \left| \left\langle \tilde{\varphi}_g \left| \hat{\mu}_M \right| \tilde{\varphi}_e \right\rangle \right|^2 Z_D(E) = E - E_\varphi \tag{8.32}$$

Equation 8.31 is a weighted harmonic mean of the energy shift from each discrete state. It is known that the harmonic mean of a sequence tends towards the smallest member of the sequence. Large outliers have little effect. In the absence of the weighting terms, Equation 8.31 tends towards the smallest of the set. The Franck-Condon terms $\Pi_{k=1}^{3P-6} \left| \left\langle 0_k \left| \upsilon_k(m) \right\rangle \right| \right|^2$ offset this effect and can lead to a state having more influence than what would normally be expected based on $E - E_{\varphi_m}$.

For each of the initial states one of the energy differences in Equation 8.31 is smallest. Because of the harmonic mean property this energy dominates. This is the energy that is closest to the unperturbed energy. Therefore, Equation 8.31 potentially gives M different results for E. Each of the M potential initial states produces one of the new total energy values E.

8.4 Experimental Trend Predictions

The roots of $J(E)$ are the energy levels of the system when coupling is included. A full solution to $J(E)=0$ is required to determine these new energy levels. Before proceeding to this solution, in Section10, it is interesting to investigate whether any trends are predicted that do not require explicitly finding these roots.

Energy levels effect spectroscopy through the energy difference between states according to Equation 4.39. The experiment of interest is between the system initially in the total ground state Ψ_{ε} (Equation 7.5) associated with uncoupled state $|\varphi_{TG}\rangle$, in comparison to the system in the excited state Ψ_{E} (Equation 7.4) associated with uncoupled state $|\varphi_{m}\rangle$. Equation 8.18 makes a trend prediction if the solution to $J(E)=0$ is predictably different for Ψ_{ε} in comparison to Ψ_{E}.

Consider first the $Z(E)$ term and for $M = 1$. Equation 8.17 shows that this term is always negative when $E<(\widetilde{E}_{g}+E_{d'})$. Let $Z(E)$ be negative, neglect the surface states, and set Equation 8.18 to zero. Solve for E. The result is an inequality, $E=E_{\varphi}+(something<0)$. Therefore, the energy E after including coupling is smaller than the energy E_{φ} of the separated states. The effect of semiconductor bulk state coupling is what lowers the energy of the coupled state.

$$E<E_{\varphi} \tag{8.33}$$

Now consider Equation 8.18 for the ground state Ψ_{ε} and with the same approximations.

$$J(\varepsilon) \approx \varepsilon - E_{TG} - G^2 \left| \langle \tilde{\varphi}_g | \hat{\mu}_M | \tilde{\varphi}_e \rangle \right|^2 Z(\varepsilon) \tag{8.34}$$

A similar inequality result.

$$\varepsilon < E_{TG} \tag{8.35}$$

Since $E_{TG} < E_{\varphi}$ and since the integration limits of $Z(E)$ are unaffected, this means the denominator of the integrand for $Z(\varepsilon)$ is larger than the denominator of the integrand for $Z(E)$, Equation 8.17. The numerator of the integrand is unaffected. So, each term in the integral of $Z(E)$ is smaller for the ground state in comparison to the excited state. The result is a general relationship between $Z(E)$ for the ground in comparison to the excited state.

$$|Z(\varepsilon)| < |Z(E)| \tag{8.36}$$

Therefore, the conclusion is that both the ground state energy and the excited state energy become smaller and also that the ground state energy is shifted less than the excited state energy. The resulting experimental prediction is that the absorption spectrum, a measure of the energy difference between these two states, is red-shifted for the coupled system in comparison to the uncoupled system.

$$E_{TG} - \varepsilon < E_{\varphi} - E \tag{8.37}$$

However, the surface states can reduce or even eliminate this effect. The reason is E can be larger or smaller than E_{θ_n} in the summation over E_{θ_n} in Equation 8.18. Also, the additional terms due to the summation over the surface states leads to additional solutions for E near E_φ. The uncoupled excited state energy may be smaller or larger than the coupled excited state energy. Although the ground state is most likely unaffected because E_{TG} is sufficiently smaller than any of the E_{θ_n}, a general trend of energy difference between the excited and ground state is not predictable. The absorption spectrum may red-shift less or could even blue shift when surface states are involved.

For $M > 1$, an experimental trend that can be predicted from the model is a broadening of the absorption spectrum. Whereas surface states presented a problem for predicting the energy dependence of the absorption spectrum, it is the surface states themselves that result in a prediction for a broadening of the absorption spectrum.

Consider that when the surface state energies E_{θ_n} are close to the excited state energy E_φ, these total N + 1 states with similar energy become available to the excitation source due to molecule / semiconductor coupling. For the separate system only the state $|\varphi\rangle$ with energy is E_φ available. Determine the nature of these new states by starting with Equation 4.20 and substitute Equation 7.44, with M = 1. Solve for the matrix $\begin{bmatrix} a & \bar{c} & \bar{b} \end{bmatrix}^T$.

$$\begin{bmatrix} E_\varphi - E & \overline{W}^{*T} & \overline{V}^{*T} \\ \overline{W} & \overline{E}_\theta - \overline{E} & \overline{0} \\ \overline{V} & \overline{0} & \overline{E}_i - \overline{E} \end{bmatrix} \begin{bmatrix} a \\ \bar{c} \\ \bar{b} \end{bmatrix} = \overline{0} \tag{8.38}$$

When the coupling is small the new states are approximately equal to the original states.

$$\begin{bmatrix} a \\ \bar{c} \\ \bar{b} \end{bmatrix} \approx \left\{ \begin{bmatrix} 1 \\ 0 \\ \vdots \\ 0 \\ 0 \\ \vdots \\ 0 \end{bmatrix}, \begin{bmatrix} 0 \\ 1 \\ \vdots \\ 0 \\ 0 \\ \vdots \\ 0 \end{bmatrix}, \cdots \begin{bmatrix} 0 \\ 0 \\ \vdots \\ 1 \\ 0 \\ \vdots \\ 0 \end{bmatrix}, \begin{bmatrix} 0 \\ 0 \\ \vdots \\ 0 \\ 1 \\ \vdots \\ 0 \end{bmatrix}, \cdots \right\} \tag{8.39}$$

As the coupling increases, new states become mixtures of the original states. The absorption experiment starts in state $\left|\varphi_{TG}\right\rangle$, which is $\left|\widetilde{\varphi}_g\right\rangle\left|\widetilde{\psi}_o\right\rangle$. The final state is described by the variation summation in Equation 7.4. Since the semiconductor bulk states are separated in energy by a larger amount than the surface states, it is expected that the new states primarily consist of $\left|\varphi\right\rangle$ and $\left|\theta_n\right\rangle$ linear combinations. These states have been created from $\left|\widetilde{\varphi}_e\right\rangle\left|\widetilde{\psi}_o\right\rangle$ and $\left|\widetilde{\varphi}_g\right\rangle\left|\widetilde{\theta}_n\right\rangle$, respectively. Therefore, the radiation induced transition to these new states is effectively transitioning to a linear combination of $\left|\widetilde{\varphi}_e\right\rangle$ and $\left|\widetilde{\theta}_n\right\rangle$. In the limit of very weak molecule / semiconductor interaction, the dipole coupling element (matrix element in Equation 4.16) primarily retains the nature of the original system, either the molecule or the semiconductor.

Figure 8.1 shows a graphical visualization of the new states created by the surface state coupling. The left column of energy levels represents the energy associated with each of three surface states $\left|\widetilde{\theta}_0\right\rangle$, $\left|\widetilde{\theta}_1\right\rangle$, and $\left|\widetilde{\theta}_2\right\rangle$. The right energy level is associated with state $\left|\widetilde{\varphi}_e\right\rangle$. The middle energy levels are associated with the four coupled states, each

composed of a linear combination of $\left|\widetilde{\theta}_0\right\rangle$, $\left|\widetilde{\theta}_1\right\rangle$, $\left|\widetilde{\theta}_2\right\rangle$, and $\left|\widetilde{\varphi}_e\right\rangle$; along with small amount of bulk state mixing which are not shown for clarity.

An absorption experiment measures the energy difference between the ground state, shown at the bottom of Figure 8.1, and the coupled states. Since $N + 1$ states are available, each with similar energy to the original excited state energy, therefore the spectrum broadens as the incident energy of the absorption spectrum is varied over the range of energy differences to the coupled state energies.

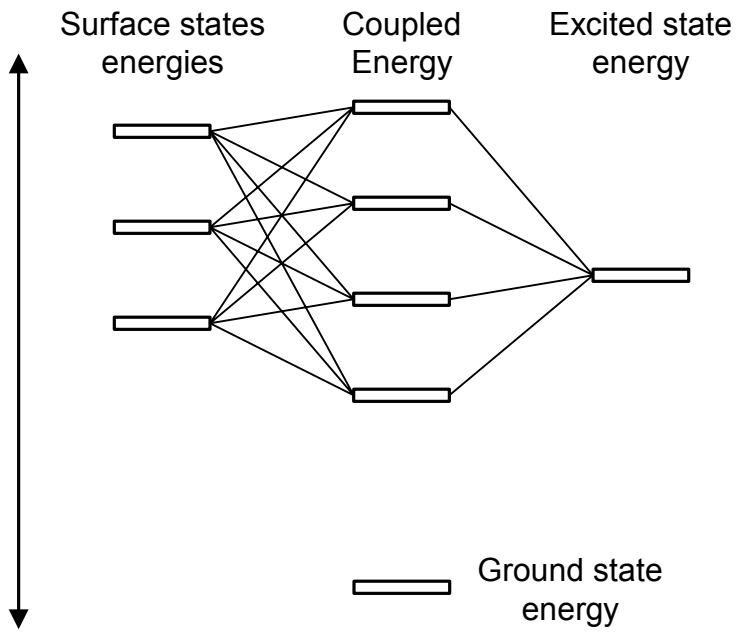

Figure 8.1 Energy diagram showing coupled state energy levels in comparison to the ground state energy level.

9.0 Absorption Intensity Prediction of Model

An important property of the absorption experiment is the intensity of the resulting spectrum. The intensity is determined by the dipole coupling element in Equation 4.16. Solve this equation for the new system to determine the effect of coupling. The states of interest are the total ground and the combined state with the molecule in its excited state, both coupled to the semiconductor.

$$\left|\left\langle \psi_{initial} \left|\hat{\mu}\right| \psi_{final} \right\rangle\right|^2 = \left|\left\langle \Psi_{\varepsilon} \left|\hat{\mu}\right| \Psi_{E} \right\rangle\right|^2 \tag{9.1}$$

The solution is separated into two approximations to simplify the math. First, ignore surface states and compute the dipole coupling element between the ground and excited state. Next, ignore the semiconductor effect on the ground state and include the effect of surface states on the excited state.

Multiple excited states are not treated because these are only used for vibronic levels in this research and in that case the intensity there is only one electronic energy level and the vibronic level intensity is treated with Franck-Condon factors which are not affected by the coupling. The energy levels, however, are affected.

9.1 Surface States Neglected

Equation 9.2 is the dipole coupling element for the first case.

$$\left|\left\langle \Psi_\varepsilon \left|\hat{\mu}\right| \Psi_E \right\rangle\right|^2 = \left|\left\langle \sum_{m'=1}^{M'} a_{m'}^{(i)} \varphi_{m'} + \sum_{s'} b_{s'}^{(i)} \psi_{s'} \left|\hat{\mu}\right| \sum_{m=1}^{M} a_m^{(f)} \varphi_m + \sum_s b_s^{(f)} \psi_s \right\rangle\right|^2 \tag{9.2}$$

A further simplification is to consider only a single excited state. Therefore, M = 1.

$$= \left|\left\langle a^{(i)} \varphi^{(i)} + \sum_{s'} b_{s'}^{(i)} \psi_{s'} \left|\hat{\mu}\right| a^{(f)} \varphi^{(f)} + \sum_s b_s^{(f)} \psi_s \right\rangle\right|^2 \tag{9.3}$$

Cross multiply the sums.

$$= \begin{vmatrix} a^{(i)*} a^{(f)} \left\langle \varphi^{(i)} \left|\hat{\mu}\right| \varphi^{(f)} \right\rangle + \sum_{s'} \sum_s b_{s'}^{(i)*} b_s^{(f)} \left\langle \psi_{s'} \left|\hat{\mu}\right| \psi_s \right\rangle + \\ a^{(f)} \sum_{s'} b_{s'}^{(i)*} \left\langle \psi_{s'} \left|\hat{\mu}\right| \varphi^{(f)} \right\rangle + a^{(i)*} \sum_s b_s^{(f)} \left\langle \varphi^{(i)} \left|\hat{\mu}\right| \psi_s \right\rangle \end{vmatrix}^2 \tag{9.4}$$

Other simplifications: approximate $b_{s'}^{(i)}$ as sufficiently small to neglect and $\left\langle \psi_{s'} \left|\hat{\mu}\right| \varphi^{(f)} \right\rangle$ also small enough to neglect. This results in Equation 9.4. Notice that the Equation 9.4 is nearly identical to a solution which neglects all coupling for the ground state. What is retained is the ground state coefficient $a^{(i)}$.

$$\left|\left\langle \Psi_\varepsilon \left|\hat{\mu}\right| \Psi_E \right\rangle\right|^2 = \left| a^{(i)*} a^{(f)} \left\langle \varphi^{(i)} \left|\hat{\mu}\right| \varphi^{(f)} \right\rangle + a^{(i)*} \sum_s b_s^{(f)} \left\langle \varphi^{(i)} \left|\hat{\mu}\right| \psi_s \right\rangle \right|^2 \tag{9.5}$$

Expand the magnitude squared.

$$\begin{aligned} &= \left|a^{(i)}\right|^2 \left|a^{(f)}\right|^2 \left|\left\langle \varphi^{(i)} \left|\hat{\mu}\right| \varphi^{(f)} \right\rangle\right|^2 + \\ &2\,\mathrm{Re}\left\{ \left|a^{(i)}\right|^2 a^{(f)} \left\langle \varphi^{(i)} \left|\hat{\mu}\right| \varphi^{(f)} \right\rangle \sum_s b_s^{(f)*} \left\langle \varphi^{(i)} \left|\hat{\mu}\right| \psi_s \right\rangle^* \right\} + \\ &\left|a^{(i)}\right|^2 \sum_s \sum_{s'} b_{s'}^{(f)*} b_s^{(f)} \left\langle \varphi^{(i)} \left|\hat{\mu}\right| \psi_{s'} \right\rangle^* \left\langle \varphi^{(i)} \left|\hat{\mu}\right| \psi_s \right\rangle \end{aligned} \tag{9.6}$$

Substitute the combined state function for each initial and final state. Also, express the dipole operator as a portion acting over the molecule coordinates and a portion acting over the semiconductor coordinates. Apply these values to each term of Equation 9.6 individually. First the transition dipole matrix element connecting the total ground state molecule and molecule excited state.

$$\left|\left\langle \varphi^{(i)}\left|\hat{\mu}\right|\varphi^{(f)}\right\rangle\right|^2 = \left\langle \widetilde{\varphi}_g\widetilde{\psi}_o\left|\hat{\mu}_M + \hat{\mu}_S\right|\widetilde{\varphi}_e\widetilde{\psi}_o\right\rangle \tag{9.7}$$

$$= \left\langle \widetilde{\psi}_o\left|\widetilde{\psi}_o\right\rangle\right\langle \widetilde{\varphi}_g\left|\hat{\mu}_M\right|\widetilde{\varphi}_e\right\rangle + \left\langle \widetilde{\varphi}_g\left|\widetilde{\varphi}_e\right\rangle\right\langle \widetilde{\psi}_o\left|\hat{\mu}_S\right|\widetilde{\psi}_o\right\rangle \tag{9.8}$$

$$= \left\langle \widetilde{\varphi}_g\left|\hat{\mu}_M\right|\widetilde{\varphi}_e\right\rangle \tag{9.9}$$

Next apply to the transition dipole matrix element connecting the total ground state and semiconductor excited state.

$$\left\langle \varphi^{(i)}\left|\hat{\mu}\right|\psi_s\right\rangle = \left\langle \widetilde{\varphi}_g\widetilde{\psi}_o\left|\hat{\mu}_M + \hat{\mu}_S\right|\widetilde{\varphi}_g\widetilde{\psi}_s\right\rangle \tag{9.10}$$

$$\left\langle \varphi^{(i)}\left|\hat{\mu}\right|\psi_s\right\rangle = \left\langle \widetilde{\psi}_o\left|\widetilde{\psi}_s\right\rangle\right\langle \widetilde{\varphi}_g\left|\hat{\mu}_M\right|\widetilde{\varphi}_g\right\rangle + \left\langle \widetilde{\varphi}_g\left|\widetilde{\varphi}_g\right\rangle\right\langle \widetilde{\psi}_o\left|\hat{\mu}_S\right|\widetilde{\psi}_s\right\rangle \tag{9.11}$$

$$\left\langle \varphi^{(i)}\left|\hat{\mu}\right|\psi_s\right\rangle = \left\langle \widetilde{\psi}_o\left|\hat{\mu}_S\right|\widetilde{\psi}_s\right\rangle \tag{9.12}$$

Substitute Equation 9.9 and Equation 9.12 into Equation 9.6.

$$\begin{aligned}&\left|\left\langle \Psi_\varepsilon\left|\hat{\mu}\right|\Psi_E\right\rangle\right|^2 = \left|a^{(i)}\right|^2\left|a^{(f)}\right|^2\left|\left\langle \widetilde{\varphi}_g\left|\hat{\mu}_M\right|\widetilde{\varphi}_e\right\rangle\right|^2 + \\ &2\,\mathrm{Re}\left\{a^{(i)}\right|^2 a^{(f)}\left\langle \widetilde{\varphi}_g\left|\hat{\mu}_M\right|\widetilde{\varphi}_e\right\rangle\sum_s b_s^{(f)*}\left\langle \widetilde{\psi}_o\left|\hat{\mu}_S\right|\widetilde{\psi}_s\right\rangle^*\Big\} + \\ &\left|a^{(i)}\right|^2\sum_s\sum_{s'} b_{s'}^{(f)*}b_s^{(f)}\left\langle \widetilde{\psi}_o\left|\hat{\mu}_S\right|\widetilde{\psi}_{s'}\right\rangle^*\left\langle \widetilde{\psi}_o\left|\hat{\mu}_S\right|\widetilde{\psi}_s\right\rangle\end{aligned} \tag{9.13}$$

A value for the coefficient $b_s^{(f)}$ is required. Start with Equation 4.20, substitute Equation 7.44, and solve for $\left[\bar{a} \quad \bar{c} \quad \bar{b}\right]^T$.

$$\begin{bmatrix} \bar{E}_\varphi - \bar{E} & \bar{W}^{*T} & \bar{V}^{*T} \\ \bar{W} & \bar{E}_\theta - \bar{E} & \bar{0} \\ \bar{V} & \bar{0} & \bar{E}_i - \bar{E} \end{bmatrix} \begin{bmatrix} \bar{a} \\ \bar{c} \\ \bar{b} \end{bmatrix} = \bar{0} \tag{9.14}$$

For the case under consideration M = 1 and N = 0. Expand each of the submatrices in Equation 9.14.

$$\begin{bmatrix} E_\varphi - E & V_1^* & V_2^* & \cdots \\ V_1 & E_1 - E & 0 & \cdots \\ V_2 & 0 & E_2 - E & 0 \\ \vdots & \vdots & 0 & \ddots \end{bmatrix} \begin{bmatrix} a \\ b_1 \\ b_2 \\ \vdots \end{bmatrix} = \bar{0} \tag{9.15}$$

Because of its diagonal nature, easily solve Equation 9.15 for the b_s coefficients, when $E \neq E_s$.

$$b_s = \frac{aV_s}{E - E_s} \tag{9.16}$$

Substitute Equation 9.16 into Equation 9.13. Recall that the subscript s indicates a summation running over all semiconductor excited states and that V_s is defined in Equation 7.37.

$$\left|\left\langle \Psi_\varepsilon \left|\hat{\mu}\right| \Psi_E \right\rangle\right|^2 = \left|a^{(i)}\right|^2 \left|a^{(f)}\right|^2$$
$$\left[\begin{array}{l} \left|\left\langle \widetilde{\varphi}_g \left|\hat{\mu}_M\right| \widetilde{\varphi}_e \right\rangle\right|^2 + \\ 2\,\mathrm{Re}\left\{\left\langle \widetilde{\varphi}_g \left|\hat{\mu}_M\right| \widetilde{\varphi}_e \right\rangle \sum_s \frac{V_s^*}{E^{(f)} - E_s} \left\langle \widetilde{\psi}_o \left|\hat{\mu}_S\right| \widetilde{\psi}_s \right\rangle^*\right\} + \\ \sum_s \sum_{s'} \frac{V_{s'}^*}{E^{(f)} - E_{s'}} \frac{V_s}{E^{(f)} - E_s} \left\langle \widetilde{\psi}_o \left|\hat{\mu}_S\right| \widetilde{\psi}_{s'} \right\rangle^* \left\langle \widetilde{\psi}_o \left|\hat{\mu}_S\right| \widetilde{\psi}_s \right\rangle \end{array}\right] \tag{9.17}$$

The next term that must be simplified is the coupling element V_s. Apply Equation 7.37 to Equation 9.17.

$$\begin{array}{l} \left|\left\langle \Psi_\varepsilon \left|\hat{\mu}\right| \Psi_E \right\rangle\right|^2 = \left|a^{(i)}\right|^2 \left|a^{(f)}\right|^2 \left|\left\langle \widetilde{\varphi}_g \left|\hat{\mu}_M\right| \widetilde{\varphi}_e \right\rangle\right|^2 + \\ \left|a^{(i)}\right|^2 \left|a^{(f)}\right|^2 2\,\mathrm{Re}\left\{\begin{array}{l} \left\langle \widetilde{\varphi}_g \left|\hat{\mu}_M\right| \widetilde{\varphi}_e \right\rangle \left\langle \widetilde{\varphi}_g \left|\hat{\mu}_M\right| \widetilde{\varphi}_e \right\rangle^* \\ \sum_s \frac{G^* \left\langle \widetilde{\psi}_s \left|\hat{\mu}_S\right| \widetilde{\psi}_o \right\rangle^*}{E^{(f)} - E_s} \left\langle \widetilde{\psi}_o \left|\hat{\mu}_S\right| \widetilde{\psi}_s \right\rangle^* \end{array}\right\} + \\ \left|a^{(i)}\right|^2 \left|a^{(f)}\right|^2 \sum_s \sum_{s'} \left(\begin{array}{l} \frac{G^* \left\langle \widetilde{\varphi}_g \left|\hat{\mu}_M\right| \widetilde{\varphi}_e \right\rangle^* \left\langle \widetilde{\psi}_{s'} \left|\hat{\mu}_S\right| \widetilde{\psi}_o \right\rangle^*}{E^{(f)} - E_{s'}} \\ \frac{G \left\langle \widetilde{\varphi}_g \left|\hat{\mu}_M\right| \widetilde{\varphi}_e \right\rangle \left\langle \widetilde{\psi}_s \left|\hat{\mu}_S\right| \widetilde{\psi}_o \right\rangle}{E^{(f)} - E_s} \end{array}\right) \left\langle \widetilde{\psi}_o \left|\hat{\mu}_S\right| \widetilde{\psi}_{s'} \right\rangle^* \left\langle \widetilde{\psi}_o \left|\hat{\mu}_S\right| \widetilde{\psi}_s \right\rangle \end{array} \tag{9.18}$$

Simplify Equation 9.18.

$$\left|\left\langle \Psi_\varepsilon \left|\hat{\mu}\right| \Psi_E \right\rangle\right|^2 =$$
$$\left|a^{(i)}\right|^2 \left|a^{(f)}\right|^2 \left|\left\langle \widetilde{\varphi}_g \left|\hat{\mu}_M\right| \widetilde{\varphi}_e \right\rangle\right|^2 \left[\begin{array}{l} 1 + 2G \sum_s \frac{\left|\left\langle \widetilde{\psi}_s \left|\hat{\mu}_S\right| \widetilde{\psi}_o \right\rangle\right|^2}{E^{(f)} - E_s} + \\ G^2 \sum_s \frac{\left|\left\langle \widetilde{\psi}_s \left|\hat{\mu}_S\right| \widetilde{\psi}_o \right\rangle\right|^2}{E^{(f)} - E_s} \sum_{s'} \frac{\left|\left\langle \widetilde{\psi}_{s'} \left|\hat{\mu}_S\right| \widetilde{\psi}_o \right\rangle\right|^2}{E^{(f)} - E_{s'}} \end{array}\right] \tag{9.19}$$

Substitute the definition of $Z_D(E)$, Equation 8.10.

$$\left|\left\langle \Psi_\varepsilon \left|\hat{\mu}\right| \Psi_E \right\rangle\right|^2 = \left|a^{(i)}\right|^2 \left|a^{(f)}\right|^2 \left|\left\langle \widetilde{\varphi}_g \left|\hat{\mu}_M\right| \widetilde{\varphi}_e \right\rangle\right|^2 \left(1 + 2GZ_D\left(E^{(f)}\right) + G^2 Z_D\left(E^{(f)}\right)^2\right) \tag{9.20}$$

Substitute for the $|a|^2$ terms. Determine by normalization.

$$|a|^2 + \sum\nolimits_s |b_s|^2 = 1 \tag{9.21}$$

Use Equation 9.16 for b_s, Equation 7.37 for the V_s value in the equation for b_s, and then solve for $|a|^2$.

$$|a(E)|^2 = \frac{1}{1 + G^2\left|\left\langle \widetilde{\varphi}_g \left|\hat{\mu}_M\right| \widetilde{\varphi}_e \right\rangle\right|^2 \sum_s \frac{\left|\left\langle \widetilde{\psi}_s \left|\hat{\mu}_S\right| \widetilde{\psi}_o \right\rangle\right|^2}{\left(E - E_s\right)^2}} \tag{9.22}$$

Substitute into Equation 9.20. Also, now that all coefficients have been eliminated, use the original notation of ε for ground energy and E for excited energy.

$$\left|\left\langle \Psi_\varepsilon \left|\hat{\mu}\right| \Psi_E \right\rangle\right|^2 = \frac{\left|\left\langle \widetilde{\varphi}_g \left|\hat{\mu}_M\right| \widetilde{\varphi}_e \right\rangle\right|^2 \left(1 + GZ_D\left(E^{(f)}\right)\right)^2}{\left(1 + G^2\left|\left\langle \widetilde{\varphi}_g \left|\hat{\mu}_M\right| \widetilde{\varphi}_e \right\rangle\right|^2 \sum_s \frac{\left|\left\langle \widetilde{\psi}_s \left|\hat{\mu}_S\right| \widetilde{\psi}_o \right\rangle\right|^2}{\left(\varepsilon - E_s\right)^2}\right)\left(1 + G^2\left|\left\langle \widetilde{\varphi}_g \left|\hat{\mu}_M\right| \widetilde{\varphi}_e \right\rangle\right|^2 \sum_s \frac{\left|\left\langle \widetilde{\psi}_s \left|\hat{\mu}_S\right| \widetilde{\psi}_o \right\rangle\right|^2}{\left(E - E_s\right)^2}\right)} \tag{9.23}$$

Equation 9.23 is the dipole transition strength for a transition between states $\left|\Psi_\varepsilon\right\rangle$ and $\left|\Psi_E\right\rangle$. An interesting quantity is to compare this dipole transition strength to the case with no coupling to the semiconductor.

$$R \equiv \frac{\left|\left\langle \Psi_\varepsilon \left|\hat{\mu}\right| \Psi_E \right\rangle\right|^2}{\left|\left\langle \varphi_{TG} \left|\hat{\mu}\right| \varphi \right\rangle\right|^2} \tag{9.24}$$

The uncoupled case is simple to derive because the semiconductor makes no transition.

$$\left|\left\langle \varphi_{TG}\left|\hat{\mu}\right|\varphi\right\rangle\right|^2 = \left|\left\langle \tilde{\varphi}_g\left|\hat{\mu}_M\right|\tilde{\varphi}_e\right\rangle\right|^2 \tag{9.25}$$

Substitute Equation 9.23 and Equation 9.25 into Equation 9.24.

$$R = \frac{\left(1+GZ_D\left(E^{(f)}\right)\right)^2}{\left(1+G^2\left|\left\langle \tilde{\varphi}_g\left|\hat{\mu}_M\right|\tilde{\varphi}_e\right\rangle\right|^2\sum_s \frac{\left|\left\langle \tilde{\psi}_s\left|\hat{\mu}_S\right|\tilde{\psi}_o\right\rangle\right|^2}{\left(\varepsilon-E_s\right)^2}\right)\left(1+G^2\left|\left\langle \tilde{\varphi}_g\left|\hat{\mu}_M\right|\tilde{\varphi}_e\right\rangle\right|^2\sum_s \frac{\left|\left\langle \tilde{\psi}_s\left|\hat{\mu}_S\right|\tilde{\psi}_o\right\rangle\right|^2}{\left(E-E_s\right)^2}\right)} \tag{9.26}$$

Simplify Equation 9.26 by defining a new term, analogous to $Z_D(E)$.

$$Y_D(E) = \sum_s \frac{\left|\left\langle \tilde{\psi}_s\left|\hat{\mu}_S\right|\tilde{\psi}_o\right\rangle\right|^2}{\left(E-E_s\right)^2} \tag{9.27}$$

Substitute Equation 9.27 into Equation 9.26.

$$R = \frac{\left(1+GZ_D\left(E^{(f)}\right)\right)^2}{\left(1+G^2\left|\left\langle \tilde{\varphi}_g\left|\hat{\mu}_M\right|\tilde{\varphi}_e\right\rangle\right|^2 Y_D(\varepsilon)\right)\left(1+G^2\left|\left\langle \tilde{\varphi}_g\left|\hat{\mu}_M\right|\tilde{\varphi}_e\right\rangle\right|^2 Y_D(E)\right)} \tag{9.28}$$

An identical derivation as for $Z(E)$ can be applied to a new term called $Y(E)$.

$$Y_D(E) \approx \int \frac{\rho\left(\tilde{E}'\right)\left\langle \tilde{\psi}_{E'}\left|\hat{\mu}_S\right|\tilde{\psi}_o\right\rangle\right|^2}{\left(E-\left(\tilde{E}_g+\tilde{E}'\right)\right)^2} d\tilde{E}' \equiv Y(E) \tag{9.29}$$

Equation 9.28 predicts the effect of the semiconductor on the intensity of the molecule transition between its ground and excited state in an absorption spectroscopy experiment. First, notice that the denominator is always larger than zero. This is because all terms of $Y_D(E)$ are squared and so $Y_D(E)$ is positive. Also G is squared and so is positive. The denominator predicts that the intensity decreases due to coupling.

In the numerator of Equation 9.28 the term $Z_D(E)$ is always negative when the molecule energy level is below the lowest energy level of the semiconductor conduction band. Therefore $Z_D(E)$ also then tends to reduce the intensity for this case. However, the position and orientation term of the G coefficient can be positive or negative. If the product GZ_D is small compared to unity, then it is the sign of G that determines the overall intensity direction. A negative value of G results in a numerator that is larger than unity and could increase the intensity, depending on the size relationship to the denominator. A positive value of G corresponds to a numerator that is smaller than unity and works with the denominator in decreasing the intensity.

If $GZ_D > 0$ (corresponding to negative G) or $GZ_D < -2$ (corresponding to large positive G) then the numerator is larger than unity independent of the sign of the product GZ_D. The relative effect of the numerator in comparison to the denominator depends on the $Y_D(E)$ and $Z_D(E)$ terms. The defining equations of these two terms are identical except the denominator of the $Y_D(E)$ integrand is squared. Therefore, it is expected that $Y_D(E)$ is smaller than $Z_D(E)$. So, any case where $|GZ_D|$ is large compared to unity results in an experimentally verifiable intensity increase, independent of the model approximation sign of G.

The problematic range where the product $|GZ_D|$ is small corresponds to weak coupling. For example, when coupling is eliminated $GZ_D = 0$ and $R = 1$. For the weak coupling case the sign of G is relevant, and in a collection of absorbers the intensity decreases. As the coupling increases, $|GZ_D|$ increases and eventually reaches a point

where the result is larger than unity independent of the sign of G. Then the absorption spectrum intensity is increased. The transition from decrease to increase is not necessarily linear in nature.

In any case, the result, which is dependent on the sign of G, is a problem for the theory. This is because the sign of G cannot be determined by experiment. It depends on the phase of the state function. A specific phase orientation cannot be forced experimentally. This was not a problem for the energy equations derived in Chapter 8. In that case the predicted energy shift depended on the magnitude squared of G. Phase dependence was eliminated.

One way around this dilemma for the intensity shift prediction is to consider that in collection of absorbers it is expected that each molecule has a quantum mechanical transition dipole, random in phase with respect to its neighbors. In this case some molecules absorb with more intensity, some with less, and the overall macroscopic effect is no change in the numerator is expected. Therefore, the overall result is determined by the denominator and the absorption spectrum intensity is predicted to reduce. Another way to consider this result is simply that too many approximations have been made and the model, as a predictor of intensity change, is simply not good enough to make an accurate prediction.

One other consideration of Equation 9.28 is that $Y_D(\varepsilon)$ is much smaller than $Y_D(E)$. Therefore the first term in the denominator can safely be neglected.

9.2 Surface States Included

Now consider how including surface states affects the intensity. For simplification, approximate the semiconductor as having no effect on the ground state. The results of previous sections justify this approximation.

$$\left|\left\langle \Psi_{\varepsilon}\left|\hat{\mu}\right|\Psi_{E}\right\rangle\right|^{2}=\left|\left\langle \varphi_{TG}\left|\hat{\mu}\right|a\varphi+\sum\nolimits_{n=1}^{N}c_{n}\theta_{n}+\sum\nolimits_{s}b_{s}\psi_{s}\right\rangle\right|^{2} \tag{9.30}$$

There are $N+1$ sets of coefficients of in Equation 9.30, each corresponds to one of the $N+1$ sets of coefficients $\begin{bmatrix} a & c_1 & \dots & c_N \end{bmatrix}^T$. Each set of coefficient corresponds to a solution for the energy. Expand the magnitude squared.

$$\begin{aligned}
&=|a|^{2}\left|\left\langle \varphi_{TG}\left|\hat{\mu}\right|\varphi\right\rangle\right|^{2}+\\
&\sum\nolimits_{n'=1}^{N}\sum\nolimits_{n=1}^{N}c_{n'}^{*}\left\langle \varphi_{TG}\left|\hat{\mu}\right|\theta_{n'}\right\rangle^{*}c_{n}\left\langle \varphi_{TG}\left|\hat{\mu}\right|\theta_{n}\right\rangle+\\
&\sum\nolimits_{s'}\sum\nolimits_{s}b_{s'}^{*}\left\langle \varphi_{TG}\left|\hat{\mu}\right|\psi_{s'}\right\rangle^{*}b_{s}\left\langle \varphi_{TG}\left|\hat{\mu}\right|\psi_{s}\right\rangle+\\
&2\,\mathrm{Re}\left\{\begin{array}{l}
a^{*}\left\langle \varphi_{TG}\left|\hat{\mu}\right|\varphi\right\rangle^{*}\sum\nolimits_{n=1}^{N}c_{n}\left\langle \varphi_{TG}\left|\hat{\mu}\right|\theta_{n}\right\rangle+\\
a^{*}\left\langle \varphi_{TG}\left|\hat{\mu}\right|\varphi\right\rangle^{*}\sum\nolimits_{s}b_{s}\left\langle \varphi_{TG}\left|\hat{\mu}\right|\psi_{s}\right\rangle+\\
\sum\nolimits_{s}\sum\nolimits_{n=1}^{N}c_{n}^{*}\left\langle \varphi_{TG}\left|\hat{\mu}\right|\theta_{n}\right\rangle^{*}b_{s}\left\langle \varphi_{TG}\left|\hat{\mu}\right|\psi_{s}\right\rangle
\end{array}\right\}
\end{aligned} \tag{9.31}$$

From Equation 9.9 $\left\langle \varphi_{TG}\left|\hat{\mu}\right|\varphi\right\rangle=\left\langle \tilde{\varphi}_{g}\left|\hat{\mu}_{M}\right|\tilde{\varphi}_{e}\right\rangle$ and from Equation 9.12 $\left\langle \varphi_{TG}\left|\hat{\mu}\right|\psi_{s}\right\rangle=\left\langle \tilde{\psi}_{o}\left|\hat{\mu}_{S}\right|\tilde{\psi}_{s}\right\rangle$. Also the dipole coupling element for the surface state is required.

$$\left\langle \varphi^{(i)}\left|\hat{\mu}\right|\theta_{n}\right\rangle=\left\langle \tilde{\psi}_{o}\left|\hat{\mu}_{S}\right|\tilde{\theta}_{n}\right\rangle \tag{9.32}$$

Substitute these into Equation 9.31.

$$\begin{aligned}
&\left|\left\langle \Psi_{\varepsilon} \left| \hat{\mu} \right| \Psi_{E} \right\rangle\right|^2 = |a|^2 \left|\left\langle \widetilde{\varphi}_g \left| \hat{\mu}_M \right| \widetilde{\varphi}_e \right\rangle\right|^2 + \\
&\sum_{n'=1}^{N} \sum_{n=1}^{N} c_{n'}^{*} \left\langle \widetilde{\psi}_o \left| \hat{\mu}_S \right| \widetilde{\theta}_{n'} \right\rangle^{*} c_n \left\langle \widetilde{\psi}_o \left| \hat{\mu}_S \right| \widetilde{\theta}_n \right\rangle + \\
&\sum_{s'} \sum_{s} b_{s'}^{*} \left\langle \widetilde{\psi}_o \left| \hat{\mu}_S \right| \widetilde{\psi}_{s'} \right\rangle^{*} b_s \left\langle \widetilde{\psi}_o \left| \hat{\mu}_S \right| \widetilde{\psi}_s \right\rangle + \\
&2\,\mathrm{Re}\left\{ \begin{array}{l} a^{*} \left\langle \widetilde{\varphi}_g \left| \hat{\mu}_M \right| \widetilde{\varphi}_e \right\rangle^{*} \sum_{n=1}^{N} c_n \left\langle \widetilde{\psi}_o \left| \hat{\mu}_S \right| \widetilde{\theta}_n \right\rangle + \\ a^{*} \left\langle \widetilde{\varphi}_g \left| \hat{\mu}_M \right| \widetilde{\varphi}_e \right\rangle^{*} \sum_{s} b_s \left\langle \widetilde{\psi}_o \left| \hat{\mu}_S \right| \widetilde{\psi}_s \right\rangle + \\ \sum_{s} \sum_{n=1}^{N} c_n^{*} \left\langle \widetilde{\psi}_o \left| \hat{\mu}_S \right| \widetilde{\theta}_n \right\rangle^{*} b_s \left\langle \widetilde{\psi}_o \left| \hat{\mu}_S \right| \widetilde{\psi}_s \right\rangle \end{array} \right\}
\end{aligned} \tag{9.33}$$

Following the approach of Equations 9.14 through 9.16, derive values for the coefficients.

$$b_s = \frac{aG \left\langle \widetilde{\varphi}_g \left| \hat{\mu}_M \right| \widetilde{\varphi}_e \right\rangle \left\langle \widetilde{\psi}_s \left| \hat{\mu}_S \right| \widetilde{\psi}_o \right\rangle}{E - E_s} \tag{9.34}$$

$$c_n = \frac{aG_W \left\langle \widetilde{\varphi}_g \left| \hat{\mu}_M \right| \widetilde{\varphi}_e \right\rangle \left\langle \widetilde{\theta}_n \left| \hat{\mu}_S \right| \widetilde{\psi}_o \right\rangle}{E - E_{\theta_n}} \tag{9.35}$$

Substitute b_s and c_n into Equation 9.33.

$$\left|\left\langle \Psi_{\varepsilon}\left|\hat{\mu}\right|\Psi_{E}\right\rangle\right|^{2}=\left|a\right|^{2}\left|\left\langle \widetilde{\varphi}_{g}\left|\hat{\mu}_{M}\right|\widetilde{\varphi}_{e}\right\rangle\right|^{2}$$
$$\left\{\begin{array}{l}1+\\ G_{W}^{2}\sum_{n=1}^{N}\dfrac{\left|\left\langle \widetilde{\theta}_{n}\left|\hat{\mu}_{S}\right|\widetilde{\psi}_{o}\right\rangle\right|^{2}}{E-E_{\theta_{n}}}\sum_{n'=1}^{N}\dfrac{\left|\left\langle \widetilde{\theta}_{n'}\left|\hat{\mu}_{S}\right|\widetilde{\psi}_{o}\right\rangle\right|^{2}}{E-E_{\theta_{n}}}+\\ G^{2}\sum_{s'}\dfrac{\left|\left\langle \widetilde{\psi}_{s'}\left|\hat{\mu}_{S}\right|\widetilde{\psi}_{o}\right\rangle\right|^{2}}{E-E_{s}}\sum_{s}\dfrac{\left|\left\langle \widetilde{\psi}_{s}\left|\hat{\mu}_{S}\right|\widetilde{\psi}_{o}\right\rangle\right|^{2}}{E-E_{s}}+\\ 2\,\mathrm{Re}\left\{\begin{array}{l}G_{W}\sum_{n=1}^{N}\dfrac{\left|\left\langle \widetilde{\theta}_{n}\left|\hat{\mu}_{S}\right|\widetilde{\psi}_{o}\right\rangle\right|^{2}}{E-E_{\theta_{n}}}+G\sum_{s}\dfrac{\left|\left\langle \widetilde{\psi}_{s}\left|\hat{\mu}_{S}\right|\widetilde{\psi}_{o}\right\rangle\right|^{2}}{E-E_{s}}+\\ G_{W}G\sum_{s}\dfrac{\left|\left\langle \widetilde{\psi}_{s}\left|\hat{\mu}_{S}\right|\widetilde{\psi}_{o}\right\rangle\right|^{2}}{E-E_{s}}\sum_{n=1}^{N}\dfrac{\left|\left\langle \widetilde{\theta}_{n}\left|\hat{\mu}_{S}\right|\widetilde{\psi}_{o}\right\rangle\right|^{2}}{E-E_{\theta_{n}}}\end{array}\right\}\end{array}\right\} \tag{9.36}$$

Reduce by applying the definition of $Z_{D}(E)$.

$$=\left|a\right|^{2}\left|\left\langle \widetilde{\varphi}_{g}\left|\hat{\mu}_{M}\right|\widetilde{\varphi}_{e}\right\rangle\right|^{2}\left[1+\left(GZ_{D}+G_{W}\sum_{n=1}^{N}\frac{\left|\left\langle \widetilde{\theta}_{n}\left|\hat{\mu}_{S}\right|\widetilde{\psi}_{o}\right\rangle\right|^{2}}{E-E_{\theta_{n}}}\right)\right]^{2} \tag{9.37}$$

Substitute for $\left|a\right|^{2}$ and also divide by the uncoupled transition dipole operator to get the ratio between coupled and uncoupled systems for the case when surface states are considered.

$$R_{surface}=\frac{\left[1+\left(GZ_{D}+G_{W}\sum_{n=1}^{N}\dfrac{\left|\left\langle \widetilde{\theta}_{n}\left|\hat{\mu}_{S}\right|\widetilde{\psi}_{o}\right\rangle\right|^{2}}{E-E_{\theta_{n}}}\right)\right]^{2}}{1+\left|\left\langle \widetilde{\varphi}_{g}\left|\hat{\mu}_{M}\right|\widetilde{\varphi}_{e}\right\rangle\right|^{2}\left\{G_{W}^{2}\sum_{n=1}^{N}\dfrac{\left|\left\langle \widetilde{\theta}_{n}\left|\hat{\mu}_{S}\right|\widetilde{\psi}_{o}\right\rangle\right|^{2}}{\left(E-E_{\theta_{n}}\right)^{2}}+G^{2}\sum_{s}\dfrac{\left|\left\langle \widetilde{\psi}_{s}\left|\hat{\mu}_{S}\right|\widetilde{\psi}_{o}\right\rangle\right|^{2}}{\left(E-E_{s}\right)^{2}}\right\}} \tag{9.38}$$

Equation 9.38 is very similar to Equation 9.28 with the two exceptions. First, the effect of ground state coupling is not included. This was an initial approximation and the effect of ground state is small. Second, the surface state summation adds to $Y_D(E)$ and $Z_D(E)$. Because this summation can result in either a positive or a negative value, the relative intensity shift depends on which of the $N+1$ states are considered. Consider the numerator of Equation 9.38, $\left[1+\left(GZ_D+G_W\sum_{n=1}^{N}\frac{\left|\left\langle\tilde{\theta}_n\left|\hat{\mu}_S\right|\tilde{\psi}_o\right\rangle\right|^2}{E-E_{\theta_n}}\right)\right]^2$, and the $E-E_{\theta_n}$ value. When $E<E_{\theta_n}$ then $E-E_{\theta_n}$ is negative. When $E>E_{\theta_n}$ then $E-E_{\theta_n}$ is positive. Therefore, it is not possible to predict whether the overall summation $\sum_{n=1}^{N}\frac{\left|\left\langle\tilde{\theta}_n\left|\hat{\mu}_S\right|\tilde{\psi}_o\right\rangle\right|^2}{E-E_{\theta_n}}$ is positive or negative. This is in contrast to the case for $Z_D(E)$. For cases where the molecule energy level is below the semiconductor then $Z_D(E)$ is always negative. Even when the molecule energy level is slightly larger then the lower edge of the semiconductor conduction band, it is still likely that $Z_D(E)$ is negative because the summation which comprises $Z_D(E)$ includes all semiconductor conduction band states and most of these states are much larger energy than the molecule excited state.

When including surface states, the contribution for the state with the largest coefficient on the combined state with molecule excited is strengthened if its energy is below most of the surface states. The same intensity is reduced if its energy is above most of the surface states. Similarly, the intensity for state with largest coefficient on the

combined state with semiconductor surface state excited is increased or decreased depending on its relative energy position.

In all cases, the strength of coupling plays a role as well. In many cases the absorption spectrum of the semiconductor in the region below the conduction band edge displays an exponential shape. This means that the lower energy states are coupled less strongly to the molecule. The result reduces the overall semiconductor effect because those states with energies below E, which tend to reverse the intensity increase effect, have a smaller coupling strength.

10.0 Closed Form Equations For Coupled Energy Levels

At this point in the work a model has been proposed and the general nature of its predictions discussed. Equation 4.39 and Equation 4.58 provide a means to calculate the absorption spectrum and the Raman spectrum of the combined molecule semiconductor system, given the energy levels and transition dipole matrix elements. Equation 8.18 (for $M=1$) and Equation 8.31 (for $M>1$) predict the energy levels. Equation 9.28 (without surface states) and Equation 9.38 (with surface states) predict the transition dipole matrix elements. The last missing piece is a solution for $Z(E)$ and $Y(E)$. These functions are found in all of Equations 8.18, 8.31, 9.28, and 9.38.

It was previously shown that $Z(E)$ is an approximate form of the correct summation of terms $Z_D(E)$, and $Y(E)$ is an approximate form of the correct summation of terms $Y_D(E)$. Yet even these approximate forms of $Z_D(E)$ and $Y_D(E)$ still require quantum mechanical computations, which are too disconnected from experimental data. What is needed is a refinement of $Z(E)$ and $Y(E)$ with parameters easily obtained from spectroscopy experiments. Once this step is resolved then closed form equations for estimating the total energy after coupling to the semiconductor are derived.

10.1 Model of $Y(E)$ and $Z(E)$

Both $Y(E)$ and $Z(E)$ require knowing $\rho(\tilde{E}')\left|\langle\tilde{\psi}_{E'}|\hat{\mu}_S|\tilde{\psi}_o\rangle\right|^2$. This is approximately the absorption spectrum of a semiconductor due to excitation of electrons from the valence band to the conduction band. Find this quantity by using experimental data combined with Equation 4.33. The problem with experimental data is it forces calculating $Y(E)$ and $Z(E)$ numerically. As a first step, use a simple approximation that enables a mathematical solution. This approximation is constant coupling over a specified select band of energies. Set $\rho(\tilde{E}')\left|\langle\tilde{\psi}_{E'}|\hat{\mu}_S|\tilde{\psi}_o\rangle\right|^2$ equal to a constant called $|k|^2$. The energy band is the conduction band of the semiconductor. Neglect states which appear at energies less than $\tilde{E}1$, the surface states. Figure 10.1 shows the resulting shape of the coupling as a function of semiconductor energy.

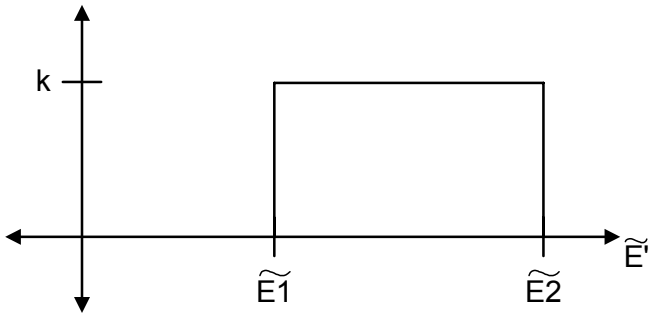

Figure 10.1. Approximated semiconductor conduction band shape.

Although this model is very simple, it is not completely unrealistic [52] [53]. A semiconductor nanoparticle absorption spectrum typically has a fast rising edge as a

function of frequency at the lower conduction band edge, then increases slowly as a function of frequency within the conduction band, and then decays at the upper conduction band edge. The in-band rise reflects the inverse relationship to the incident frequency $1/\nu$ in Equation 4.33.

The purpose of this approximation is to acquire an intuitive understanding as to how $Y(E)$ and $Z(E)$ affect energy and absorption intensity. Substitute a constant $|k|^2 \equiv \rho(\tilde{E}')\left|\langle \tilde{\psi}_{E'} | \hat{\mu}_S | \tilde{\psi}_o \rangle\right|^2$ into Equation 8.17.

$$Z(E) = \int_{\tilde{E}1}^{\tilde{E}2} \frac{|k|^2}{E - (\tilde{E}_g + \tilde{E}')} d\tilde{E}' \tag{10.1}$$

Before proceeding with the integration, it is helpful to plot the function in the integrand. This is shown in Figure 10.2 The region in the box of Figure 10.2 is the area that is integrated in Equation 10.1 To simplify notation, $E' \equiv \tilde{E}_g + \tilde{E}'$, $E1 \equiv \tilde{E}_g + \tilde{E}1$, and $E2 \equiv \tilde{E}_g + \tilde{E}2$. Notice that as E approaches $E1$, the integrated area increases dramatically. When E is larger than $E1$, but less than $E2$, then there is a discontinuity in the integral. The computed area, and therefore $Z(E)$, is always negative as long as the value of E is less than $E1$ (note that the numerator of Equation 10.1 is always positive).

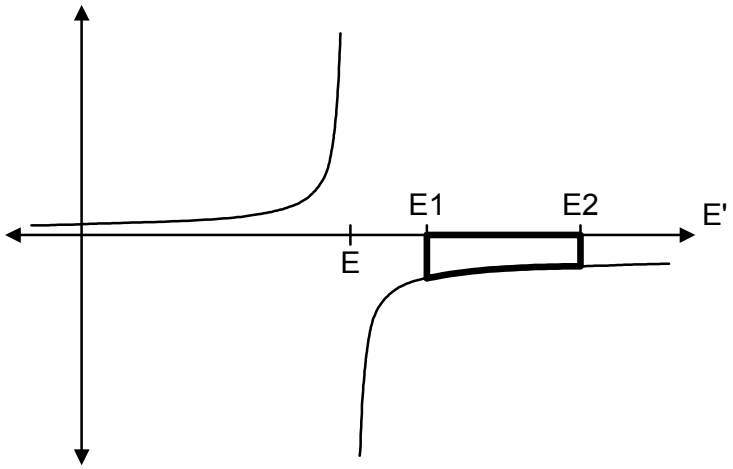

Figure 10.2 Plot of $|k|^2 / E - E'$.

Integrate Equation 10.1, using the constraint $E < E1$.

$$Z(E) = |k|^2 \ln\left(\frac{E1 - E}{E2 - E}\right); \quad E < E1 \tag{10.2}$$

A similar integration equation and result is applied for the case of $Y(E)$.

$$Y(E) = \int_{E1}^{E2} \frac{|k|^2}{\left(E - \left(E_g + E'\right)\right)^2} dE' \tag{10.3}$$

$$Y(E) = |k|^2 \frac{E2 - E1}{(E - E2)(E - E1)} \tag{10.4}$$

For E within the range of $E1$ and $E2$ the discontinuity is sometimes resolved by adding a phenomenological lifetime term to the energy, $\frac{|k|^2}{E - E' - j\Gamma}$. This gives the realistic physical effect of a lifetime to the states. For the simple case studied here,

symmetry of the problem provides a simpler solution. Figure 10.3 shows $\frac{|k|^2}{E-E'}$ when E is in this range. Note that the function is symmetric for $E1 < E < 2E - E1$. When $\rho(\tilde{E}')|\langle\tilde{\psi}_{E'}|\hat{\mu}_S|\tilde{\psi}_o\rangle|^2$ is a constant, the positive and negative areas cancel, and $Z(E)$ is written as an integral over a shortened range.

$$Z(E) = \int_{2E-E1}^{E2} \frac{|k|^2}{E-E'} dE' \tag{10.5}$$

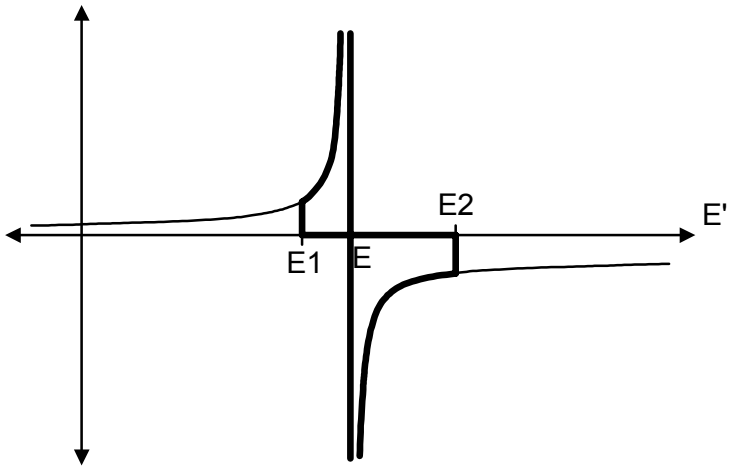

Figure 10.3. Plot of $|k|^2 / E - E'$ when $E > E1$.

Equation 10.5 now has a solution.

$$Z(E) = |k|^2 \ln\left(\frac{E-E1}{E2-E}\right); \quad E1 < E < E2 \tag{10.6}$$

Compare Equation 10.6 and Equation 10.2. A general solution for $Z(E)$ valid for all E, when $\rho(\tilde{E}')\left|\langle\tilde{\psi}_{E'}|\hat{\mu}_S|\tilde{\psi}_o\rangle\right|^2$ is a constant, results from comparing these equations.

$$Z(E) = |k|^2 \ln\left(\left|\frac{E1 - E}{E2 - E}\right|\right) \tag{10.7}$$

Figure 10.4 demonstrates the function $Z(E)$, Equation 10.7, for two values of k and for two sets of $\{E1, E2\}$.

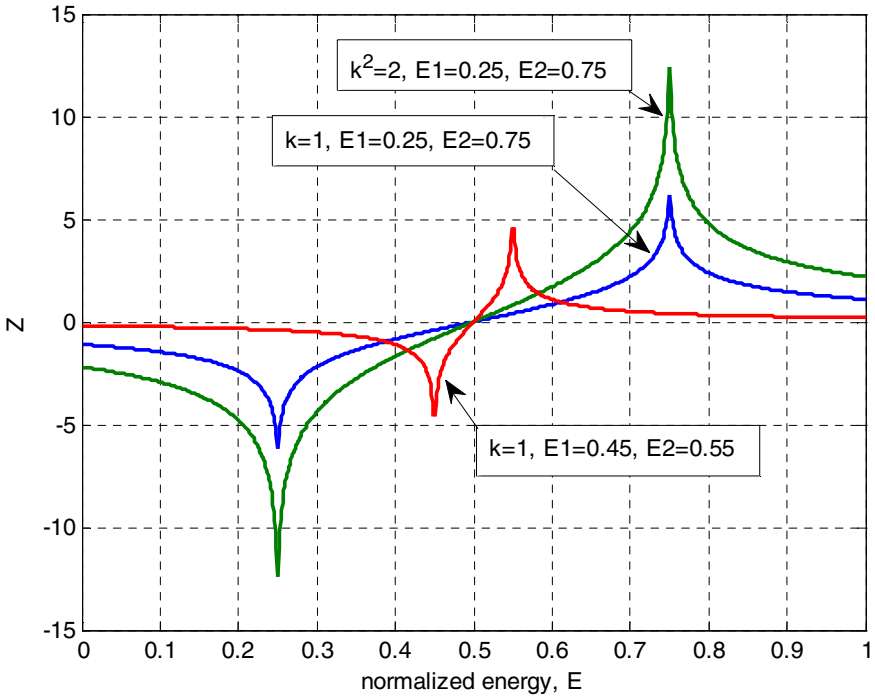

Figure 10.4. Plot of $Z(E)$. The values of the horizontal axis, E, are simply a range of values selected with respect to $E1$ and $E2$. The figure shows generally the shape of $Z(E)$ both within and external to the semiconductor conduction band.

When $E < E1$ the function $Z(E)$ is negative. When $E1 < E < E2$ the function $Z(E)$ increases from a negative value to a positive value and crosses zero at the midpoint $E = (E1 + E2)/2$. When $E > E2$ the function $Z(E)$ is positive. As $E1$ approaches $E2$ the function $Z(E)$ is everywhere closer to zero, in comparison to when $E1$ and $E2$ are further separated in energy. This indicates that a wide semiconductor conduction band more strongly influences the coupling. Also, as the coupling parameter k increases, the function $Z(E)$ increases proportionately.

10.2 Energy Shift Trend for Single Excited Energy Level

Substitute Equation 10.7 into the result for energy calculation, Equation 8.18, with surface states neglected. Equation 8.18 is the case for $M = 1$, a single excited energy level.

$$|k|^2 G^2 \left| \langle \tilde{\varphi}_g | \hat{\mu}_M | \tilde{\varphi}_e \rangle \right|^2 \ln\left(\left| \frac{E1 - E}{E2 - E} \right| \right) = E - E_\varphi \tag{10.8}$$

Equation 10.8 is nonlinear and must be solved numerically. This is the tradeoff for reducing the order of $Z_D(E)$ by approximating it with the continuous function $Z(E)$. Before numerically solving Equation 10.8, it is useful to plot the individual terms of Equation 10.8 to gain insight into the effect of coupling strength k on the coupled energy E. First define K and $F(E)$.

$$K \equiv |k|^2 G^2 \left| \langle \tilde{\varphi}_g | \hat{\mu}_M | \tilde{\varphi}_e \rangle \right|^2 \tag{10.9}$$

$$F(E) \equiv \ln\left(\left| \frac{E1 - E}{E2 - E} \right| \right) \tag{10.10}$$

This simplifies Equation 10.8. Figure 10.4 also represents the general characteristics of $F(E)$ since $Z(E)$ and $F(E)$ differ by only a constant. Notice that K has units of energy.

$$KF(E) = E - E_\varphi \tag{10.11}$$

Plot Equation 10.11 and observe the effect of K, $E1$, $E2$, and E_φ on the energy shift $E - E_\varphi$. Figure 10.5 shows this plot. Equation 10.11 is a function of the variable E. The solution to Equation 10.11 is the point, $E = E_c$, at which $E - E_\varphi$ is equal to $KF(E)$. This point is indicated as E_c in the figure.

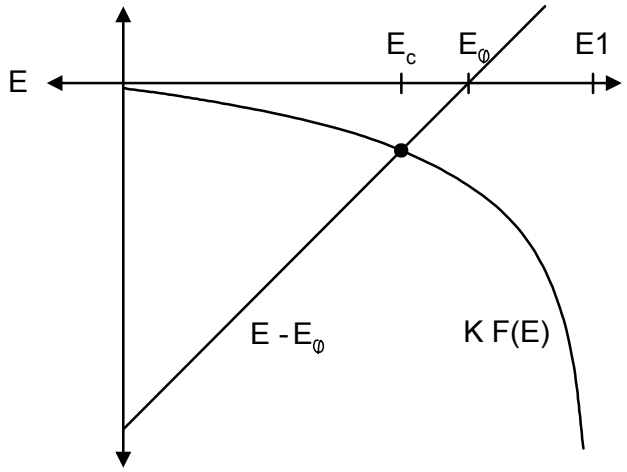

Figure 10.5 Plot of $KF(E)$ and $E - E_\varphi$ vs. E.

Now consider the effect of increasing K or $E2$. This shifts $KF(E)$ more negative. The result is that the energy difference $E_c - E_\varphi$ must increase in order to remain equal to $KF(E_c)$. This is shown in Figure 10.6. Therefore, an increase in coupling, either through $|k|^2$, $G(R,\theta,\alpha)$, $\left|\langle \tilde{\varphi}_g | \hat{\mu}_M | \tilde{\varphi}_e \rangle\right|^2$, or more states to couple (larger $E2$) results in an increase in the energy shift $E - E_\varphi$. The effect of $G(R,\theta,\alpha)$is reasonable because $G(R,\theta,\alpha)$is inversely proportional to the distance between the molecule and semiconductor. So coupling due to $G(R,\theta,\alpha)$ increases as the two

individual systems approach each other. This distance can decrease if, for example, a bridge anchor group between the excited portion of the molecule and the semiconductor is reduced in length. A limitation of the theory is that as the coupling increases then the approximation of weak coupling no longer applies.

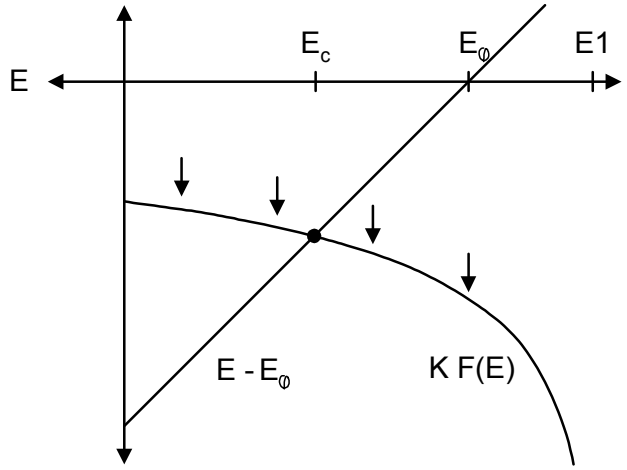

Figure 10.6 Plot of $KF(E)$ vs. E for a larger value of K than in Figure 10.5. The arrows indicate the direction of the curve shift.

Another consideration is the proximity of E_φ to $E1$. Figure 10.7 shows a curve with the same coupling as Figure 10.5 except with E_φ shown close to $E1$. Compare Figure 10.7 to Figure 10.5 and observe the energy shift increases as E_φ approaches $E1$. Notice, however, that the effect of K appears larger than the effect of $E1$ - E_φ until E_φ gets very near $E1$.

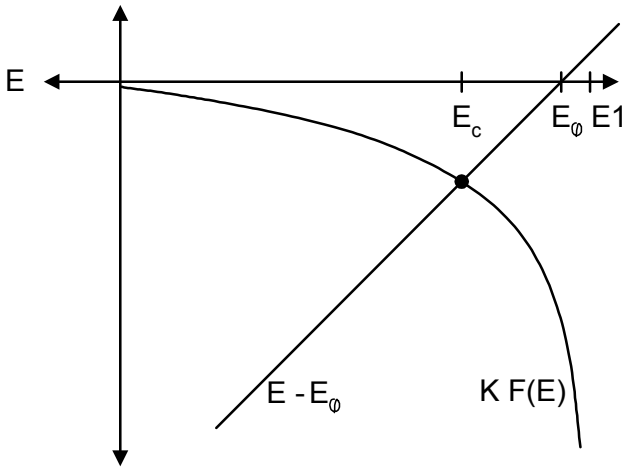

Figure 10.7 Effect of E_{φ} moving closer to E1.

When $E > E1$, all of the trends reverse. This is because in Equation 10.7 the numerator starts to increase which makes $Z(E)$ become less negative as E increases past $E1$. When E is half-way in between $E1$ and $E2$ then $Z(E)$ is zero. In this case the semiconductor has no influence on the molecule energy level and the energy red-shift and intensity increase seen in an absorption experiment are eliminated. Above this mid-point, the absorption experiment energy begins to blue-shift and the intensity is reduced. Figure 10.8 shows this effect.

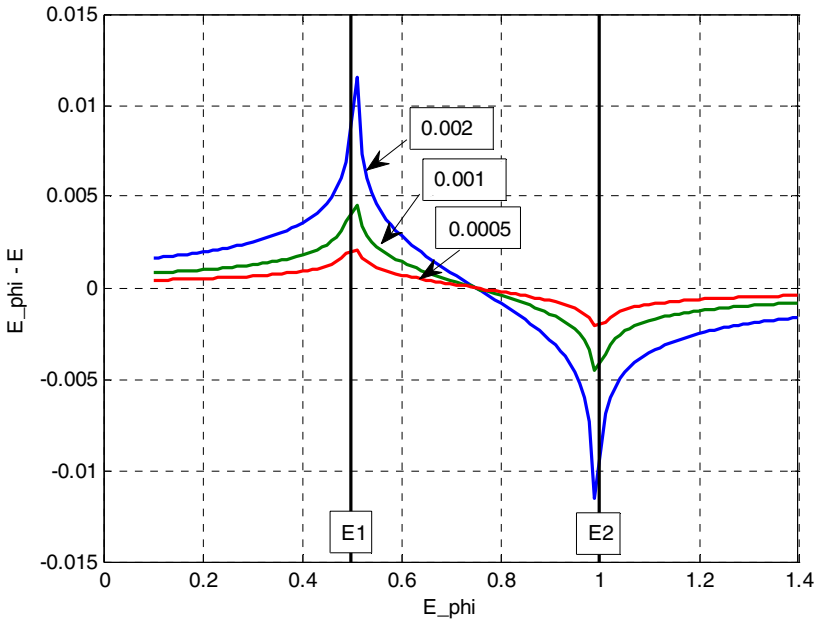

Figure 10.8 Numerical simulation showing the energy shift as a function of the relationship between the uncoupled excited state energy E_φ and the shifted energy due to coupling E. Positive values indicate a shift to lower energy. Negative values indicate a shift to larger energy.

Figure 10.8 is a plot of a numerical solution of Equation 10.11, displayed as $E_\varphi - E$ vs. E_φ. The vertical axis represents the amount that the energy of the coupled state $|\varphi\rangle$ shifts to another energy as a result of the semiconductor coupling on the molecule. The horizontal axis shows where the starting energy, E_φ, resides in comparison to the semiconductor band energy $E1$. Three values of K have been selected, $\{0.002, 0.001, 0.0005\}$, along with setting $E1 = 0.5$ and $E2 = 1.0$. The values for $E1$ and $E2$ are selected to enable visualizing trends and do not represent measured

experimental values. In fact, all of the values $E1$, $E2$, K, E_φ are displayed over a much larger range than is valid for the theory. This is the reason to plot $E_\varphi - E$ instead of shift as a percentage of E_φ. Although plotting as a percentage (normalized to E_φ) provides a more universal result, the result would be skewed due to the unrealistic range of values. Correct value ranges are applied in the experimental section of the thesis.

Equation 10.11, as displayed in Figure 10.8, shows interesting phenomena in the range $E1 < E_\varphi < E2$. The vertical black bars in Figure 10.8 indicate this range. Notice that the shift to a lower energy continues to increase for a short range of energies into the semiconductor conduction band. This effect is greater for large values of K. Figure 10.9 shows the cause of this phenomenon, using exaggerated scales to clarify the issue. As E_φ increases above $E1$ the intersection with $KF(E)$ remains in the negative trending range of $KF(E)$. This results in the nonlinearly increasing shift shown in Figure 10.8 above $E1$ (the value of $E1$ is 0.5 in Figure 10.8). When E_φ increases such that $E_\varphi - E$ intersects with the positive trending range of $KF(E)$ then the energy shift suddenly decreases. Figure 10.9 shows the line $E_\varphi - E$ nearly intersecting at point X. At the intersection of point X is when the energy shift steps to a new smaller value. At this intersection there are two solutions to the equation. It seems likely that this effect is not physical and is due to the numerical approximations of the model. Therefore, care must be taken when using the model for initial energy levels significantly within the semiconductor conduction band. The range where the theory applies is derived as follows. Consider that $E_\varphi = \widetilde{E}_e + \widetilde{E}_o$ and $E1 = \widetilde{E}_g + \widetilde{E}_{s=1}$. The proximity of E_φ to $E1$ is

$E1 - E_{\varphi} = \left(\widetilde{E}_{s=1} - \widetilde{E}_{o}\right) - \left(\widetilde{E}_{e} - \widetilde{E}_{g}\right)$. Therefore, the theory is applicable for molecules with their LUMO (lowest unoccupied molecular orbital) to HOMO (highest occupied molecular orbital) energy difference smaller than the semiconductor bandgap energy. This is the case for nearly all systems under consideration for DSSC applications.

In creating Figure 10.8 the intersection at point X is taken as the root, justified by the fact that in a real system the discontinuity at energy $E1$ is not correct. Perhaps a more physically realistic $Z(E)$ exhibits a slight curvature near $E1$ and in this case multiple roots may not appear.

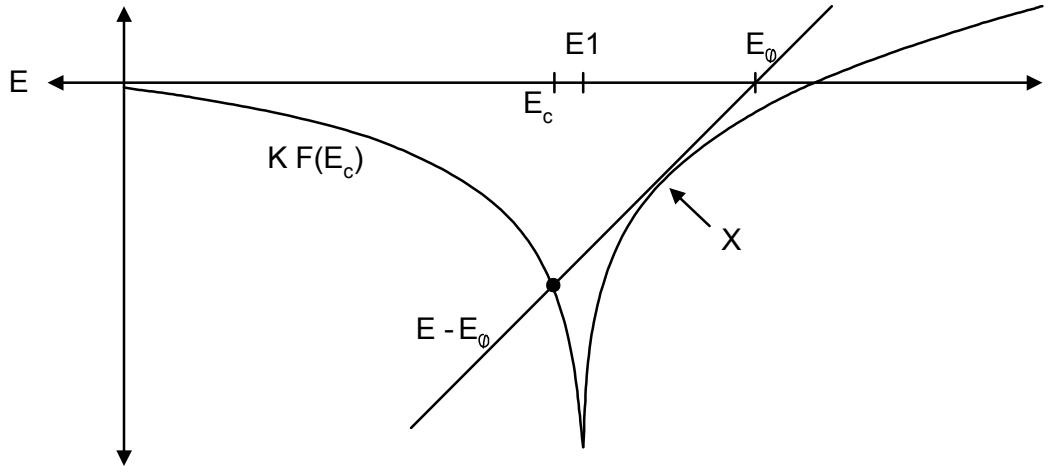

Figure 10.9 Effect of E_{φ} within the range of $E1 < E_{\varphi} < E2$.

Also, observe in Figure 10.8 that when E_{φ} is at the midpoint of the semiconductor conduction band energy then $E = E_{\varphi}$ as expected. One last observation for Figure 10.8 is that the amount of shift decreases as K decreases. When $K = 0$ there is no shift.

10.3 Effect of Surface States

Substitute Equation 10.7 into the result for energy calculation, Equation 8.18, with surface states included. The definition for K is shown in Equation 10.9.

$$K\frac{G_W^2}{G^2}\sum_{n=1}^{N}\frac{\left|\left\langle\widetilde{\theta}_n\left|\hat{\mu}_S\right|\widetilde{\psi}_o\right\rangle\right|^2}{E-E_{\theta_n}}+K\ln\left(\left|\frac{E1-E}{E2-E}\right|\right)=E-E_\varphi \tag{10.12}$$

The effect of surface states depends on the coupling strength and position of E_φ with respect to the surface state energies. If E_φ is less than the lowest surface state energy then the denominator of each term in the summation over surface states in Equation 10.12 is always negative. This is because if E_φ is less than the lowest surface state energy then $E < E_{\theta_n}$; $n = 1,\ldots,N$. Therefore, surface states enhance the red-shift and intensity change.

As E_φ increases into the surface state range then the denominator can be positive or negative, depending on the relationship between E_φ and the energy values E_{θ_n}. The red-shift effect becomes less pronounced.

When E_φ is larger than all of the surface state energies then each term in the summation over surface states is most likely positive. In this case the coupled energy E can become larger than the uncoupled excited sate energy E_φ, resulting in a blue-shift in comparison to the uncoupled system. The relative value of G_W in comparison to G and the relative strength of each $\left|\left\langle\widetilde{\theta}_n\left|\hat{\mu}_S\right|\widetilde{\psi}_o\right\rangle\right|^2$ in comparison to $\rho\left(\widetilde{E}'\right)\left|\left\langle\widetilde{\psi}_{E'}\left|\hat{\mu}_S\right|\widetilde{\psi}_o\right\rangle\right|^2$

determine the effect of surface states in comparison to bulk states. In either case, the denominator of the surface state summation most likely consists of smaller energy differences in comparison to the bulk state summation, which results in the overall summation to consist of larger terms. Therefore, the surface states are expected to have significant influence in comparison to the bulk states.

10.4 Energy Shift Trend for Vibronic Energy Levels

The analysis of vibronic levels at the excited electronic state results in a solution with multiple states $|\varphi_m\rangle$. As for the case with $M=1$, the important prediction for $M>1$ is quantifying the energy shift magnitude. An additional new prediction for this case is the relative shift of individual energy levels. This results in a change of the vibronic absorption spectrum shape. Substitute Equation 10.7 into Equation 8.31 (using the approximation $Z(E)\approx Z_D(E)$), and use Equation 10.9 for K.

$$K\ln\left(\left|\frac{E1-E}{E2-E}\right|\right)=\frac{1}{\sum_{m=1}^{M}\frac{\Pi_{k=1}^{3P-6}\left|\langle 0_k\left|\upsilon_k(m)\right\rangle\right|^2}{E-E_{\varphi_m}}} \tag{10.13}$$

Figure 10.10 shows a plot of the left and right side functions of Equation 10.13 for $M=2$. These are $K\ln\left(\left|\frac{E1-E}{E2-E}\right|\right)$ and $\left(\sum_{m=1}^{M=2}\frac{\Pi_{k=1}^{3P-6}\left|\langle 0_k\left|\upsilon_k(m)\right\rangle\right|^2}{E-E_{\varphi_m}}\right)^{-1}$. Recall that $F(E)\equiv\ln\left(\left|\frac{E1-E}{E2-E}\right|\right)$. The intersections, E_{c1} and E_{c2}, of these two functions provides the new shifted energy levels. Notice similar characteristics as for the $M=1$ case. For example, as K increases, so does the energy shift. Also, for small K, the energy level E_{φ_1} is shifted less than the energy level E_{φ_2}. This is because E_{φ_2} is closer to the lower band of the semiconductor conduction band.

However, Figure 10.10 also shows a new phenomenon that is not seen for $M=1$. One of the new energy levels, E_{c2}, cannot take a value any smaller than $\left(E_{\varphi_1}+E_{\varphi_2}\right)/2$.

At this point the function $\left(\sum_{m=1}^{M}\frac{\Pi_{k=1}^{3P-6}\left|\langle 0_k\left|\upsilon_k(m)\right\rangle\right|^2}{E-E_{\varphi_m}}\right)^{-1}$ reaches a limit due to the discontinuity at $\left(E_{\varphi_1}+E_{\varphi_2}\right)/2$. This is a problem for the theory.

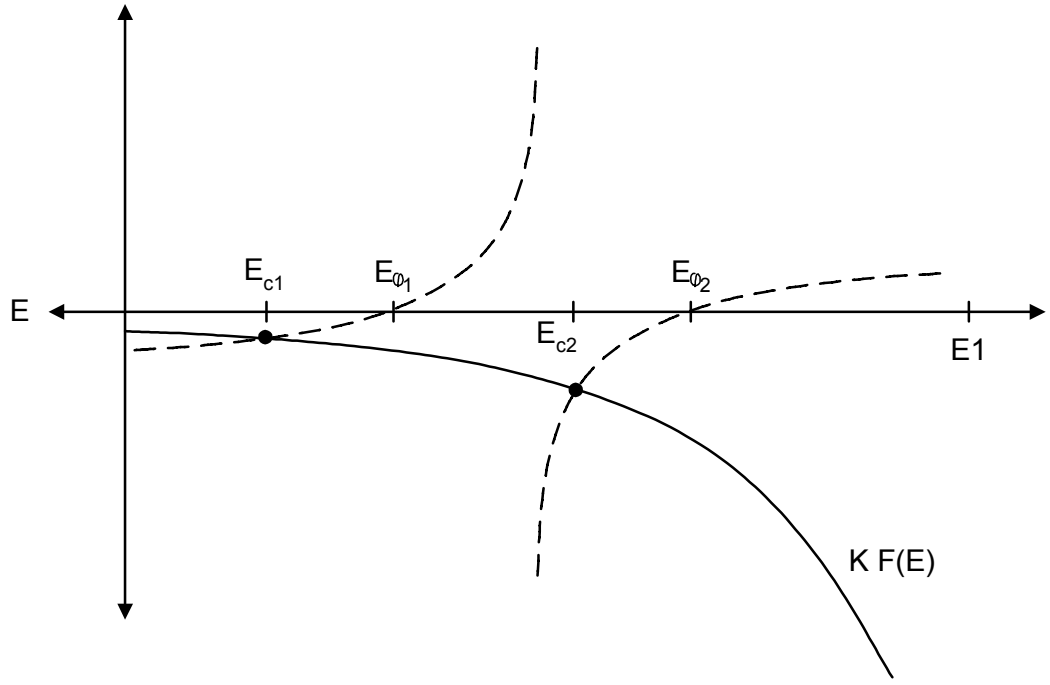

Figure 10.10

$KF(E)$ is the solid curve and $\left(\sum_{m=1}^{M}\frac{\Pi_{k=1}^{3P-6}\left|\langle 0_k\left|\upsilon_k(m)\right\rangle\right|^2}{E-E_{\varphi_m}}\right)^{-1}$ with $M=2$ is the dashed curve.

As long as K is small and therefore the relative energy shift is small, the limitation due to the discontinuity is not a problem. Therefore, one could interpret this as simply a limitation of the theory to cases with weak coupling. The flaw with this

argument, however, is that for vibrational levels, and when M is large, the energy levels E_{φ_i} are very close together. Sufficiently close that Equation 10.13 effectively predicts no energy shift due to semiconductor coupling. The lowest energy level shifts dramatically (the point E_{c1} has no such limitation) and all other energy levels are unchanged.

The cause of this problem is due to the form of Equation 7.57, which is rewritten without surface states included.

$$\overline{H} = \begin{bmatrix} \overline{E}_{\varphi} & \overline{U}^{*T} \\ \overline{U} & \overline{E}_i \end{bmatrix} \tag{10.14}$$

The submatrix $\overline{U}$ has M columns. The number of rows is determined by the number of semiconductor conduction band states. Temporarily define this number as S. Then submatrix $\overline{U}$ is S x M. Each term of $\overline{U}$ is described by Equation 7.55, which is simplified under the approximation of constant G. Write with three separated terms.

$$U_{s,m} \equiv \langle \psi_s | \hat{H} | \varphi_m \rangle = \{ G\mu(\tilde{\varphi}_g, \tilde{\varphi}_e) \} \quad \mu(\tilde{\psi}_s, \tilde{\psi}_o) \quad \left\langle \Pi_{i=1}^{3P-6} \chi_{\upsilon'_i=0} \middle| \Pi_{j=1}^{3P-6} \chi_{\upsilon_j(m)} \right\rangle \tag{10.15}$$

The first term is related to the coupling strength K. Recall Equation 10.9, $K \equiv |k|^2 G^2 \left| \langle \tilde{\varphi}_g | \hat{\mu}_M | \tilde{\varphi}_e \rangle \right|^2$. Define a new value K'.

$$K' \equiv G\mu(\tilde{\varphi}_g, \tilde{\varphi}_e) \tag{10.16}$$

The second term is the semiconductor transition dipole and the third term is the vibrational Franck-Condon factor for the mth vibronic state. Write the submatrix $\overline{U}$ as an outer vector product. This factorization is possible because of the separated molecule and semiconductor terms.

$$\overline{U} = K'\left(\mathbf{s} \cdot m^T\right) \tag{10.17}$$

The two vectors are defined according to the second and third terms of Equation 10.15.

$$\mathbf{s} \equiv \left[\mu\left(\widetilde{\psi}_{s=1}, \widetilde{\psi}_o\right) \quad \ldots \quad \mu\left(\widetilde{\psi}_{s=S}, \widetilde{\psi}_o\right)\right]^T \tag{10.18}$$

$$m \equiv \left[\left\langle \Pi_{i=1}^{3P-6} \chi_{\upsilon'_i=0} \middle| \Pi_{j=1}^{3P-6} \chi_{\upsilon_j(m=1)} \right\rangle \quad \ldots \quad \left\langle \Pi_{i=1}^{3P-6} \chi_{\upsilon'_i=0} \middle| \Pi_{j=1}^{3P-6} \chi_{\upsilon_j(m=M)} \right\rangle\right]^T \tag{10.19}$$

Now substitute Equation 10.17 into Equation 10.14.

$$\overline{H} = \begin{bmatrix} \overline{E}_\varphi & K'\left(\mathbf{s} \cdot m^T\right)^{*T} \\ K'\left(\mathbf{s} \cdot m^T\right) & \overline{E}_i \end{bmatrix} \tag{10.20}$$

Finding the new energy levels is equivalent to finding the eigenvalues of Equation 10.20. However, because submatrix $\overline{U}$ is defined by an outer product, it is singular. Also, submatrices $\overline{E}_\varphi$ and $\overline{E}_i$ are diagonal. Therefore, submatrix $\overline{U}$ has a rather suspicious form and it is not surprising that only two of the eigenvalues (the largest and smallest) are different from the diagonal terms $\overline{E}_\varphi$ and $\overline{E}_i$. When K' is zero, all eigenvalues are equal to $\overline{E}_\varphi$ and $\overline{E}_i$. As K' increases, the largest and smallest eigenvalues experience a change from their initial values. No other eigenvalues change significantly from their values for K' zero.

The source of the problem is the assumptions of nonzero ground dipole and orientational term G being independent of quantum mechanical state. These assumptions were selected to simplify the mathematics. But they lack a solid physical

justification. It would be helpful if an approximation could be found which retains the mathematical simplicity of Equation 10.13, while avoiding the problems which limit the energy value shift.

One approach is treating vibronic levels individually. Set $M = 1$ and solve Equation 10.11 M times, once for each vibronic level. This approach is a variational theory Equation 7.1 which neglects the effect of coupling individual vibronic levels to each other through the semiconductor.

$$\Psi_{E_m} = a_m(E)\varphi_m + \sum_s b_s(E)\psi_s, \quad m = 1,2,\ldots M \tag{10.21}$$

Consider the effect of this approximation on the vibronic spectrum. Figure 10.11 shows an example for $M = 4$. According to Equation 10.11 the energy levels closer to the semiconductor spectrum shift more than the energy levels further away. Therefore, it is predicted that the vibronic spectrum shifts to lower energy and also compresses when coupled to the semiconductor. This prediction is moderated when molecule energy levels are within the energy range $E_\varphi > E1$ because in this case the shift starts to decrease. Surface states also reduce this effect. Therefore, this approach predicts compression of the vibronic spectrum with a possible broadening of the spectrum when the molecule energy levels are either within the range of the semiconductor surface state or the semiconductor conduction band energy levels.

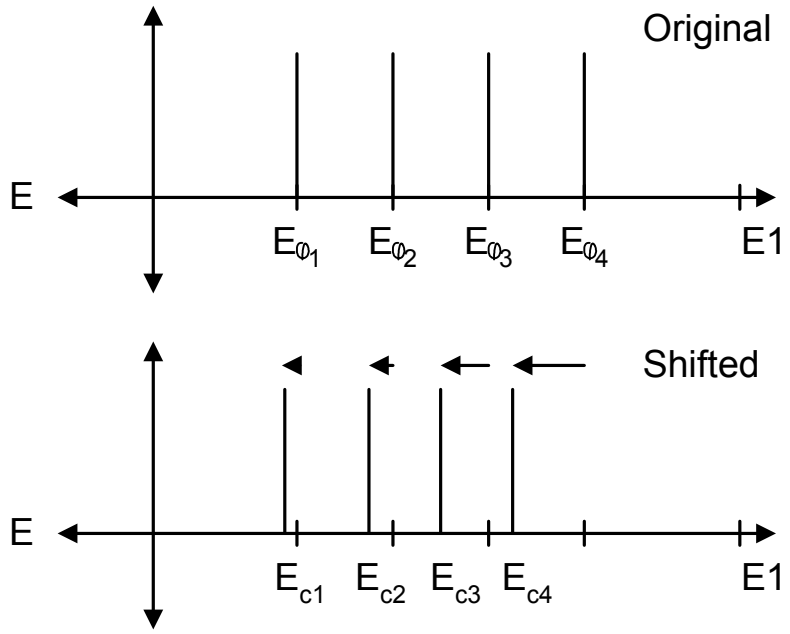

Figure 10.11 Exaggerated effect of proximity to $E1$ on the shift of vibronic energy levels.

Experimental evidence suggests that semiconductor coupling leads to a broadening of the vibronic spectrum [59]. Therefore, although Equation 10.21 does predict broadening when surfaces states are also included or when the molecule is within the semiconductor conduction band, the fact that it also predicts narrowing for certain cases indicates perhaps this approach is not sufficiently close to physical reality. Treating the system as individual $M = 1$ systems does not properly account for coupling through the semiconductor. A more useful approximation can be determined by considering some general properties of Equation 10.13. The goal is to justify a reasonable simplification but which retains the essential features of Equation 10.13.

The harmonic mean tends towards the value of the smallest element in the list. For each energy solution in Equation 10.13, it is expected that the energy closest to E_{φ_n} is the smallest element. Therefore, separate this term from the summation. The denominator of Equation 10.13 now consists of two terms. The first term contains the energy E_{φ_n} of interest. The second term is the summation of all other energies.

$$K \ln\left(\left|\frac{E1-E}{E2-E}\right|\right) = \frac{1}{\frac{\Pi_{k=1}^{3P-6}\left|\langle 0_k \mid \upsilon_k(n)\rangle\right|^2}{E-E_{\varphi_n}} + \sum_{\substack{m=1,\\ m\neq n}}^{M} \frac{\Pi_{k=1}^{3P-6}\left|\langle 0_k \mid \upsilon_k(m)\rangle\right|^2}{E-E_{\varphi_m}}} \tag{10.22}$$

Temporarily approximate the energy denominator of the second term as equal to the energy E_{φ_n}. So set $E = E_{\varphi_n}$. This approximation is justified when the new energy E is approximately equal to E_{φ_n}. Given the weak coupling assumption (small expected energy shift), this approximation is reasonable.

$$K \ln\left(\left|\frac{E1-E}{E2-E}\right|\right) = \frac{1}{\frac{\Pi_{k=1}^{3P-6}\left|\langle 0_k \mid \upsilon_k(n)\rangle\right|^2}{E-E_{\varphi_n}} + \sum_{\substack{m=1,\\ m\neq n}}^{M} \frac{\Pi_{k=1}^{3P-6}\left|\langle 0_k \mid \upsilon_k(m)\rangle\right|^2}{E_{\varphi_n}-E_{\varphi_m}}} \tag{10.23}$$

Now the second term in the denominator of Equation 10.23 is independent of E. Define a new function.

$$T(n) \equiv \sum_{\substack{m=1,\\ m\neq n}}^{M} \frac{\Pi_{k=1}^{3P-6}\left|\langle 0_k \mid \upsilon_k(m)\rangle\right|^2}{E_{\varphi_n}-E_{\varphi_m}} \tag{10.24}$$

Substitute Equation 10.24 into Equation 10.23.

$$K\ln\left(\left|\frac{E1-E}{E2-E}\right|\right)=\frac{1}{\frac{\Pi_{k=1}^{3P-6}\left|\langle 0_k\left|\upsilon_k(n)\right\rangle\right|^2}{E-E_{\varphi_n}}+T(n)} \tag{10.25}$$

Manipulate the right side of Equation 10.25 into a single fraction and then cross multiply the terms on each side of the equation.

$$\left\{\Pi_{k=1}^{3P-6}\left|\langle 0_k\left|\upsilon_k(n)\right\rangle\right|^2+T(n)\left(E-E_{\varphi_n}\right)\right\}K\ln\left(\left|\frac{E1-E}{E2-E}\right|\right)=E-E_{\varphi_n} \tag{10.26}$$

Equation 10.26 is written in a form similar to Equation 10.11, the result for $M=1$. When $T(n)=0$ Equation 10.26 is exactly in the form of Equation 10.11. Therefore, it is useful to investigate the properties of $T(n)$. Consider the sign of $T(n)$. Each term with $E_{\varphi_n}>E_{\varphi_m}$ is positive. This is the case when the vibronic energy level E_{φ_m} is below the energy level of interest. Each term with $E_{\varphi_n}<E_{\varphi_m}$ is negative. This is the case when the vibronic energy level E_{φ_m} is above the energy level of interest. If all energy levels are evenly spaced and the numerator terms are equal then the sign of $T(n)$ depends on the relative number of energy levels higher than E_{φ_n} in comparison to the number of energy levels lower than E_{φ_n}. For this simplistic view of $T(n)$, the sign of $T(n)$ tends positive when the level of interest is one of the higher vibronic energy levels and tends negative when the level of interest is one of the lower vibronic energy levels.

The function $T(n)$ is multiplied by $E-E_{\varphi_n}$ in Equation 10.26 and it has already been established that, in the energy region of interest, typically $E<E_{\varphi_n}$. Therefore, the

sign of $T(n)(E - E_{\varphi_n})$ tends positive when the level of interest is one of the smaller vibronic energy levels and tends negative when the level of interest is one of the larger vibronic levels.

Now an interesting feature of Equation 10.13 can be understood. Treat the first term of Equation 10.26 as a new coupling parameter.

$$K''(n) \equiv \left\{\Pi_{k=1}^{3P-6}\left|\langle 0_k \left| \upsilon_k(n)\right\rangle\right|^2 + T(n)(E - E_{\varphi_n})\right\}K \tag{10.27}$$

The effect of the other vibronic energy levels on the level of interest is to increase this coupling parameter for smaller energy vibronic energy levels and decrease this parameter for larger energy vibronic energy levels. This effect directly counteracts the $M = 1$ effect shown in Figure 10.11 in which levels closer to the semiconductor are shifted more. In fact, this effect is very reasonable. As has already been demonstrated, energy levels below a large set of energy levels get shifted to smaller energy and energy levels above a large set of energy levels get shifted to larger energy. This is exactly the effect shown in Figure 10.8. The vibronic levels work against the direct semiconductor effect because all of the vibronic levels are below the semiconductor levels. The indirect effect of the semiconductor is to enable the vibronic levels to couple, through the semiconductor, to each other, and therefore, potentially broaden the vibronic spectrum.

While normally orthogonal, proximity of the semiconductor enables the molecule states to couple to each other and lower the combined energies. Surface states can either increase or decrease this effect, depending on whether they are energetically larger or smaller than the combined semiconductor with excited molecule energies.

All Franck-Condon terms, $\left|\left\langle 0_k \left| \upsilon_k(n) \right\rangle\right|^2$, are less than unity. This is because of the normalization of the sum of these factors. The vibronic levels redistribute energy but do not change the total energy. Without the additional energy shift contribution of adjacent states $\left|\varphi_m\right\rangle$, the predicted shift of all individual vibronic energy levels would be less. Therefore, the additional shift caused by adjacent levels can be interpreted as a natural consequence of the Franck-Condon normalization.

In terms of a possible effect on the vibronic absorption spectrum shape, the vibronic levels furthest from the semiconductor energy levels and the vibronic levels with the largest Franck-Condon terms can shift to lower energy by a larger amount than adjacent states, due to the influence of other vibronic states. Therefore, it is possible for the peak of the spectrum and the lower energy portion of the spectrum to experience the largest shift. A quantitative treatment is included in the next section.

Based on this analysis, Equation 10.26 is selected as the working equation for $M > 1$. However, one additional simplification is required. Unfortunately, terms in the summation for $T(n)$ are discontinuous with a singularity if any $E_{\varphi_n} = E_{\varphi_m}$. An example of this is a degenerate state. Even for cases with all $E_{\varphi_n} \neq E_{\varphi_m}$, a single level $E_{\varphi_n} \approx E_{\varphi_m}$ could dominate the result. The result is an individual energy level shifting well beyond any reasonable physically justifiable value.

A solution is to recognize that the $1/\left(E_{\varphi_n} - E_{\varphi_m}\right)$ terms are already the result of many approximations. Therefore a further mathematical approximation which eliminates the nonphysical characteristic of this result, while essentially keeping its general functional shape, seems easy to justify. Such an approach is similar to the

phenomenological lifetime term typically added to absorption cross-section equations [47]. Several courses of action are possible. For example, one approach is to simply limit the terms $1/\left(E_{\varphi_n} - E_{\varphi_m}\right)$ to a maximum or minimum value. However, this approach is difficult to express in simple mathematical form.

Another solution is a mathematical expression which approximates $1/\left(E_{\varphi_n} - E_{\varphi_m}\right)$, yet without the singularity. Equation 10.28 is one possibility, with $\alpha < 0$.

$$T'(n) \equiv \sum_{\substack{m=1, \\ m \neq n}}^{M} \left\{ \Pi_{k=1}^{3P-6} \left| \langle 0_k \left| \upsilon_k(n) \right\rangle \right|^2 \right\} e^{\alpha \left| E_{\varphi_n} - E_{\varphi_m} \right|} \operatorname{sgn}\left(E_{\varphi_n} - E_{\varphi_m}\right) \tag{10.28}$$

Figure 10.12 shows a plot of $1/\left(E_n - E_{\varphi_m}\right)$ in comparison to $e^{\alpha \left| E_{\varphi_n} - E_{\varphi_m} \right|} \operatorname{sgn}\left(E_{\varphi_n} - E_{\varphi_m}\right)$.

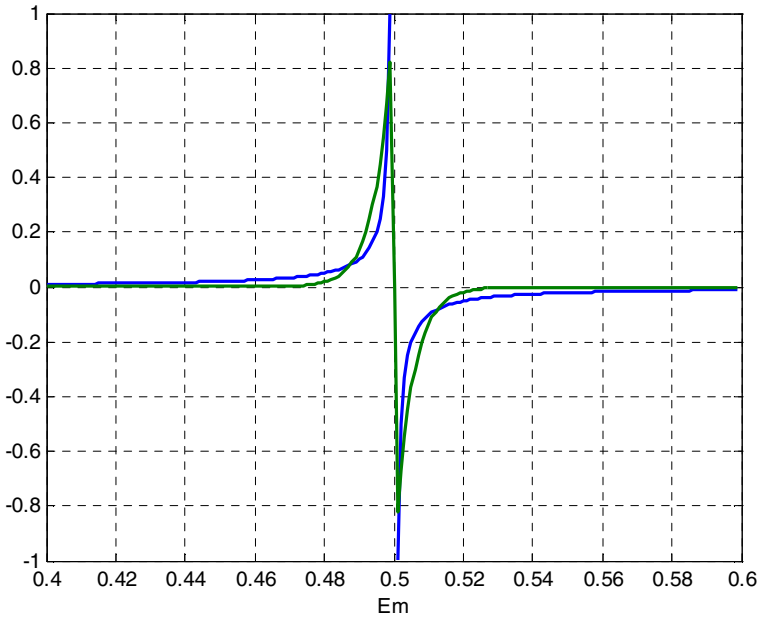

Figure 10.12 Plot of $1/\left(E_n - E_{\varphi_m}\right)$ and $e^{\alpha \left| E_{\varphi_n} - E_{\varphi_m} \right|} \operatorname{sgn}\left(E_{\varphi_n} - E_{\varphi_m}\right)$. $E_n = 0.5$.

The essential characteristics of $1/\left(E_n - E_{\varphi_m}\right)$ are kept while eliminating the singularity. The function $T'(n)$ becomes a phenomenological parameter. It is consistent with the general trends expected by the exact theory, but is not directly derived from the theory. The argument for $T'(n)$ is that, in the absence of assumptions necessary to obtain a simple mathematical solution, the theory is expected to show behavior generally similar to the behavior seen by the use of $T'(n)$. The parameter α is chosen as a function of the specific problem such that $1/\left(E_n - E_{\varphi_m}\right)$ is best approximated in the range of interest. In Figure 10.12, $\alpha = 200$, and the result is scaled by 1000. This extra scale factor is only included for demonstration of Figure 10.12 and is not included in the Equation 10.28.

The final form of the equation for calculation of the new energy levels E is given by Equation 10.29. The approach is to solve Equation 10.29 M times, once for each initial values of E_{φ_n} where $n = 1,2,\ldots,M$.

$$\left\{\Pi_{k=1}^{3P-6}\left|\left\langle 0_k \left| \upsilon_k(n) \right\rangle\right|^2 + T'(n)\left(E - E_{\varphi_n}\right)\right\} K \ln\left(\left|\frac{E1 - E}{E2 - E}\right|\right) = E - E_{\varphi_n} \qquad (10.29)$$

Notice Equation 10.28 depends on the approximation $E \approx E_{\varphi_n}$, and E is determined by Equation 10.29. Therefore, some accuracy to the $E \approx E_{\varphi_n}$ approximation is regained if Equation 10.29 is solved iteratively. Once all $n = 1,2,\ldots,M$ values of E are determined, substitute them back into Equation 10.29 as $E^{(\eta+1)} = E^{(\eta)}{}_{\varphi_n}$ and recalculate each E with Equation 10.29. Repeat until the new calculated energy levels match the previous iteration energy levels to within a predetermined level of tolerance.

11.0 Compare Predictions with Experiment

Now the model is complete. A method of calculating an approximate absorption and Raman spectrum for a light collecting molecule when coupled to a semiconductor is available. The model is sufficiently simple to enable intuitive understanding of the coupling effect. One final and important task is to check the model against experimental data.

Three checks are performed. First, for the case with a single excited electronic energy level, compare an experimental spectrum shift ($M > 1$ case) to the model parameters. Next, compare an experimental vibronic spectrum shift and broadening to the model prediction. Finally, compare an experimental intensity change to the model parameters. It is seen that, while a direct comparison is difficult both due to the level of approximation in the model and the many interactions of the experimental environment which are not modeled, the model parameters and predictions are at least reasonable in comparison to the experimental data. Certain limitations of the model are uncovered but in other cases the model performs well. For example, the spectral broadening prediction shows good agreement with experiment.

11.1 TiO_2 Experimental Data

Approximate the semiconductor TiO_2 spectrum as constant over the conduction band. The energies $E1$ and $E2$ are required. It is known that the bandgap energy of TiO_2 is 3.2 eV.

$$\widetilde{E}_{s=1} - \widetilde{E}_o = 3.2eV \tag{11.1}$$

Add and subtract $\widetilde{E}_g$ to the left side of Equation 11.1. Use the fact that $E_{TG} = \widetilde{E}_g + \widetilde{E}_o$ (Equation 5.47) and $E_s = \widetilde{E}_g + \widetilde{E}_s$ (Equation 5.51).

$$E_{s=1} - E_{TG} = E_{s=1} = 3.2eV \tag{11.2}$$

Set $E_{TG} = 0$. This is the reference energy. Energy $E1$ is then equal to $E_{s=1}$. To obtain $E2$, use experimental data [54], [39], [55], [56], [28], [57] and estimate the width of the TiO_2 conduction band equal to 1.2 eV. The values for $E1$ and $E2$ are substituted into Equation 10.11 for computing energy shift amounts due to semiconductor coupling.

$$E - E_\varphi = K \ln\left(\left|\frac{3.2eV - E}{4.4eV - E}\right|\right) \tag{11.3}$$

Equation 11.3 has three unknowns, E, E_φ, and K. Remember from Equation 10.9 $K \equiv |k|^2 G^2 \left|\left\langle \widetilde{\varphi}_g \left| \hat{\mu}_M \right| \widetilde{\varphi}_e \right\rangle\right|^2$ and since its components are all positive, therefore K is always positive. The $|k|^2$ value is determined by the experimental semiconductor absorption, G

is the orientation portion of the dipole coupling element, and $\left|\left\langle \widetilde{\varphi}_g \left| \hat{\mu}_M \right| \widetilde{\varphi}_e \right\rangle\right|^2$ is the isolated molecule transition strength.

If experimental measurements of any two of E, E_φ, or K are known, then the third can be found. One issue with Equation 11.3 is that it contains absolute energies. A procedure similar to how Equation 11.2 was obtained from Equation 11.1 converts absolute energies into relative energies. So, all energies are relative to the total ground state energy.

11.2 Estimation of Coupling Constant for Retinoic and Carotenoic Acid on TiO_2

Absorption spectra of a series of retinoic and carotenoic acids both isolated and attached to TiO_2 have been published [40]. These molecules represent a sequence of increasing length and number of conjugated double bonds. The retinoic acid (labeled RA5 in the paper) has five conjugated double bonds. The sequence of carotenoic acids (labeled CA6, CA7, CA8, CA9, and CA11 in the paper) has six, seven, eight, nine, and eleven conjugated double bonds. Organic molecules such as these are experimentally useful due to simple structure, absorbance within the solar spectrum, as well as conveniently providing varying chain lengths. Retinoic acid is the oxidized form of Vitamin A.

For each molecule the shift $E_\varphi - E$ is measured. This data provides two of the unknowns in Equation 11.3: E and E_φ. So, use Equation 11.3 to determine the coupling value K. Once K is known, check whether the value is reasonable using approximate values for the transition dipole elements, density of states, and relative dipole distance. Intensity data is not given in the paper and so the intensity increase prediction is not included when comparing to this measured data. Table 11.1 shows experimental results [40].

Molecule	$E_{free}\left(1B_u^+ \leftarrow 1A_g^-\right)$, nm	$E_{bound}\left(1B_u^+ \leftarrow 1A_g^-\right)$, nm	Shift, nm
RA5	345	365	20
CA6	378	395	17
CA7	406	419	13
CA8	425	439	14
CA9	441	454	13
CA11	471	483	12

Table 11.1. Data from [40].

The second column of Table 11.1 approximately corresponds to $\widetilde{E}_e - \widetilde{E}_g$. Ideally this column is exactly $\widetilde{E}_e - \widetilde{E}_g$ but the peak is due to the vertical vibronic transition, not the isolated electronic transition. Figure 11.1 shows these two transitions.

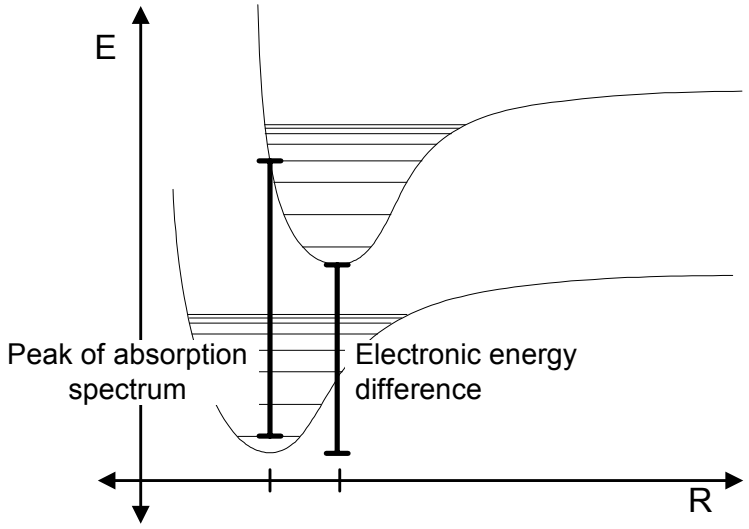

Figure 11.1. Distinguish between the vertical peak of absorption spectrum $E_{free}\left(1B_u^+ \leftarrow 1A_g^-\right)$ and electronic energy difference $\widetilde{E}_e - \widetilde{E}_g$. The electronic energy difference is approximately the 0-0 transition.

Approximate the electronic energy difference with the absorption peaks.

$$E_{free}\left(1B_u^+ \leftarrow 1A_g^-\right) = \widetilde{E}_e - \widetilde{E}_g \tag{11.4}$$

Add and subtract $\widetilde{E}_o$ to the right side of Equation 11.4. The result is the combined state energy E_φ.

$$E_{free}\left(1B_u^+ \leftarrow 1A_g^-\right) = E_\varphi - E_{TG} = E_\varphi \tag{11.5}$$

Set $E_{TG} = 0$. This is the reference energy. Forcing the energy of $\left|\varphi_{TG}\right\rangle$ to zero means the semiconductor coupling effect on the ground state cannot be included in the calculations. This is acceptable because previously it was shown that coupling has a minor effect on the ground state.

The third column of Table 11.1 corresponds, again approximately, to $E - \varepsilon$, where E and ε are solutions to Equation 8.11 for the coupled states Ψ_E and Ψ_ε. Since in both the bound and the free case the table values are approximated as the 0-0 transition, in order to use as the electronic energy transition, therefore, when comparing the shift the error of this simplification approximately cancels.

$$E_{bound}\left(1B_u^+ \leftarrow 1A_g^-\right) = E - \varepsilon \tag{11.6}$$

The ground state is reference and is approximately unaffected by the semiconductor. Therefore $\varepsilon = E_{TG} = 0$.

$$E_{bound}\left(1B_u^+ \leftarrow 1A_g^-\right) = E \tag{11.7}$$

Substitute Equation 11.7 and Equation 11.5 into Equation 11.3.

$$E_{bound}\left(1B_u^+ \leftarrow 1A_g^-\right) - E_{free}\left(1B_u^+ \leftarrow 1A_g^-\right) = K \ln\left(\left|\frac{3.2eV - E_{bound}\left(1B_u^+ \leftarrow 1A_g^-\right)}{4.4eV - E_{bound}\left(1B_u^+ \leftarrow 1A_g^-\right)}\right|\right) \tag{11.8}$$

Solve for K. Convert all energies to electron volts. The units of K are also in units of electron volts, eV.

$$K = \frac{E_{bound}^{(eV)}\left(1B_u^+ \leftarrow 1A_g^-\right) - E_{free}^{(eV)}\left(1B_u^+ \leftarrow 1A_g^-\right)}{\ln\left(\left|\frac{3.2eV - E_{bound}^{(eV)}\left(1B_u^+ \leftarrow 1A_g^-\right)}{4.4eV - E_{bound}^{(eV)}\left(1B_u^+ \leftarrow 1A_g^-\right)}\right|\right)} \tag{11.9}$$

Figure 11.1 shows the result for each of the molecules RA5 (345nm), CA6 (378nm), CA7 (406nm), CA8 (425nm), CA9 (441nm), and CA11 (471nm). It is expected that all six molecules have similar coupling constants. The data for all molecules except RA5 appear similar. Equation 11.8 predicts a very large coupling constant for RA5. This could be correct. Alternatively, it could be that Equation 11.8 overstates the red-shift reduction due to the absorption energy of $|\varphi\rangle$ within the semiconductor energy. For example, the boxcar semiconductor coupling is an approximation. When the absorption energy of $|\varphi\rangle$ is within the conduction band then some of the approximations in the theoretical development are challenged. However, the theory is still valid. A value of K near 0.05 eV for RA5 is obtained if the red-shift of RA5 is set lower than the red-shift of CA11.

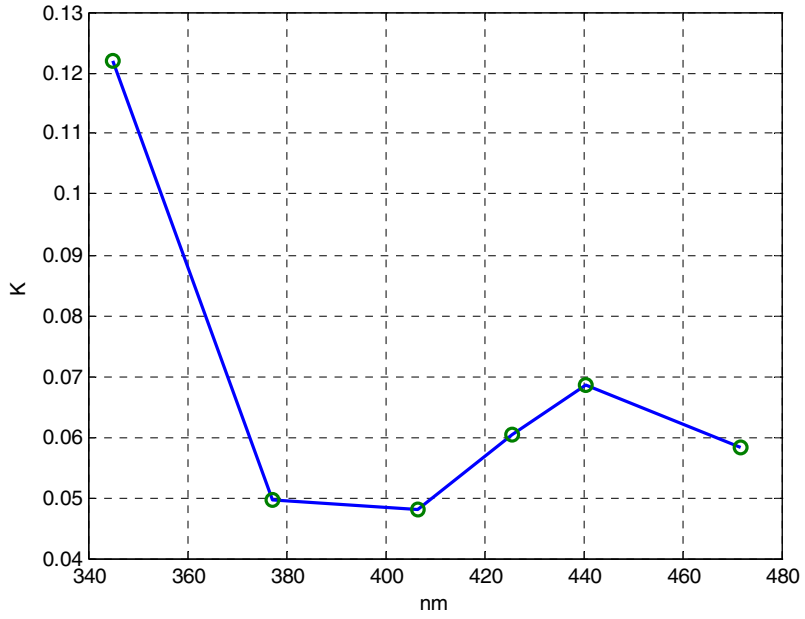

Figure 11.2. Vertical axis is estimated value of K, units of eV. The horizontal axis is the location of the spectral peak with respect to wavelength for the uncoupled case.

Check whether the values of K shown in Figure 11.2 are reasonable using approximate values of each component of K. First, estimate $\langle \tilde{\varphi}_g | \hat{\mu}_M | \tilde{\varphi}_e \rangle$ as $10D \quad (debye)$. In SI units this is $10D \frac{1 \cdot 10^{-21}}{c} Cm/D = 3 \cdot 10^{-29} Cm$.

For $|k|^2$, calculate the density of states with Equation 5.26. The TiO_2 electron effective mass is equal to the rest electron mass [58]. The energy at the center of the conduction band is an "average" for the density of states and scale by $10D$ for the contribution of $\langle \tilde{\psi}_{E'} | \hat{\mu}_S | \tilde{\psi}_o \rangle$. The value $10D$ is selected as an approximation. The accuracy of this value is not critical when simply checking for reasonable K. The

combination $\rho(\tilde{E}')\left|\langle\tilde{\psi}_{E'}|\hat{\mu}_S|\tilde{\psi}_o\rangle\right|^2$ is approximated as constant. The result is $|k|^2 = 1\cdot 10^{-33}\,(Cm)^2/J$.

$$|k|^2 = \left(\frac{8\sqrt{2}\pi}{h^3}\right)(9.11\cdot 10^{-31})^{\frac{3}{2}}\left(\frac{4}{3}\pi\left(20\cdot 10^{-9}\right)^3\right)\sqrt{0.6eV}\,(10D)^2 \qquad (11.10)$$

Finally a value for G is required. From Figure 6.2, it is seen that the numerator of G is in range ± 2. The denominator depends on the distance between the quantum mechanical dipoles. Approximate this distance on the nanometer scale. The result is $-2\cdot 10^{37} < G < 2\cdot 10^{37}\ \ N/C^2 m$. One immediate problem with the theory is that the unknown orientation part puts G into a very broad range of possible values.

$$|G| < \frac{2}{4\pi\left(\varepsilon_o = 8.854\cdot 10^{-12}\ C^2/Nm^2\right)\left(1\cdot 10^{-9} m\right)^3} \qquad (11.11)$$

In any case, at least the maximum value of G is constrained and so apply these results to an estimate of K. Use Equation 10.9 for K. The calculation is shown in Equation 11.12 and the result is $K < 10{,}000eV$. While it is fortunate for the theory that the estimated values of K in Figure 11.2 do not exceed this maximum theoretical value, it is unfortunate that the unknown orientation term G dominates the result, making the range check on K useless. This is a limitation of the model.

$$K < \left(4\cdot 10^{-33}\,(Cm)^2/J\right)\left(\pm 2\cdot 10^{37}\ N/C^2 m\right)^2\left(3\cdot 10^{-29} Cm\right)^2 \frac{eV}{1.602\cdot 10^{-19} J} \qquad (11.12)$$

11.3 Effect of TiO_2 on Carotenoid – Vibronic Spectrum Comparison

A second paper [42] treats the same molecule, CA9 as the experimental comparison in Section 11.2 [40]. The IUPAC (International Union of Pure and Applied Chemistry) name for the molecule is 8'-apo-β-caroten-8'-oic-acid and is abbreviated ACOA [42]. In both works [40] [42] solutions are dissolved in ethanol and the molar ratio to TiO_2 is 1:100 [40] [42]. The experimental red-shift observed is slightly different for the two papers. The second paper [42] shows red-shift starting from an initial value of 437 nm and increasing to a maximum value of 446 nm as the TiO_2 colloidal concentration increases to the same level as [Xian 2005]. The red-shift is 9 nm. This is a smaller shift than the paper considered in the previous section [Xian 2005], with the previous peak shifting from 441 nm to 454 nm, a difference of 13 nm. One difference in the experimental conditions between these papers is this second paper [42] acidified the ethanol to keep the colloidal suspension intact. This may affect the coupling strength.

This second paper shows clearly the absorption shift and broadening when ACOA is attached to colloidal TiO_2, in comparison to free ACOA. It is interesting to compare the predicted spectral broadening of the model developed in this thesis, Equation 10.29, to the experimental results [42]. Doing so is a two step process. First, apply Equation 10.29 to compute the new energy levels. Use the iterative calculation process described for Equation 10.29. Second, apply Equation 4.39 to calculate the absorption spectrum. Compare against the unshifted spectrum by applying Equation 4.39 without first computing new shifted energy levels.

The required parameters of Equation 10.29 are listed below. Ideally a theory requires no adjustable parameters for experimental fit. Subsequent analysis shows that only the single parameter K is required for this purpose. The rest are either simply basic physical descriptors of the system (ACOA molecule and TiO_2 semiconductor) or have little impact on the result (parameter α).

1. Coupling strength K.
2. Semiconductor conduction band energy levels $E1$ and $E2$.
3. Franck-Condon factors $\left|\langle 0_k \left| \upsilon_k(n) \right\rangle\right|$.
4. Original unshifted vibronic energy levels E_{φ_n}.
5. The parameter α used to approximate the denominator of $T(n)$ such that the non-physical singularities are eliminated.

Select K to center the peak of the shifted spectrum to match the experimental result by applying Equation 10.29. The value of K is iteratively determined by comparing the predicted spectrum to the experimental spectrum and adjusting K until the red-shift matches. In this case the match is against the peak of the spectrum, which is not the E_{00} transition (E_{mi} in Figure 4.1). This introduces a slight error in the calculation because the individual vibronic energy level changes are not uniform. Note that the intent of the Equation 10.29 model is to predict the spectral broadening shape, not to quantitatively predict red-shift (qualitatively the red-shift is predicted). Therefore it is acceptable to select K such that an identical red-shift is achieved. This is similar to the

process followed in the Section 11.2 of this thesis. The required value of K is 0.279 eV. Although the molecule ACOA presently considered is identical to the molecule CA9 of Section11.2, the value of K required for a similar red-shift is different. The reason this value of K is different from the value of K in Section 11.2 is because these values have different meaning. Section 11.2 is for the $M=1$ case, Equation 10.11. The present value of K is for the $M>1$ case, Equation 10.29.

The next required experimental values, the semiconductor conduction band energies, were previously explained in Section 11.1. The values are $E1=3.2eV$ and $E2=4.4eV$.

Acquire the necessary original unshifted energy levels E_{φ_n} and the Franck-Condon factors $\left|\left\langle 0_k \left| \upsilon_k(n) \right\rangle\right|\right.$ with Equation 4.36 and Equation 4.37 respectively. These equations require experimentally determined displacement values and ground state vibronic energy levels. Unfortunately, this data is not available for ACOA. However, values for β-carotene are available [59]. The physical difference between ACOA and β-carotene is a cyclohexene instead of a carboxyl terminating group. This difference does not significantly change the molecule vibrational properties and justifies the use of the β-carotene values for ACOA modeling. A total of three normal modes are considered. For the dimensionless displacement, $\Delta_k=\{1.2,0.95,0.65\}$. For the vibrational levels, $\omega_k=\{1525,1155,1005\}cm^{-1}$.

The final necessary parameter is α. A value of $\alpha=100$ is selected. Requiring this extra parameter is certainly not ideal. Fortunately, numerical calculations with Matlab indicate the predicted spectrum, shown later, is fairly insensitive to the parameter

α. Varying α over several orders of magnitude has little effect on the result. This is a nice outcome because parameter α has no physical significance. Furthermore, the insensitivity is easy to understand. What dominates the result for the equation which uses α, Equation 10.28, is the relative number of energy levels above and below the energy level of interest. Equal numbers of levels above and below approximately cancel. What is left is simply the residual, Franck-Condon weighted, difference in numbers of energy levels. Since the Franck-Condon terms are all small, they do not significantly influence the energy cancellations.

What is nice about this theory is that only the parameter K is necessary for adjusting against the experimental results. Equation 11.13 fully expands Equation 10.29 with all terms explicitly shown. Equation 11.14 expands $T'(n)$ of Equation 10.13. These are the exact equations applied in Matlab in order to calculate the new energy levels when a small molecule is attached to a semiconductor.

$$\begin{aligned} &\left\{\left(\Pi_{k=1}^{3}\frac{1}{\upsilon_k(n)!}\left(\frac{\Delta_k^2}{2}\right)^{\upsilon_k(n)}e^{-\frac{\Delta_k^2}{2}}\right)+T'(n)\left(E-\left(E_{eg}+\sum_{k=1}^{3}\upsilon_k(n)\hbar\omega_k^{(e)}\right)\right)\right\} \\ &K\ln\left(\left|\frac{E1-E}{E2-E}\right|\right)=E-\left(E_{eg}+\sum_{k=1}^{3}\upsilon_k(n)\hbar\omega_k^{(e)}\right) \end{aligned} \tag{11.13}$$

$$\begin{aligned} T'(n)\equiv\sum_{\substack{m=1,\\ m\neq n}}^{M}&\left(\Pi_{k=1}^{3}\frac{1}{\upsilon_k(m)!}\left(\frac{\Delta_k^2}{2}\right)^{\upsilon_k(m)}e^{-\frac{\Delta_k^2}{2}}\right) \\ &e^{\alpha\hbar\left|\sum_{k=1}^{3}\left(\upsilon_k(n)\omega_k^{(e)}-\upsilon_k(m)\omega_k^{(e)}\right)\right|}\operatorname{sgn}\left(\hbar\sum_{k=1}^{3}\left(\upsilon_k(n)\omega_k^{(e)}-\upsilon_k(m)\omega_k^{(e)}\right)\right) \end{aligned} \tag{11.14}$$

As a baseline, first compute the spectrum of ACOA without TiO_2 effects. Substitute the Franck-Condon factors Equation 4.37 and the explicit form of the vibronic

energy values Equation 4.36 into the equation for absorption spectrum calculation, Equation 4.39. Convolve with a Gaussian of half-width 550 cm^{-1}. This is approximately 14 nm wide. For each of the three normal modes, the quantum numbers zero through five are included. This results in $6 \cdot 6 \cdot 6 = 216$ individual vibronic levels. So, $M = 216$. The value of Γ in Equation 4.39 is 50 cm^{-1}. Figure 11.3 shows the original spectrum, as calculated by Equation 4.39.

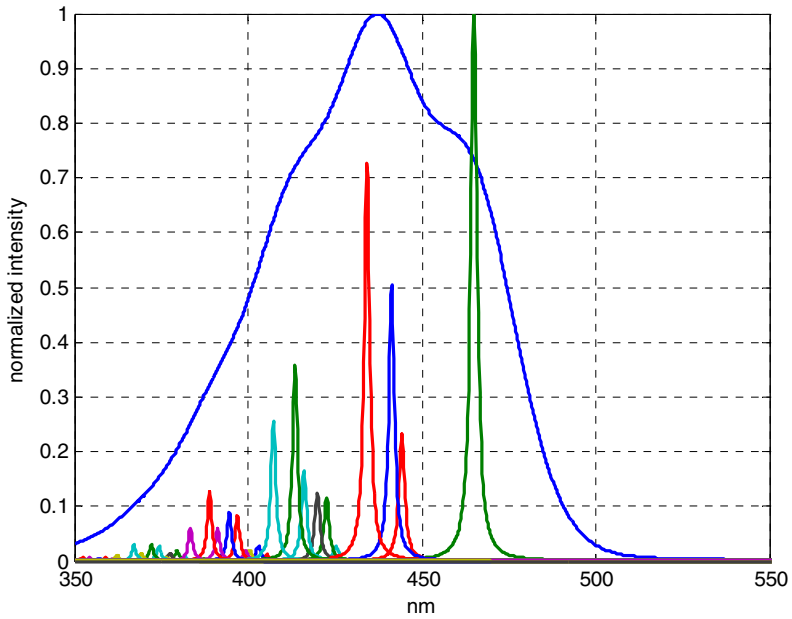

Figure 11.3 Original Spectrum. The individual shapes in the summation of Equation 4.39 are shown underneath the overall spectrum. The overall spectrum is a summation of individual vibration levels and then convolved with a Gaussian.

Next, apply the model, Equation 11.13 and Equation 11.14 to predict the properties of ACOA attached to TiO_2. The resulting absorption spectrum is shown in Figure 11.4. It is very interesting that since the spectrum is broadened, the underlying

vibronic spectra become more visible. This suggests a possible analytical method to separate individual vibration levels, by a molecule weakly coupled to a semiconductor.

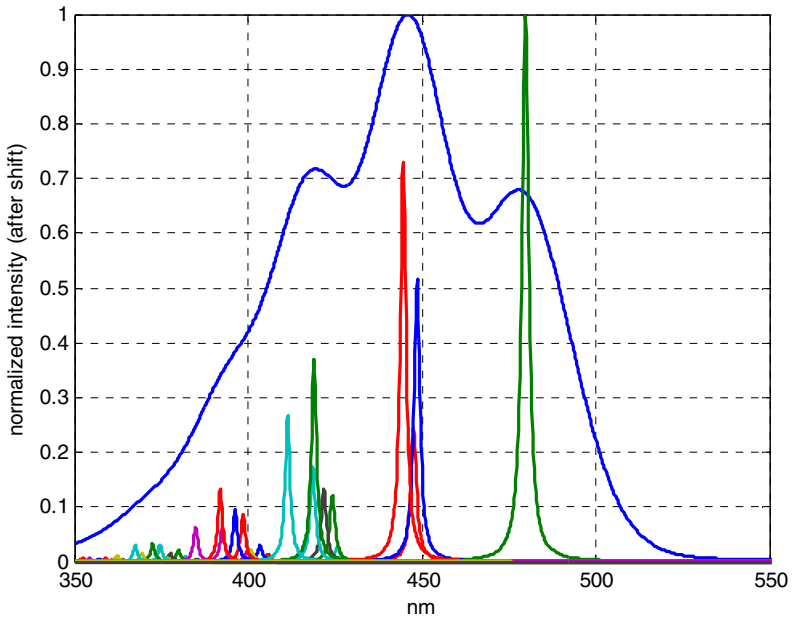

Figure 11.4. Predicted molecule vibronic spectrum after coupling to TiO_2 semiconductor.

Next compare the original absorption spectrum to the shifted absorption spectrum. Original peak is 437 nm. Shifted peak is 446 nm. This matches the shift of the paper, as expected since the constant K has been chosen for this purpose.

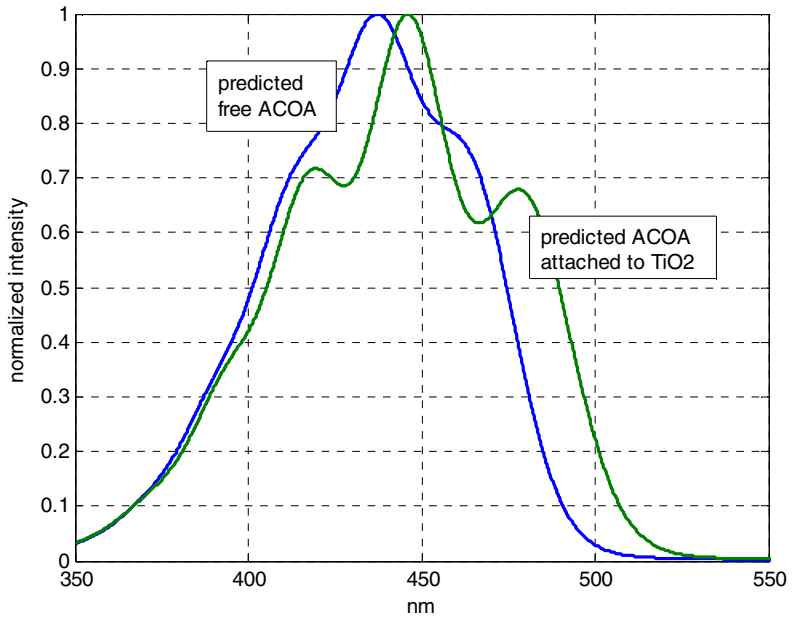

Figure 11.5. Original molecule spectrum vs. coupled to semiconductor.

One difference between the broadened spectrum in Figure 11.5 and the experimental results [42] is that the experimental spectrum shows less structure. The result of Figure 11.5 show nearly identical shifting and overall broadening but with a difference of showing more underlying structure. One possible cause of this difference is that surface states are neglected in the application of Equation 11.3 but in the experiment [42] the effect of surface states could add more underlying vibronic spectra. Also, a change in the solvent interaction could occur upon binding to TiO_2. Also, the binding of molecule to semiconductor probably increases the lifetime.

Account for these effects by adjusting the Gaussian width. Keep all other parameters the same except apply a slightly broader convolved Gaussian of width at the half height 700 cm^{-1} (approximately 17 nm width) to include these effects. The result is

shown in the upper plots of Figure 11.6. Compare with the experimental results [42] in the lower plots of Figure 11.6. Note that the individual figures are displayed with identical horizontal and vertical axis scaling. This facilitates comparing the spectrum.

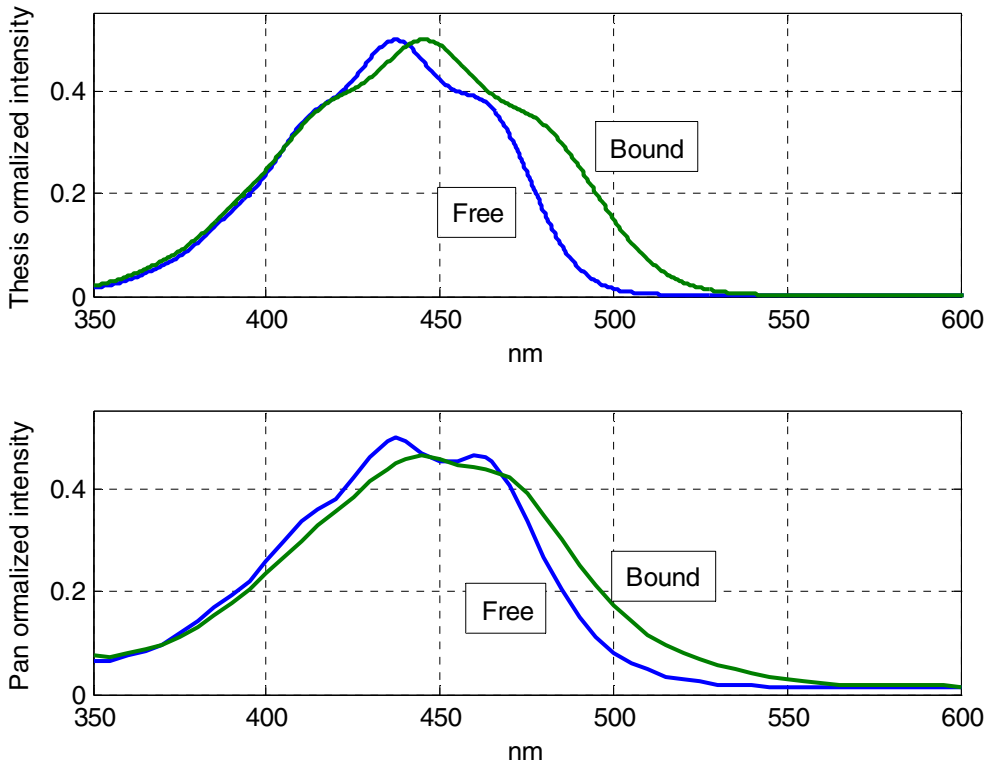

Figure 11.6. Theory (upper plots) compared to Experiment [42] (lower plots).

In comparing the theory to experiment, first notice that the original absorption spectrum are not exactly identical. This is due to the approximation of using β-carotene quantities in place of the data for ACOA. So, the comparison is against relative change in spectral shape, compared to the original spectrum.

The theory correctly predicts a greater amount of red-shift for the longer wavelength measurements. It is hypothesized that this shift is due to coupling of the

vibrational states to each other through the influence of coupling to the semiconductor states. In the absence of such coupling, the absorption spectrum would compress as a function of wavelength: the higher energy vibronic levels would shift more than the lower energy vibronic levels due to being closer, energetically, to the semiconductor.

The theory also shows a decrease in the intensity for the longer wavelength peak, similar to the experimental data. Equation 11.13 and Equation 11.14 does not include the absorption magnitude portion of the model and this is why the overall intensity shift is constant for the theoretical result.

11.4 Effect of TiO2 On Alizarin – Intensity Change Comparison

Experimental results [43] [44] are available which show alizarin spectra before and after binding with colloidal TiO_2. The free alizarin, in methanol, shows peak absorption at 430 nm. When mixed with colloidal TiO_2, in the same methanol solution, the peak red-shifts to 500 nm. The large alizarin red-shift might be a charge transfer phenomena and therefore unsuitable for application of the theory. Unfortunately, no other works could be found which include experimental data on intensity changes as a function of coupling. Often published papers normalize the intensity prior to reporting results. Also, the intensity theory itself, result of thesis Section 9, is suspect due to the dependence on sign of orientational term G. Therefore, the following analysis is included only to show a possible technique for application of the results of Section 9. The predictions should be treated with caution.

Applying Equation 11.8 to the experimental data in [43] results in a coupling prediction of 0.413 eV. Compare to the results for carotenoic acid in Section 11.2. The coupling is much stronger for alizarin because the red-shift is larger.

The paper also measures an intensity increase of approximately 50% after coupling to TiO_2. Use this data with the red-shift data to calculate $G(R,\theta,\alpha)$ and $|k|^2$. This then enables a check of the dipole distance R. If a reasonable value for R is predicted, it provides some additional confidence as to the applicability of the theory. First write $Y(E)$, Equation 10.4, with the experimental data included.

$$Y(E) = |k|^2 \frac{4.4eV - 3.2eV}{\left(E_{bound}^{(eV)} - 4.4eV\right)\left(E_{bound}^{(eV)} - 3.2eV\right)} \tag{11.18}$$

Substitute into Equation 9.28, neglecting the effect of the ground state. Neglecting the ground state was previously shown as a decent approximation.

$$R = \frac{\left(1 + G|k|^2 \ln\left(\left|\frac{3.2eV - E_{bound}^{(eV)}}{4.4eV - E_{bound}^{(eV)}}\right|\right)\right)^2}{\left(1 + K\frac{1.2eV}{\left(E_{bound}^{(eV)} - 4.4eV\right)\left(E_{bound}^{(eV)} - 3.2eV\right)}\right)} \tag{11.19}$$

The numerator of Equation 11.19 is a function of $G|k|^2$ instead of K. Note that $G|k|^2$ is dimensionless. Solve Equation 11.19 for $G|k|^2$.

$$G|k|^2 = \frac{\sqrt{R\left(1 + K\frac{1.2eV}{\left(E_{bound}^{(eV)} - 4.4eV\right)\left(E_{bound}^{(eV)} - 3.2eV\right)}\right)} - 1}{\ln\left(\left|\frac{3.2eV - E_{bound}^{(eV)}}{4.4eV - E_{bound}^{(eV)}}\right|\right)} \tag{11.20}$$

All terms on the right side of Equation 11.20 are experimentally known values: $R = 1.5$, $K = 0.413eV$, and $E_{bound}^{(eV)} = (1240/500)eV$. Substitute these values into Equation 11.20 and calculate $G|k|^2$. The negative sign is due to the orientation component in the numerator of G.

$$G|k|^2 = -0.229 \tag{11.21}$$

The value of $\langle \tilde{\varphi}_g | \hat{\mu}_M | \tilde{\varphi}_e \rangle$ is approximated as $10D$. Substitute into Equation 10.9, after rearranging the equation to place $|k|^2 G^2$ on the left side.

$$|k|^2 G^2 = \frac{0.413eV \cdot 1.6 \cdot 10^{-19} \, J/eV}{\left(10D \frac{1 \cdot 10^{-21}}{c} Cm/D\right)^2} \tag{11.22}$$

Use Equation 10.21 and Equation 10.22 to solve for G and $|k|^2$ individually. The calculated results are $G = -2 \cdot 10^{38} \, N/C^2 m$ and $|k|^2 = 9 \cdot 10^{-40} \, (Cm)^2 / J$. Next, apply the calculated value of G with Equation 11.11 to predict an upper bound value of the quantum mechanical dipole separation $R_{\max}$.

$$R_{\max} = \left(\frac{2}{4\pi\varepsilon_o |G|}\right)^{1/3} \tag{11.23}$$

According to the result in Equation 11.23, the value is $R_{\max} \approx 0.5nm$. This is perhaps smaller than expected but is within tolerance given the many approximations.

12.0 Conclusion

A model of the molecule and semiconductor coupling based on first principles of quantum physics has been created. The theory developed in this thesis qualitatively predicts an absorption spectrum red-shift, intensity change, and quantitatively calculates the broadening shape of the molecule absorption spectrum due to semiconductor coupling of the quantum mechanical transition dipole interaction. The nature of the broadening is shown to be a result of vibronic levels coupling to each other, through the effect of the semiconductor.

This research provides the initial step for further investigation of the coupling effects. Some future work could include numerical calculation of the absorption related parameters (instead of estimating them), the effect of solvent, full numerical calculations of the surface states, and further experiments better tuned to verify the predictions of the model. The surface states can be approximately treated using a decaying exponential below the conduction band edge in the calculation of $Z(E)$. Also, it would be interesting to use experimental data for $Z(E)$ instead of the constant approximation.

Quantum mechanical calculations to remove the constraint of constant orientation term G would be interesting. Initial Matlab studies showed good promise, but were not developed sufficiently to include in the thesis at this time. Neglecting the ground state molecule dipole moments is certainly an approximation worth removing but this also complicates the resulting mathematical model.

Raman spectrum results were not shown but the theory is very easily extended to Raman spectroscopy. This is because once the new energy levels are calculated using the results of this thesis, the Raman spectrum can be calculated using the equations derived in Section 4. Comparing predicted and actual Raman results would be interesting future work.

The dependence of the intensity change on the sign of G is certainly a problem for the theory. It is likely that this is due to the many approximations and future work to investigate simple methods such that this limitation is eliminated would be worth pursuing. Fortunately, the energy level results do not depend on the sign of G and so the main contribution of this thesis, spectral broadening characterization, is not influenced by this one issue.

Earlier forms of the model are general and not specific to a molecule coupled to a semiconductor. For example, in Section 6 the coupling Hamiltonian is applied to a simple dipole. An interesting path for future research is to apply the model to simpler systems and use this approach to eliminate some of the approximations necessary in the later forms of the model.

A final idea for continuing with this research is to pursue the potential analytic benefit of using a semiconductor to separate out vibronic levels of an attached molecule. While admittedly the environmental change, the different lifetime, and binding effects probably wash out the benefit of improved vibronic resolution, it might be possible to find certain molecules and semiconductors and environments for which the effect proves useful.

13.0 Appendix – Determinant Derivation

Proof of 3x3 block matrix determinant [60]. The 2x2 block matrix determinant is well known and can be found in most standard mathematical tables [61].

$$\begin{vmatrix} A & B \\ C & D \end{vmatrix} = |D|\,|A - BD^{-1}C| \tag{13.1}$$

Use Equation 13.1 to find the determinant of X, where X is a 3x3 block matrix.

$$X = \begin{bmatrix} A' & B' & C' \\ B'^{T} & D' & 0 \\ C'^{T} & 0 & E' \end{bmatrix} \tag{13.2}$$

All variables in Equation 13.2 are block matrices. First define four new matrices.

$$A \equiv A' \tag{13.3}$$

$$B \equiv \begin{bmatrix} B' & C' \end{bmatrix} \tag{13.4}$$

$$C \equiv \begin{bmatrix} B' & C' \end{bmatrix}^{T} \tag{13.5}$$

$$D \equiv \begin{bmatrix} D' & 0 \\ 0 & E' \end{bmatrix} \tag{13.6}$$

Substitution of Equations 13.3, 13.4, 13.5, and 13.6 into the matrix $\begin{bmatrix} A & B \\ C & D \end{bmatrix}$ results in the matrix X. Therefore, apply these to Equation 13.1.

$$\left|D\right|\left|A-BD^{-1}C\right|=\begin{vmatrix}D' & 0\\ 0 & E'\end{vmatrix}\left|A'-\begin{bmatrix}B' & C'\end{bmatrix}\begin{bmatrix}D' & 0\\ 0 & E'\end{bmatrix}^{-1}\begin{bmatrix}B' & C'\end{bmatrix}^{T}\right| \tag{13.7}$$

Simplify.

$$\left|D\right|\left|A-BD^{-1}C\right|=\left|D'\right|\left|E'\right|\left|A'-B'D'^{-1}B'^{T}-C'E'^{-1}C'^{T}\right| \tag{13.8}$$

14.0 Appendix – Matlab Files

The following Matlab code generates the plots in Figure 11.3 through Figure 11.6

```
%%%%%%%%%%%%%%%%%%%%%%%%%%%%%%%%%%%%%%%%%%%%%%%%%%%%%%%%%%%%%%%%%%%%%%%%
%
% Vibrational Spectrum Calculations
% Application of theory developed in thesis to generate
% figures 11.3, 11.4, 11.5, and 11.6.
%
% January 2009
%
% Greg Zweigle
%
%%%%%%%%%%%%%%%%%%%%%%%%%%%%%%%%%%%%%%%%%%%%%%%%%%%%%%%%%%%%%%%%%%%%%%%%
clear;

% Constants
hbar = 6.626e-34/2/pi;
cval = 299792458;
nval = 1;
cm_to_rad = 2*pi*100*cval;
cm_to_ev = cm_to_rad * hbar / 1.602e-19;


%%%%%%%%%%%%%%%%%%%%%%%%%%%%%%%%%%%%%%%%%%%%%%%%%%%%%%%%%%%%%%%%%%%%%%%%
% Pan data to compare against.
%%%%%%%%%%%%%%%%%%%%%%%%%%%%%%%%%%%%%%%%%%%%%%%%%%%%%%%%%%%%%%%%%%%%%%%%
load pan_data.txt;
pan_nm = pan_data(:,1);
pan_unshifted = pan_data(:,2);
pan_shifted = pan_data(:,3);

%%%%%%%%%%%%%%%%%%%%%%%%%%%%%%%%%%%%%%%%%%%%%%%%%%%%%%%%%%%%%%%%%%%%%%%%
% These are the adjustable parameters of the calculation.
%%%%%%%%%%%%%%%%%%%%%%%%%%%%%%%%%%%%%%%%%%%%%%%%%%%%%%%%%%%%%%%%%%%%%%%%

% Loop over all quantum numbers up to this value.
max_v = 5;

% Select the electronic transition frequency.
% Trying to get center of absorption spectra at 437nm.
weg_cm = 1240/(465*cm_to_ev);

% Gamma value in the denominator.
gamma = 50;

% Gaussian variance.
sig = 550;

% Frequency sampling interval, units of cm-1.
freq_interval = 10;

%%%%%%%%%%%%%%%%%%%%%%%%%%%%%%%%%%%%%%%%%%%%%%%%%%%%%%%%%%%%%%%%%%%%%%%%
% Molecule parameters and expected spectrum.
%%%%%%%%%%%%%%%%%%%%%%%%%%%%%%%%%%%%%%%%%%%%%%%%%%%%%%%%%%%%%%%%%%%%%%%%

% Expected spectrum.  I approximated this based on the plot in the paper.
spectrum_exp = [1 3.5 4.75 4.25 5 5.25 4 3.75 3];
spectrum_exp = spectrum_exp ./ max(max(spectrum_exp));  % Normalize.
offset = -850;
wo_exp_cm = [weg_cm+offset:500:weg_cm+4000+offset];
```

```
% Betacarotene values from the paper.
ugeo = 16.6;
num_norm_modes = 3;
omega_cm(1:num_norm_modes) = [1525 1155 1005];
delta(1:num_norm_modes) = [1.12 0.95 0.65];

%%%%%%%%%%%%%%%%%%%%%%%%%%%%%%%%%%%%%%%%%%%%%%%%%%%%%%%%%%%%%%%%%%%
% Calculate the unshifted spectrum.
%%%%%%%%%%%%%%%%%%%%%%%%%%%%%%%%%%%%%%%%%%%%%%%%%%%%%%%%%%%%%%%%%%%

% Set the wo array to be centered around weg_cm.
wo_array_cm = [weg_cm-5*omega_cm(3):freq_interval:weg_cm+15*omega_cm(1)];

% Make a Gaussian to convolve with the original spectrum.
mygauss = exp(-(wo_array_cm-mean(wo_array_cm)).^2/2/sig^2);

% For the broadened spectrum, use a broader Gaussian.
sig2 = 700;
mygauss2 = exp(-(wo_array_cm-mean(wo_array_cm)).^2/2/sig2^2);

% Constant out front.
k_front = 4*pi^2*ugeo^2/3/hbar/cval/nval * gamma / pi * wo_array_cm .^2;

% Loop over the excited state quantum numbers.
fi = 1;
for v1 = 0:max_v,
  for v2 = 0:max_v,
    for v3 = 0:max_v,

      % Save for later to compare against shifted frequencies.
      orig_levels_cm(fi) = weg_cm + v1*omega_cm(1) + v2*omega_cm(2) + v3*omega_cm(3);

      % Franck-Condon term.
      fc_coeff(fi) =  1 ./ (factorial(v1)*factorial(v2)*factorial(v3)) .* ...
          (delta(1)^2/2)^v1 * (delta(2)^2/2)^v2 * (delta(3)^2/2)^v3 .* ...
          exp(-(delta(1)^2 + delta(2)^2 + delta(3)^2)/2);

      % Calculate the spectrum of each normal mode individually.
      spectrum_calc(fi,:) = k_front * fc_coeff(fi) ./ ...
          ((orig_levels_cm(fi) - wo_array_cm).^2 + gamma^2);

      fi = fi + 1;

    end;
  end;
end;

% Store the total number of excited frequencies: this is M in the thesis.
M_val = fi - 1;

% Normalize the individual spectrum.
spectrum_calc = spectrum_calc ./ max(max(spectrum_calc));

% Sum the individual spectrum.
spectrum_total = sum(spectrum_calc);

% Convolve with the Gaussian then shift by half of the length of the
% Gaussian in order to recenter.  Also, normalize.
tmp1 = conv(mygauss,spectrum_total);
tmp2 = tmp1(round(length(mygauss)/2):length(tmp1));
spectrum_filtered_total = tmp2(1:length(spectrum_total));
spectrum_filtered_total = spectrum_filtered_total ./ max(spectrum_filtered_total);

% Plot calculated vs. experimental.
figure(1);
subplot(1,1,1);
plot(1240./(wo_array_cm*cm_to_ev),spectrum_filtered_total,...
     1240./(wo_array_cm*cm_to_ev),spectrum_calc,'LineWidth',2);
xlabel('nm');
```

```
ylabel('normalized intensity');
grid;
axis([350 550 0 1]);

%%%%%%%%%%%%%%%%%%%%%%%%%%%%%%%%%%%%%%%%%%%%%%%%%%%%%%%%%%%%%%%%%%%%%%%
% Compute the shifted frequencies, use thesis algorithm.
%%%%%%%%%%%%%%%%%%%%%%%%%%%%%%%%%%%%%%%%%%%%%%%%%%%%%%%%%%%%%%%%%%%%%%%
last_shift_levels_cm = zeros(1,length(orig_levels_cm));
[shift_levels_cm] = ...
  section11_eshift(M_val, wo_array_cm, cm_to_ev, fc_coeff, ...
                   orig_levels_cm, last_shift_levels_cm);

% Run it again except this time with the shifted levels.
% This is an iterative approach and only one iteration is needed.
last_shift_levels_cm = shift_levels_cm;
[shift_levels_cm] = ...
  section11_eshift(M_val, wo_array_cm, cm_to_ev, fc_coeff, ...
                   orig_levels_cm, last_shift_levels_cm);

%%%%%%%%%%%%%%%%%%%%%%%%%%%%%%%%%%%%%%%%%%%%%%%%%%%%%%%%%%%%%%%%%%%%%%%
% Calculate the shifted spectrum.
%%%%%%%%%%%%%%%%%%%%%%%%%%%%%%%%%%%%%%%%%%%%%%%%%%%%%%%%%%%%%%%%%%%%%%%

% Loop over the excited state quantum numbers.
fi = 1;
for v1 = 0:max_v,
  for v2 = 0:max_v,
    for v3 = 0:max_v,

      spectrum_calc2(fi,:) = k_front .* fc_coeff(fi) ./ ...
          ((shift_levels_cm(fi) - wo_array_cm).^2 + gamma^2);

      fi = fi + 1;

    end;
  end;
end;

% Normalize the individual spectrum.
spectrum_calc2 = spectrum_calc2 ./ max(max(spectrum_calc2));

% Sum the individual spectrum.
spectrum_total2 = sum(spectrum_calc2);

% Convolve with the Gaussian then shift by half of the length of the
% Gaussian in order to recenter.  Also, normalize.
tmp1 = conv(mygauss,spectrum_total2);
tmp2 = tmp1(round(length(mygauss)/2):length(tmp1));
spectrum_filtered_total2 = tmp2(1:length(spectrum_total2));
spectrum_filtered_total2 = spectrum_filtered_total2 ./ max(spectrum_filtered_total2);

% Try with a broader Gaussian.
% Convolve with the Gaussian then shift by half of the length of the
% Gaussian in order to recenter.  Also, normalize.
tmp1 = conv(mygauss2,spectrum_total2);
tmp2 = tmp1(round(length(mygauss2)/2):length(tmp1));
spectrum_filtered_total3 = tmp2(1:length(spectrum_total2));
spectrum_filtered_total3 = spectrum_filtered_total3 ./ max(spectrum_filtered_total3);

% Plot the result, with a horizontal scale of nanometers to compare with paper easily.
figure(2);
subplot(1,1,1);
plot(1240./(wo_array_cm*cm_to_ev),spectrum_filtered_total, ...
     1240./(wo_array_cm*cm_to_ev),spectrum_filtered_total2,...
    'LineWidth',2);
xlabel('nm');
ylabel('normalized intensity');
grid;
axis([350 550 0 1]);
```

```
% Plot the shifted with the underlying spectrum.
figure(3);
subplot(1,1,1);
plot(1240./(wo_array_cm*cm_to_ev),spectrum_filtered_total2,...
     1240./(wo_array_cm*cm_to_ev),spectrum_calc2,'LineWidth',2);
xlabel('nm');
ylabel('normalized intensity (after shift)');
grid;
axis([350 550 0 1]);

% Use the broader Gaussian.
% Plot the result, with a horizontal scale of nanometers to compare with paper easily.
figure(4);
subplot(1,1,1);
plot(1240./(wo_array_cm*cm_to_ev),spectrum_filtered_total * 0.5, ...
     1240./(wo_array_cm*cm_to_ev),spectrum_filtered_total3 * 0.5,...
    'LineWidth',2);
xlabel('nm');
ylabel('Pan normalized intensity');
grid;
axis([350 600 0 0.55]);

% Compare against Pan.
figure(5);
subplot(2,1,1);
plot(1240./(wo_array_cm*cm_to_ev),spectrum_filtered_total * 0.5, ...
     1240./(wo_array_cm*cm_to_ev),spectrum_filtered_total3 * 0.5,...
    'LineWidth',2);
xlabel('nm');
ylabel('Thesis normalized intensity');
grid;
axis([350 600 0 0.55]);
subplot(2,1,2);
pan_nm = pan_data(:,1);
pan_unshifted = pan_data(:,2);
pan_shifted = pan_data(:,3);
plot(pan_nm,0.5 / 40 * pan_unshifted, ....
     pan_nm,0.5 / 40 * pan_shifted, ....
    'LineWidth',2);
xlabel('nm');
ylabel('Pan normalized intensity');
grid;
axis([350 600 0 0.55]);

% Display numerical shift values for each frequency.
[1240 ./ (orig_levels_cm * cm_to_ev)' ...
1240 ./  (shift_levels_cm * cm_to_ev)' ...
1240 ./ (orig_levels_cm * cm_to_ev)' - 1240 ./  (shift_levels_cm * cm_to_ev)' ...
(orig_levels_cm * cm_to_ev)' ...
(shift_levels_cm * cm_to_ev)' ...
(orig_levels_cm * cm_to_ev)' - (shift_levels_cm * cm_to_ev)']

% Display the amount of shift in nanometers.
orig_peak_ind = find(spectrum_filtered_total >= max(spectrum_filtered_total));
shifted_peak_ind = find(spectrum_filtered_total2 >= max(spectrum_filtered_total2));
[1240./(wo_array_cm(orig_peak_ind)*cm_to_ev) ...
 1240./(wo_array_cm(shifted_peak_ind)*cm_to_ev) ...
 1240./(wo_array_cm(orig_peak_ind)*cm_to_ev) - ...
 1240./(wo_array_cm(shifted_peak_ind)*cm_to_ev)]
```

15.0 References

[1] Lewis, N.S.; Nocera, D. G. *Proceedings of the National Academy of Sciences of the United States of America* **2006**, 103 (43), 15729.

[2] Wrighton, M.S. *Accounts of Chemical Research* **1979**, 12 (9), 303.

[3] O'Regan, B.; Gratzel, M. *Nature* **1991**, 353, 737.

[4] Bisquert, J.; Cahen, D.; Hodes, G.; Ruhle, S.; Zaban, A. *The Journal of Physical Chemistry B* **2004**, 108 (24), 8106.

[5] Frank, A.J.; Kopidakis, N.; Lagematt, J. *Coordination Chemistry Reviews* **2004**, 248, 1165.

[6] Tributsch, H. *Coordination Chemistry Reviews* **2004**, 248, 1511.

[7] Hagfeldt, A.; Gratzel, M *Chemical Reviews* **1995**, 95, 49.

[8] Kalyanasundaram, K.; Gratzel, M. *Coordination Chemistry Reviews* **1998**, 77, 347.

[9] Cahen, D.; Hodes, G.; Gratzel, M.; Guillemoles, J. F.; Riess, Ilan *The Journal of Physical Chemistry B* **2000**, 104, 2053.

[10] Argazzi, R.; Iha, N. Y. M.; Zabri, H.; Odobel, F.; Bignozzi, C. A. *Coordination Chemistry Reviews* **2004**, 248, 1299.

[11] Muscat, J. P.; Newns, D. M. *Progress in Surface Science* **1978**, 9, 1.

[12] Fleischmann, M.; P. J. Hendra; A. J. McQuillan *Chemical Physics Letters* **1974**, 26 (2), 163.

[13] Fujishima, A.; Honda, K. *Nature* **1972**, 238, 37.

[14] Cesar, I.; Kay, A.; Gonzalez, M.; Gratzel, M. *Journal of the American Chemical Society* **2006**, 128, 4582.

[15] Marcus, R. A. *The Journal of Chemical Physics* **1993**, 98 (7), 5604.

[16] Gao, Y. G.; Georgievskii, Y.; Marcus, R. A. *The Journal of Chemical Physics* **2000**, 112 (7), 3358.

[17] Creutz, C.; Brunschwig, B. S.; Sutin, N. *The Journal of Physical Chemistry B* **2005**, 109 (20), 10251.

[18] Creutz, C.; Brunschwig, B. S.; Sutin, N. *The Journal of Physical Chemistry B* **2006**, 110 (5), 25181.

[19] Zhu, X. Y. *The Journal of Physical Chemistry B* **2004**, 108 (26), 8778.

[20] Ai, X.; Anderson, N. A.; Guo, J.; Lian, T. *The Journal of Physical Chemistry B* **2005**, 109, 7088.

[21] Lombardi, J. R.; Birke, R. L.; Lu, T.; Xu, J. *The Journal of Chemical Physics* **1986**, 84 (8), 4174.

[22] Lombardi, J. R.; Birke, R. L. *The Journal of Chemical Physics* **2007**, 126, 244709.

[23] Ramakrishna, S.; Willig, F.; May, V. *Physical Review B* **2000**-II, 62 (24), R16330.

[24] Ramakrishna, S.; Willig, F.; May, V. *The Journal of Chemical Physics* **2001**, 115 (6), 2743.

[25] Zimmerman, C.; Willig, F.; Ramakrishna, S.; Burfeindt, B.; Pettinger, B.; Eichberger, R.; Storck, W. *The Journal of Physical Chemistry B* **2001**, 105, 9245.

[26] Wang, L.; Ernstorfer, R.; Willig, F.; May, V. *The Journal of Physical Chemistry B* **2005**, 109, 9589.

[27] Wang, L.; Willig, F.; May, V. *The Journal of Chemical Physics* **2006**, 124, 014712.

[28] Persson, P.; Lundqvist, M. J.; Ernstorfer, R.; Goddard III, W. W.; Willig, F. *Journal of Chemical Theory and Computation* **2006**, 2, 441.

[29] Fano, U. *Physical Review* **1961**, 124 (6), 1866.

[30] Wang, L.; Willig, F.; May, V. *The Journal of Chemical Physics* **2007**, 126, 134110.

[31] Pollard, J. A.; Zhang, D.; Downing, J. A.; Knorr, F. J.; McHale, J. L. *The Journal of Physical Chemistry A* **2005**, 109 (50), 11443.

[32] Hoertz, P. G.; Staniszewski, A.; Marton, A.; Higgins, G. T.; Incarvito, C. D.; Rheingold, A. L.; Meyer, G. J *Journal of the American Chemical Society* **2006**, 128, 8234.

[33] Wang, Z. S.; Cui, Y.; Dan-oh, Y.; Kasada, C.; Shinpo, A.; Hara, K. *The Journal of Physical Chemistry C* **2007**, 111 (19), 7224.

[34] Edvinsson, T.; Li, C.; Pschirer, N.; Schneboom, J.; Eickemeyer, F.; Sens, R.; Boschloo, G.; Herrmann, A.; Mllen, K.; Hagfeldt, A. *The Journal of Physical Chemistry C* **2007**, 111 (42), 15137.

[35] Sudeep, P. K.; Takechi, K.; Kamat, P. V. *The Journal of Physical Chemistry C* **2007**, 111 (1), 488.

[36] Liang, M.; Xu, W.; Cai, F.; Chen, P.; Peng, B.; Chen, J.; Li, Z. *The Journal of Physical Chemistry C* **2007**, 111 (1), 4465.

[37] Sayhun, M. R. V.; Serpone, N. *Journal of Photochemistry and Photobiology A: Chemistry* **1998**, 115, 231.

[38] Nawrocka, A.; Krawczyk, S. *The Journal of Physical Chemistry C* **2008**, 112 (27), 10233.

[39] Persson, P.; Bergstrm, R.; Lunell, S. *The Journal of Physical Chemistry B* **2000**, 104 (44), 10348.

[40] Xiang, J.; Rondonuwu, F. S.; Kakitani, Y.; Fujii, R.; Watanabe, Y.; Koyama, Y.; Nagae, H.; Yamano, Y.; Ito, M. *The Journal of Physical Chemistry B* **2005**, 109 (36), 17066.

[41] Xiang, J.; Rondonuwu, F. S.; Kakitani, Y.; Fujii, R.; Watanabe, Y.; Koyama, Y.; Nagae, H.; Yamano, Y.; Ito, M. J. *The Journal of Physical Chemistry B Supplemental Information* **2005**, 109 (36), 17066.

[42] Pan, J.; Benk, G.; Xu, Y.; Pascher, T.; Sun, L.; Sundstrm, V.; Polvka, T. *Journal of the American Chemical Society* **2002**, 124 (46), 13949.

[43] Huber, R.; Sporlein, S.; Moser, J.; Gratzel, M.; Wachtveitl, J. *The Journal of Physical Chemistry B* **2000**, 104, 8995.

[44] Duncan, W. R.; Stier, W. M.; Prezhdo, O. V. *Journal of the American Chemical Society* **2005**, 127 (21), 7941.

[45] Levine, R. N. *Quantum Chemistry, 5th Edition;* Prentice Hall: New Jersey, 2000.

[46] Eisberg, R.; Resnick, R. *Quantum Physics of Atoms, Molecules, Solids, Nuclei, and Particles, 2nd Edition;* John Wiley and Sons: New York, 1985.

[47] McHale, J. L *Molecular Spectroscopy;* Prentice Hall: New Jersey, 1999.

[48] Shockley, W. *Electrons and Holes in Semiconductors*; D. Van Nostrand: New York, 1950.

[49] D.A. Neamen, *Semiconductor Physics and Devices;* Irwin, 1992.

[50] Mandel, L. *Physical Review A* **1979**, 20 (4), 1590.

[51] Kovalenko, A. F.; Holovko, M. F. *Journal of Physics B: Atomic, Moleccular and Optical Physics* **1992,** 25, L223.

[52] Mor, G. K.; Varghese, O. K.; Paulose, M.; Shankar, K.; Grimes, C. A. *Solar Energy Materials and Solar Cells* **2006**, 90, 2011.

[53] Asahi, R.; Tata, Y.; Mannstadt, W.; Freeman, A. J. *Physical Review B* **2000**, 61 (11), 7459.

[54] Gong, X. Q.; Selloni, A. *The Journal of Physical Chemistry B* **2005**, 109, 19560.

[55] Persson, P.; Gebhardt, J. C. M.; Lunell, S. *The Journal of Physical Chemistry B* **2003**, 107, 3336.

[56] Rothenberger, G.; Fitzmaurice, D.; Gratzel, M. *The Journal of Physical Chemistry* **1992**, 96, 5983.

[57] Sorantin, P. I.; Schwarz, K. *Inorganic Chemistry* **1992**, 31, 567.

[58] Toyoda, T.; Tsuboya, I. *Review of Scientific Instruments* **2003**, 74 (1), 782.

[59] Burt, J. A.; Zhao, X.; McHale, J. L. *The Journal of Chemical Physics* **2004**, 120 (9), 4344.

[60] Abadir, K. M.; Magnus, J. R. *Matrix Algebra;* Cambridge University Press: New York, 2005.

[61] CRC Standard Math Tables 27th Ed.